THE ROLES OF THE PROTEIN TYROSINE PHOSPHATASES PTPN3 AND PTPN4 IN T CELLS AND PTPN11 IN TISSUE REMODELING

by

Timothy J Bauler

A dissertation submitted in partial fulfillment
of the requirements for the degree of
Doctor of Philosophy
(Microbiology and Immunology)
in The University of Michigan
2009

Doctoral Committee:

Associate Professor Philip D. King, Chair
Professor Wesley A. Dunnick
Assistant Professor Ivan P. Maillard
Assistant Professor Mary X.D. O'Riordan

Acknowledgements

Biomedical research is becoming increasingly collaborative, and the work presented here is no exception. Thom Saunders and Elizabeth Hughes in the Transgenic Animal Model Core facility were instrumental in the generation of the PTPN3 and PTPN4 knockout strains. Tomas Mustelin and Yutaka Arimura were collaborators for the PTPN3 project. Wiljan Hendriks (PTPN13 ΔPTP/ΔPTP), Gen-Sheng Feng (SHP-2 fl/fl), and Eric J. Brown (ERT2-Cre) were exceptionally generous to share valuable mouse strains. The SHP-2 project was started in collaboration with Eric Langewisch, and furthered with Erby Wilkinson (pathology) and Nobuhiro Kamiya (bone histology).

The King lab has been a wonderful place to be a graduate student. This is in no small part due to the leadership of "The King", who is full of great ideas and guidance, is a fun person to be around, and whose open door mentorship policy has been responsible for much of my growth as a scientist. My coworkers in the lab, Phil, Jen, and Francesc made work enjoyable and were always willing to share techniques/advice. My committee was extremely supportive when all my data was negative, and has been full of ideas on how to focus these projects and address what is important.

I need to thank my parents, siblings, and extended family who provide my foundation and set me off on this path. I must also thank my wife Laura who not only supplied insight and technical support for the science, but also has been by my side throughout the journey.

Table of Contents

List of Figures

Abstract

PTPN3 and PTPN4 are closely-related non-receptor PTP that contain FERM and PDZ domains. Both PTP have been implicated as negative-regulators of early signal transduction through the TCR, acting to dephosphorylate the TCRζ chain. To determine if PTPN3 functions as a physiological negative-regulator of TCR signaling in primary T cells we generated gene-trapped and gene-targeted mouse strains that lack expression of catalytically-active PTPN3. Numbers and ratios of T cells in primary and secondary lymphoid organs and TCR-induced signal transduction, cytokine production, and proliferation were normal in PTPN3-deficient mice. To address if the lack of a T cell phenotype in PTPN3-deficient mice can be explained by functional redundancy of PTPN3 with PTPN4, we generated PTPN4-deficient and PTPN4/PTPN3 double-deficient mice. As in PTPN3 mutants, T cell development and homeostasis and TCR-induced cytokine synthesis and proliferation were found to be normal in PTPN4-deficient and PTPN4/PTPN3 double-deficient mice. PTPN13 is another FERM and PDZ domain-containing PTP that is distantly related to PTPN3 and PTPN4. Therefore, to determine if PTPN13 might compensate for the loss of PTPN3 and PTPN4 in T cells, we generated mice that lack functional forms of all three PTP. However, triple-mutant T cells are phenotypically indistinguishable from PTPN13 single-deficient T cells. We conclude that PTPN3 and PTPN4 are dispensable for TCR signal transduction.

SHP-2 (PTPN11) is essential for signaling from multiple classes of cell surface receptors. Mice deficient in SHP-2 expression exhibit defective gastrulation and fail to survive, which has precluded the use of non-conditional SHP-2 deficient mice to examine the role of SHP-2 in mature animals. To study this, we have used a conditional SHP-2 deficient mutant together with an ubiquitin promoter-driven ERT2-Cre transgene to mediate drug inducible deletion of SHP-2 in multiple tissues in adult mice. Using this model, we have determined that induced deletion of SHP-2 results in lethality preceded by weight loss. Epidermal acanthosis, anemia and premature thymic involution were also observed in these mice. Roles for SHP-2 in the homeostasis of the skeletal system are further demonstrated by the striking bone and cartilage remodeling defects resulting from the loss of SHP-2 in this model.

Chapter 1: Introduction

A common event in cellular signal transduction pathways is the tyrosine phosphorylation of proteins which results in diverse cellular outcomes such as motility, differentiation, growth, and proliferation. This phosphorylation is mediated by protein tyrosine kinases (PTK). By contrast, protein tyrosine phosphatases (PTP) remove phosphate groups from protein tyrosyl residues and thus oppose the actions of PTK.

Although an appropriate cellular response to stimuli resulting in protein tyrosine signals requires both PTK and PTP, PTK have been more extensively studied. The first PTK was identified, purified, and cloned ten years prior to similar studies of the first PTP. Furthermore, following the initial characterization of PTP, PTP were shown to have log magnitude higher levels of enzymatic activity compared to PTK. The limited number of PTP identified and the high enzymatic activity of these PTP resulted in the hypothesis that PTP exhibit limited substrate specificity and function primarily as cellular housekeeping enzymes. The steady identification of additional PTP and the further characterization of substrates of the earliest described PTP have gradually led to the appreciation that PTP are as similarly diverse in form, function, and specificity as PTK.

1.1 Protein Tyrosine Phosphatases

The human genome encodes 107 genes whose protein products are classified as members of the PTP family [1]. Of these, 81 genes are catalytically active and dephosphorylate tyrosine residues, whereas the majority of the remainder are inactive or dephosphorylate inositol phospholipids [1]. The approximately 280 residue catalytic domain of PTP is characterized by the PTP signature motif (I/V)HCxxGxxR(S/T), which forms a significant fraction of the phosphate binding pocket [2]. The cysteine residue in the signature motif initiates catalysis by nucleophilic attack on the phosphate atom, while the arginine residue provides stability to the subsequent cysteine-phosphate intermediate. In addition to the PTP signature motif, there are nine further motifs spread throughout the primary sequence of PTP domains that are highly conserved, including motifs involved in substrate recognition and catalysis [3]. Most PTP have additional modular domains other than the catalytic domain, many of which are involved in protein-protein interactions [1]. Similar to PTK, these domains in PTP can serve to direct expression of PTP to distinct cellular compartments, function in intramolecular catalytic regulation, or aid in substrate specificity determination.

The mammalian genome encodes 38 “classical” PTP that dephosphorylate tyrosine residues only, in contrast to dual-specific phosphatases that dephosphorylate serine and threonine in addition to tyrosine [4,5]. These classical PTP can be subdivided into receptor-like and non-transmembrane PTP [4,6]. There are 21 transmembrane, receptor-like PTP genes, and the majority of these have tandem PTP domains. The non-transmembrane PTP family consists of 17 members, most of which have modular domains that affect localization and function (Fig 1). The work described herein has

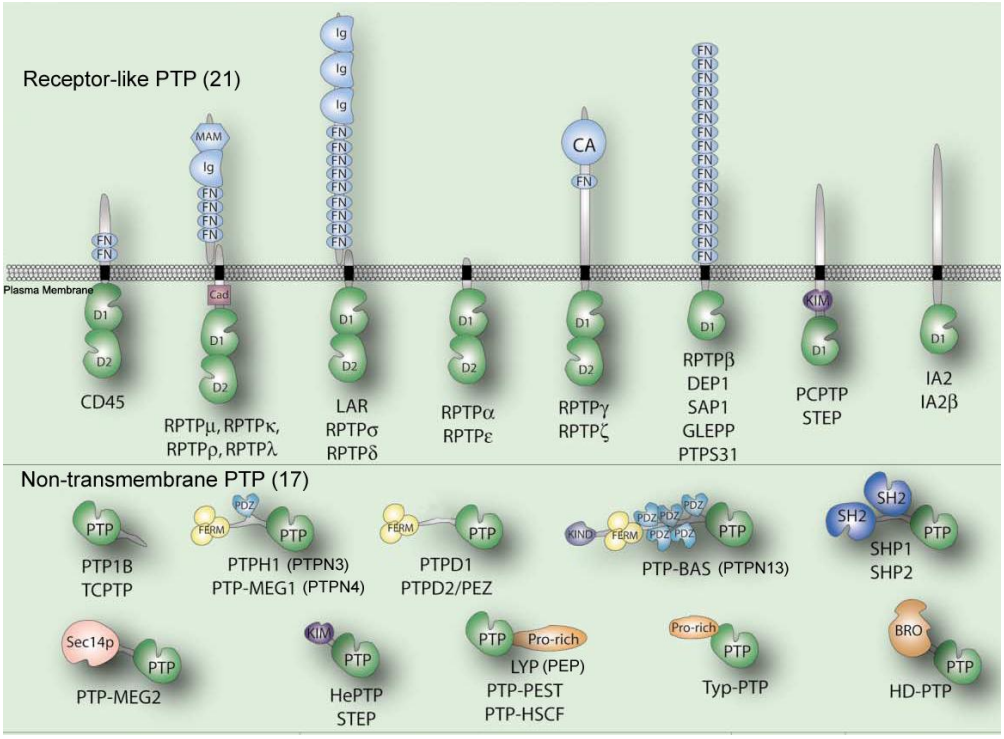

Figure 1 Classical PTP encoded by the human/mouse genomes

Schematic of the domain organization of the 38 classical PTP. Abbreviations: BRO, baculovirus BRO homology; CA, carbonic anhydrase-like; Cad, cadherin-interaction domain; FERM, band 4.1-ezrin-radixin-moesin homology; FN, fibronectin-like; Ig, immunoglobulin-like; KIM, kinase interaction motif; KIND, kinase N lobe-like domain; MAM, meprin, A2, RPTPμ homology; PDZ, postsynaptic density-95/discs large/ZO1 homology; Sec14p, Sec14p homology; SH2, src homology 2. From Alonso et al [1].

focused on the roles of three members of the classical non-transmembrane PTP family in cellular signal transduction.

1.2 Tyrosine Phosphorylation in TCR Signal Transduction

Cells of the immune system utilize cell surface receptors to respond to diverse stimuli, including pathogens, cytokines and growth factors, and other immune cells. The signaling cascades stimulated by many of these receptors utilize PTK and PTP to transduce signals. The signals originating at the clonally distributed, cell surface expressed T cell antigen receptor (TCR) have been particularly well studied. These signals have been shown to be at least partially responsible for T cell maturation in the

thymus, including gene rearrangement, growth, positive and negative selection, and lineage decisions. Additionally, TCR signals are required for T cell function in the periphery, including T cell growth, proliferation, differentiation, migration, target cell lysis, and B cell help.

T cells become activated subsequent to TCR-mediated recognition of MHC-peptide complexes on the surface of antigen presenting cells (APC) [7]. The TCR is comprised of a heterodimer of polypepides, TCRα and TCRβ, each of which is assembled by somatic DNA recombination. This results in a highly diverse TCR repertoire capable of recognizing the myriad of self MHC-peptide combinations. A second signal originating from a costimulatory receptor such as CD28 must accompany the TCR signal to generate a productive T cell response [8]. One of the first events in the now well-established TCR signaling cascade is the phosphorylation and activation of the Src-family PTK (SrcFK), LCK and FYN [9]. SrcFK are noncovalently associated with the intracellular tail of the coreceptors CD4 and CD8, which results in local aggregation important for SrcFK activation following coreceptor-MHC binding [10]. LCK and FYN phosphorylate immunoreceptor tyrosine-based activation motifs (ITAMs) present within the cytoplasmic tails of invariant CD3 and TCRζ proteins that form part of the TCR complex [11]. Subsequently, the Syk-family kinase, ZAP-70, is recruited to the complex by the recognition of phosphorylated ITAMs, and, in turn, is activated via SrcFK-mediated phosphorylation. Activated ZAP-70 phosphorylates the transmembrane adapter protein, linker for activation of T cells (LAT) on four tyrosine residues [12]. Phosphorylated LAT serves as a scaffold for the membrane recruitment of additional signaling intermediates leading to the development of multiprotein signaling complexes.

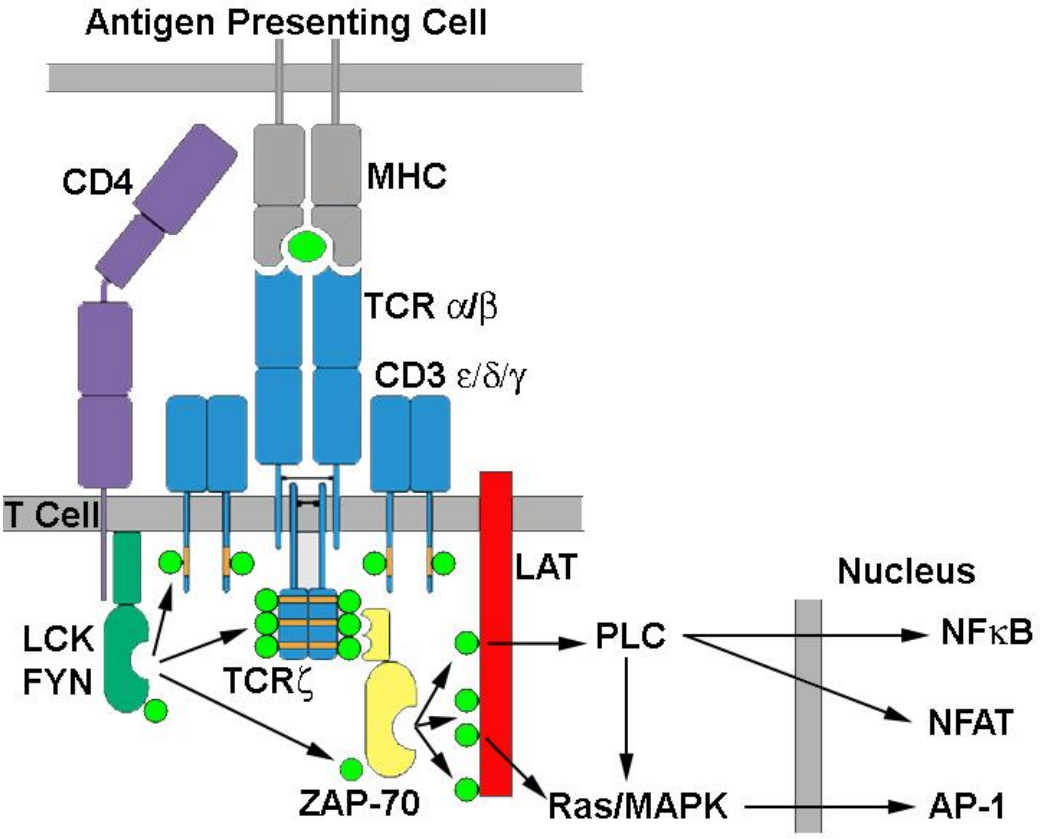

Figure 2 T cell signal transduction overview

The proximal signaling events in T cells that ultimately lead to transcription factor mobilization and synthesis of new gene programs following MHC-peptide recognition are depicted. See text for details. Phosphorylated tyrosine residues are represented by small green circles.

Phospholipase C (PLC) and Grb2 are two important binding partners of LAT, which activate the Ca^{2+}/Protein Kinase C and Ras-MAPK pathways, respectively. These signaling pathways ultimately result in the nuclear mobilization of the transcription factors NFAT, NF-κB, and AP-1 (Fig 2) [13]. The transcription of new gene programs that result in cytokine secretion, cytokine receptor expression, cell division, and effector cell differentiation are driven by these transcription factors.

This signaling machinery is required for both peripheral T cell activation and T cell development in the thymus [7,13]. Hematopoiesis begins in the bone marrow, where self-renewing hematopoietic stem cells proliferate and divide into precursors of the

myeloid and lymphoid lineages. Multipotent progenitor cells migrate from the bone marrow to the thymus, where these most recent thymic immigrants are termed double-negative (DN)-1 cells, as they do not express either the CD4 or CD8 coreceptors. These DN1 cells progress through three additional DN stages (DN2-4), which are defined based upon expression of CD44 and CD25. TCRβ locus recombination occurs during the DN3 stage, and a productive rearrangement generates signals, emanating from this rearranged β chain paired with a surrogate α chain, that are required for expansion and advancement to the DN4 stage. Thymocytes then progress into the double positive (DP) stage, initiating expression of both CD4 and CD8. At the DP stage, TCRα gene rearrangement results in cell surface expression of the mature TCR heterodimer. T cells that express a TCR with affinity for self MHC-peptide complexes receive survival signals in positive selection. However, in negative selection, T cells expressing a TCR with high affinity for self MHC-self peptide receive signals resulting in apoptosis. These selection steps ensure that T cells exiting into the periphery will be capable of generating responses to foreign, but not self, antigens, in a process designated central tolerance. Positive selection mediated by antigen presented by MHC Class II will result in loss of CD8 from the surface of the DP thymocyte to generate CD4+CD8- single-positive (SP) thymocytes, whereas selection on antigen presented in the context of MHC Class I will result in loss of CD4 from the cell surface to generate CD8+CD4- SP thymocytes. These fully differentiated thymocytes subsequently exit the thymus to initiate surveillance in the periphery. Mature T cells circulate throughout the tissues and following activation, CD4 T cells differentiate into T helper cells and CD8 T cells differentiate into cytotoxic T cells.

1.3 T cells in Human Disease

A more complete understanding of the molecular mechanisms by which T cells develop and become activated presents new opportunities to treat and prevent a variety of human diseases. Vaccinations have been undeniably successful in decreasing human disease to a diverse subset of pathogens, including smallpox and measles. However, increased knowledge of the immune response can improve current vaccines and provide strategies to develop novel vaccines. Furthermore, the generation of shelf-stable vaccines to be used in developing nations is a major public health goal. Early vaccines were based upon attenuated microorganisms, however acellular vaccines have the potential for increased safety and stability. Improved understanding of how vaccine administration route and the specific cell types activated by a given antigen generate variably effective T cell memory will increase the effectiveness of vaccination.

Cancer is a leading cause of death in developed countries, and increasing life expectancies will only increase the prevalence of cancer in the population. Harnessing the power of T cells for use as immunotherapy for cancer is an opportunity to create a specific and long-lasting anti-tumor immunity. Breaking T cell tolerance to tumors, generating more immunogenic tumor antigens, and circumventing the immune avoidance mechanisms of tumors remain significant barriers to successful treatment of cancer by T cell immunotherapy.

Two situations in which an immune response develops to innocuous antigens include allergies and graft rejection. Allergies are becoming increasingly common in the industrialized societies, and represent a considerable burden on the health care system. Significant categories of allergic responses include allergic rhinitis caused by inhalation

of environmental allergens such as pollens, food allergies to proteins from nuts and dairy products, and allergic asthma to danders and pollens resulting in airway inflammation, bronichial constriction, and increased mucus production. Allergic responses develop following allergen-mediated activation of mast cells, which release chemokines, cytokines, and lipid mediators. These mast cell products activate APC which further direct the development of an antigen-specific T cell response to allergens. T cells migrate to the effected tissue and direct the late allergic response. Furthermore, T cell memory develops and will continue to result in an immune response to the innocuous allergens upon subsequent antigen exposure.

In transplantation, the immune system recognizes antigens in the graft as foreign and attacks the transplanted organ. This graft rejection is mediated primarily by T cells. Long-term graft survival requires immunosuppressive drugs, which increase the risk of infection and cancer. In allogeneic bone marrow transplantation following radiation therapy to treat leukemia or lymphoma, mature T cells from the graft can attack host tissues, in a process termed graft-versus-host disease (GVHD). Protection against relapse is partially dependent upon a graft-versus-leukemia (GVL) response. T cell depleted bone marrow transplantation removes both the damaging effects of GVHD but also eliminates the beneficial GVL.

Autoimmunity, the adaptive immune response to self, is the third category of an immune response developing to innocuous antigens. Autoimmune diseases include type I diabetes, systemic lupus erythematosus, rheumatoid arthritis, multiple sclerosis, Graves' disease, and autoimmune hemolytic anemia. The chronic nature of many autoimmune disorders is due to the continued presence of self-antigens in the body, which results in

recurrent inflammation and tissue destruction. Both autoantibody production by B cells and T cell cytolytic responses are important for tissue destruction in various autoimmune syndromes.

1.4 Misregulation of T cell Signaling can result in Autoimmunity

The importance of understanding the regulation of TCR signaling is illustrated by the severe autoimmune disorders that result from the altered expression or activity of many T cell signaling molecules. T cell-intrinsic initiation of autoimmunity is thought to occur by at least four independent means [14]. The first is defective negative selection, where autoimmune T cells can enter the periphery if a positive regulator of TCR signal transduction is present at abnormally low levels or is mutated and thus suboptimally active.

A second cause of T cell intrinsic autoimmunity is impaired peripheral tolerance. The term peripheral tolerance refers to the multiple failsafe mechanisms in place to prevent autoimmunity after lymphocytic exit from primary immune tissues. Antigen recognition by T cells in the absence of costimulatory signals results in anergy and later apoptotic death. Defective signal transduction from death receptors can result in the evasion of apoptotic death, ultimately resulting in autoimmunity. The importance of apoptosis in the avoidance of autoimmunity is exemplified by the autoimmune phenotypes of mice and humans with impaired Fas-FasL death receptor signaling, and mice deficient in the proapoptotic Bcl-2 family member Bim [15-19]. Failure of peripheral tolerance can also result in autoimmunity by a less well characterized, and

controversial, mechanism following infection [20]. Pathogen-activated T cells can cross-react with self-tissues, resulting in autoimmunity [21,22].

Thirdly, increased survival signals in positive selection in the thymus or T cell homeostasis in the periphery can result in autoimmunity. Each of these processes requires repeated weak interactions between TCR and MHC-peptide complexes. If signals emanating from the TCR are too strong, for example due to the inactivity or absence of a negative regulatory molecule, increased positive selection in the thymus, or increased survival/homeostatic proliferation in the periphery will result. T cells undergoing homeostatic proliferation show enhanced levels of activation and memory markers, and are therefore more prone to the promotion of autoimmunity via alteration of B cell homeostasis [23,24].

Finally, defective or absent regulatory T cells (T_{reg}) can cause autoimmune disease. *Scurfy* mice and human IPEX patients, each of which lack the transcription factor essential to the development of T_{reg}, reveal the importance of T_{reg} in the avoidance of autoimmunity [25-29]. Absence of T_{reg} results in a failure to restrain the immune response, leading to the induction of inflammatory bowel disease, type 1 diabetes, eczema, lymphoproliferation, and infiltration of T cells into solid organs [30].

Accordingly, deficiencies or mutations in T cell signal transduction genes are known to confer risk to a wide spectrum of autoimmune disorders [31]. For example, PTEN, SHIP, and Cbl-b function in the signal transduction pathway emanating from the costimulatory receptor CD28 and are required for the avoidance of autoimmunity. CD28 engagement by costimulatory molecules expressed on the surface of APC results in the membrane recruitment of the lipid kinase PI3K. The inositol phospholipid $PI(4,5)P_2$ is

phosphorylated by PI3K to generate PI(3,4,5)P_3, which recruits the guanine nucleotide exchange factor Vav and the serine/threonine kinase AKT to the membrane, resulting in the activation of these signaling intermediates [32]. The consequent activation of further downstream signaling molecules ultimately leads to T cell cytokine production, proliferation, and survival [33]. T cell-specific deletion of the PI(3,4,5)P_3 lipid phosphatase PTEN in mice results in lymphadenopathy, splenomegaly, enlarged thymi, impaired negative selection, defective peripheral tolerance, hyperresponsive peripheral T cells, and CD4+ lymphomas leading to premature death [34,35]. The lipid phosphatase SHIP, which like PTEN dephosphorylates PI(3,4,5)P_3, also has a role in the prevention of autoimmunity, as demonstrated by the more severe phenotype of PTEN-SHIP double-deficient mice as compared to PTEN-only deficient mice [36]. The ubiquitin ligase Cbl-b functions in T cell signaling as a negative regulator of Vav activation. T cells from Cbl-b deficient mice do not require CD28-mediated costimulation to proliferate, and thus develop self-reactive and hyperresponsive T cells, resulting in spontaneous autoimmunity [37,38].

The development of autoimmune disease has also been associated with mutations in the PTP CD45, SHP-1, and PEP, and the transmembrane negative regulator of T cell costimulation, CTLA-4. The specific pathologies resulting from misregulation of these molecules will be discussed in detail in later sections.

1.5 PTP and TCR Signal Transduction

While the role of PTK in TCR signal transduction have been extensively studied, the identity of PTP that regulate this pathway is less clear. T cells express at least 17

classical PTP, including three receptor-like PTP and 14 non-receptor PTP [39]. While PTP are canonically considered negative regulators of TCR signaling, at least one PTP is known to function as positive regulator [40]. CD45, is a transmembrane PTP characterized by hematopoietic-restricted expression and is well-established to dephosphorylate SrcFK [41]. Phosphorylation of SrcFK on a tyrosine near the COOH terminus (Y505 in LCK) is known to result in inactivity of SrcFK as a consequence of binding of phospho-Y505 by the SH2 domain of the protein. This permits SH3 domain interaction with the proline-rich region of SrcFK, ultimately resulting in an intramolecular fold that allosterically inhibits the catalytic domain [42-44]. Dephosphorylation of Y505 by CD45 thus relieves this inhibition and is crucial for the optimal activation of SrcFK [45].

Indeed, CD45-deficient mice provide confirmation of a positive regulatory role for CD45 in TCR signal transduction. These mice exhibit a severe-combined immunodeficiency (SCID) phenotype and nearly completely lack peripheral T and B cells [46]. In these mice, the threshold for positive selection is raised, as evidenced by the failure of thymocytes to develop in weak affinity TCR transgenic systems, where all T cells in the mouse express TCR with affinity to one specific peptide [47]. Human mutations in CD45 have also been shown to result in a SCID phenotype [48,49]. In contrast, T and B cells isolated from $CD45^{E613R}$ knock-in mice exhibit high levels of proliferation and activation, resulting in autoimmune nephritis and premature death of the animals [50]. The $CD45^{E613R}$ mutation promotes constitutive activation of CD45 by inhibition of dimerization [51]. This autoimmunity as a result of CD45 gain of function

mutations is further evidence for the role of CD45 as a positive regulator of T cell signal transduction.

The first PTP established as a physiological negative-regulator of proximal TCR signaling was SHP-1. SHP-1 is predominantly expressed in hematopoietic cells, and shows aberrant expression or activity in mice carrying the *motheaten* or *motheaten-viable* alleles, respectively [52]. The names of these alleles originate from the appearance of homozygous mice, which exhibit patchy hair loss, and differ only in the severity of disease. *Motheaten* mice exhibit severe autoimmune disease as a result of increased numbers of monocytes and neutrophils and infiltration of these cell types into peripheral tissues. This inflammation and tissue damage causes premature death due to hemorrhagic pneumonitis [53]. SHP-1 has been shown to dephosphorylate and inactivate LCK, FYN, and ZAP-70 [54]. Consistent with this mechanism of action, negative regulatory roles for SHP-1 in T cell positive and negative selection, T cell proliferation, and T helper cell differentiation have been described [55,56].

A role for PEST domain-enriched tyrosine phosphatase (PEP) as a negative regulator of TCR signal transduction is also well-established. PEP expression is restricted to the hematopoietic compartment, and has been shown to associate with the inhibitory PTK CSK and dephosphorylate LCK, FYN, and ZAP-70 [57,58]. PEP-deficient mice exhibit enhanced positive selection in both MHC Class I and MHC Class II TCR transgenic systems [59]. Strikingly, while young PEP-deficient mice appear normal, older (4-6 month old) mice develop severe splenomegaly and lymphadenopathy, resulting primarily from an increased number of effector/memory T cells [59]. Accordingly, while TCR signal transduction pathways appear intact in naïve T cells from

these mice, effector/memory T cells exhibit enhanced and sustained phosphorylation of LCK^{Y394}, the autoregulatory tyrosine residue. Interestingly, gain of function mutations in human patients, PEP^{R620W}, also result in generalized autoimmunity [60,61]. These mutations are associated with a wide variety of autoimmune phenotypes, including type 1 diabetes, rheumatoid arthritis, systemic lupus erythematosus, and Graves' disease.

A delicate balance of kinase and phosphatase activity is required for normal T cell signal transduction. Therefore, a more detailed understanding of the molecular pathways that regulate T cell activation might result in the development of novel treatment regimens for disorders in which T cells figure prominently. In this body of work, we specifically sought to define a role for additional PTP in the regulation of TCR signal transduction, since the role of PTP in this process is significantly less well known than that for PTK. For example, while the molecules that phosphorylate the ITAMs of CD3 and TCRζ and the adapter protein LAT have been known for more than ten years, the PTP that dephosphorylate these molecules, to prevent continuous TCR signals and thus uncontrolled T cell development and/or activation, are completely unknown.

1.6 Do PTPN3 and PTPN4 Regulate TCR Signal Transduction?

PTPN3 and PTPN4 have been recently implicated in negative regulation of TCR signal transduction [62,63]. In mice, these PTP are 50% identical and 67% homologous at the amino acid level. They consist of an NH_2-terminal FERM (band 4.1, Ezrin, Radixin, and Moesin) domain, a central PDZ (PSD-95, Dlg, ZO-1) domain, and a COOH-terminal PTP domain. FERM and PDZ domains bind the cytosolic domain of transmembrane proteins [64-66]. Both domains have also been shown to bind directly to

the phospholipid $PI(4,5)P_2$ [67,68]. The FERM domains of PTPN3 and PTPN4 are required for PTP membrane localization in T cells [69].

A screen in the Jurkat T cell leukemia line seeking to identify candidate negative regulators of TCR signal transduction performed by Tomas Mustelin's group revealed that over-expression of PTPN3 and PTPN4 resulted in an approximate 75% and 40% reduction, respectively, of TCR-induced activation of the promoter for the T cell growth-promoting cytokine, IL-2 [70]. Mutation of the catalytic cysteine residue or expression of a FERM domain-deleted form of these PTP abrogated this inhibitory effect, illustrating the importance of enzymatic activity and protein localization [69,70]. This screen provided the primary rationale for determining the role of PTPN3 and PTPN4 in TCR signal transduction. Both overexpression of PTPN3 and PTPN4 inhibited IL-2 promoter activity to a greater extent than SHP-1, which at the time this screen was completed was the only PTP for which a physiological role in TCR signaling was known. PTPN3 overexpression resulted in the second strongest inhibition, with only PEP inhibiting IL-2 promoter activity to a greater extent. PEP would, soon after the onset of our work, be definitively determined a potent physiological negative regulator of TCR signal transduction [59].

Following the beginning of our efforts to determine the physiological role of PTPN3 and PTPN4 in TCR signal transduction, a mechanism for the proposed inhibition by PTPN3 on IL-2 promoter activity was proposed by Nicolai van Oers and colleagues [71]. To determine PTP with the ability to desphosphorylate TCRζ, Jurkat T cells were fractionated, and candidate PTP were immunoblotted to determine their presence in fractions exhibiting TCRζ-dephosphorylating activity. PTPN3 was one of only two PTP

found in the appropriate fractions. Further experiments on derivatives of PTP domains termed substrate traps, due to the replacement of an invariant aspartic acid residue to severely slow catalysis, revealed PTPN3 as the only PTP of 47 tested to bind TCRζ *in vitro*. Catalytically-active PTPN3 purified from insect cells was also shown to dephosphorylate TCRζ *in vitro.* Furthermore, overexpression of PTPN3 in COS fibroblasts transfected to express phosphorylated TCRζ revealed desphosphorylation of TCRζ compared to empty vector-expressing cells [71]. Recently, a PTPN4 substrate trap has similarly been shown to bind TCRζ *in vitro*, while catalytically-active PTPN4 dephosphorylated TCRζ *in vitro* [72]. In this second study PTPN4 has also been shown to dephosphorylate TCRζ when overexpressed in 293T cells [72]. These experiments generated considerable excitement about the role of PTPN3 and PTPN4 in TCR signaling. Chapters 2 and 3 directly test the hypothesis that PTPN3 and PTPN4 are physiological negative regulators in TCR signal transduction [73,74].

1.7 SHP-2: PTP with Multiple Functions

The ubiquitously expressed PTP SHP-2 is highly related to the first and best characterized PTP regulator of T cell signal transduction, SHP-1. SHP-2 contains a COOH-terminal PTP domain and NH_2-terminal tandem Src-homology 2 (SH2) domains, which bind phosphorylated tyrosine residues. SHP-2 deficient mice fail to survive beyond embryonic day 10 due to defective gastrulation, at least partially due to suboptimal and greatly shortened fibroblast growth factor (FGF)-induced MAPK activation [75]. In the absence of a viable mouse model of SHP-2 deficiency, biochemical experiments described many binding partners for SHP-2 and implicated

SHP-2 in a myriad of cellular signaling pathways. The relevance of many of these binding partners and pathways to the physiological functions of SHP-2 remains unclear.

More recently, a flanked-by-*loxp* (floxed) allele of SHP-2 has been developed to circumvent the embryonic lethality of the complete knockout allele [76]. As the Cre recombinase specifically splices out of the genome sequences between *loxp* sites, crossing mice carrying the SHP-2 floxed allele to mice expressing Cre expressed from tissue-specific promoters can define the role of SHP-2 in individual cell types or tissues. This conditional deletion of SHP-2 in mice has led to a clearer understanding of the role of SHP-2 in many different tissues and corresponding cellular signaling pathways. Accordingly, these recently described physiologically relevant roles for SHP-2 are summarized below.

The role of SHP-2 in growth factor signal transduction, originally demonstrated in complete SHP-2 knockout mice, has been verified in tissue-specific knockout mice. In neural stem/progenitor cell (NSC)-specific deletion of SHP-2, NSC exhibited decreased proliferation in response to FGF signals, with defective activation of the mitogen activated protein kinase (MAPK) ERK and reduced activation of the transcription factor c-Myc. This impaired proliferation of NSC coupled with reduced differentiation into neurons results in early postnatal lethality [77]. Furthermore, ERK activation was abrogated in cardiac myocyte-specific deletion of SHP-2, indicating roles for SHP-2 in signal transduction from insulin-like growth factor-1 (IGF-1), and epidermal growth factor (EGF) [78]. Finally, involvement of SHP-2 in EGF and hepatocyte growth factor signaling was shown in liver-specific knockout mice, in the context of liver regeneration following partial hepatectomy. In these mice, a SHP-2-Gab1 complex was shown

required for activation of ERK and the downstream expression of the transcription factors c-Fos, c-Jun, c-Myc, and the cyclins A, E, and B1 [79].

SHP-2-mediated regulation of hormone receptor signal transduction has been shown in three mouse models. First, deletion of SHP-2 from postmitotic CNS neurons results in obesity in mice, due to leptin receptor-mediated disregulation of metabolism in the hypothalamus [76]. In wild-type neurons, leptin signals stimulate a metabolic response, however, in SHP-2 deficient neurons, leptin signals fail to activate ERK. Second, mammary gland-specific deletion of SHP-2 revealed a role for SHP-2 in positive regulation of prolactin-stimulated STAT5 activation, and negative regulation of STAT3-inducing signals [80]. Finally, striated muscle-specific knockout of SHP-2 leads to defective insulin-induced glucose uptake in cardiac myocytes and skeletal muscle cells as a result of attenuated ERK activation [81].

A definitive role for SHP-2 in T cell signaling has remained elusive. SHP-2 has, however, been long proposed to be the effector molecule of inhibitory surface receptors, and has recently been implicated in positive regulation of TCR signal transduction.

1.7.1 SHP-2 in T cell Inhibitory Receptor Signaling

SHP-2 has been shown to associate with a number of T cell inhibitory receptors, including CTLA-4, PD-1, BTLA-1, CEACAM-1, and CD31 [40,82-84]. CTLA-4-mediated inhibition of the CD28 costimulation pathway has led CTLA-4 to be the most well-characterized of the T cell inhibitory receptors. Expression of CTLA-4 is induced following T cell activation and CTLA-4 competes with CD28 to bind B7 molecules on APC [85]. CTLA-4 binds B7 with higher affinity than does CD28, limiting the costimulatory signal delivered by CD28, and additionally transduces a negative signal to

limit T cell proliferation. The phenotype of CTLA-4 deficient mice provides evidence for a CTLA-4-mediated physiological role in limiting T cell expansion [86,87]. Within a week after birth, T cells from these mice express activation markers, proliferate, and infiltrate into tissues, resulting in death by one month of age. A role for CTLA-4 in maintenance of peripheral tolerance is furthered by the genetic association studies which have found numerous links between CTLA-4 single-nucleotide polymorphisms (SNPs) and many autoimmune diseases in humans [85].

The intracellular tail of CTLA-4 is required for transduction of the negative regulatory signal, and SHP-2 is co-immunoprecipitated with the CTLA-4 tail [82]. A complex between CTLA-4, SHP-2, and TCRζ can also be detected by immunoprecipitation [88]. The association of SHP-2 with CTLA-4 and TCRζ has led to the hypothesis that SHP-2 is the effector molecule of CTLA-4, acting to dephosphorylate the ITAMs of TCRζ [89,90].

1.7.2 A role for SHP-2 in TCR Signaling

Following the generation of a conditional SHP-2 allele, the hypothesis that SHP-2 is the effector molecule for inhibitory receptors like CTLA-4 and PD-1 could be directly tested by SHP-2 gene ablation restricted to the T cell compartment. SHP-2 deletion mediated by LCK-Cre instead revealed a role for SHP-2 as a positive regulator of pre-TCR signaling [91].

SHP-2 fl/fl LCK-Cre mice exhibit a decreased number of thymocytes and higher percentages of DN thymocytes. Further investigation into this phenotype revealed altered ratios of DN4/DN3 cells, indicating that SHP-2 is required for optimal pre-TCR signal transduction at the DN3-DN4 checkpoint. The precise mechanism for the role of SHP-2

has yet to be determined, but ERK was shown to be inefficiently phosphorylated in SHP-2 deficient thymocytes in response to simulated TCR signals. Studies of mature peripheral T cells isolated from these mice suggest SHP-2 is a positive regulator of TCR signal transduction in mature T cells as well. However these experiments remain inconclusive, due to the possibility that altered T cell development in the thymus results in this peripheral phenotype.

We attempted to directly address the role of SHP-2 in positive and negative selection by the generation of SHP-2 fl/fl CD4-Cre mice. We also sought to determine the role of SHP-2 in mature T cells, utilizing the recently developed ERT2-Cre transgene [92]. Adult SHP-2 fl/fl ERT2-Cre mice were injected with tamoxifen with the expectation that SHP-2 would be deleted from not only peripheral T cells, but all tissues. In the course of these experiments, we have identified a variety of unexpected phenotypes, including a block in hematopoiesis, skin dysplasia, and skeletal malformations. These studies are described in detail in chapter 4.

Chapter 2: Normal TCR Signal Transduction in Mice that Lack Catalytically-active PTPN3 Protein Tyrosine Phosphatase

2.1 Abstract

PTPN3 (PTPH1) is a cytoskeletal protein tyrosine phosphatase that has been implicated as a negative-regulator of early TCR signal transduction and T cell activation. To determine if PTPN3 functions as a physiological negative-regulator of TCR signaling in primary T cells we generated gene-trapped and gene-targeted mouse strains that lack expression of catalytically-active PTPN3. PTPN3 phosphatase-negative mice were born in expected Mendelian ratios and exhibited normal growth and development. Furthermore, numbers and ratios of T cells in primary and secondary lymphoid organs were unaffected by the PTPN3 mutations and there were no signs of spontaneous T cell activation in the mutant mice with increasing age. TCR-induced signal transduction, cytokine production and proliferation was normal in PTPN3 phosphatase-negative mice. This was observed using both quiescent T cells and recently-stimulated T cells where expression of PTPN3 is substantially up-regulated. We conclude, therefore, that the phosphatase activity of PTPN3 is dispensable for negative-regulation of TCR signal transduction and T cell activation.

2.2 Introduction

T cells recognize peptide fragments of foreign antigens together with self MHC molecules displayed on the surface of APC [93]. This specific recognition is achieved through a clonally-distributed, cell surface-expressed TCR. In quiescent T cells, TCR binding to peptide-MHC induces T cell cytokine synthesis, proliferation and differentiation into effector cells that aid in the elimination of antigen from the host.

Over the past two decades much has been learned of the intracellular signaling pathways that emanate from the TCR which instruct T cell responses [94-97]. One of the first events after TCR engagement is activation of the SrcFK, LCK and FYN. The precise mechanism by which these PTK become activated is uncertain but is likely to involve locally-induced PTK aggregation, PTK-interacting adapter proteins and the CD45 PTP [9,98-100]. Directly or indirectly these events lead to phosphorylation of a positive-regulatory tyrosine contained in the kinase domain of the PTK which results in increased kinase activity. Upon activation, SrcFK phosphorylate tyrosine residues contained in ITAMs located in the cytoplasmic tails of TCR signaling chains such as TCRζ. The phosphorylated ITAMs are then recognized by the Src homology-2 domains of the Syk-family PTK, ZAP-70, which is thus recruited to the TCR signaling complex and activated, in part through transphosphorylation by SrcFK [12]. Activated ZAP-70 phosphorylates the LAT transmembrane adapter protein which couples the TCR to the activation of transcription factors such as AP1, NFκB and NFAT [95]. Together, these transcription factors initiate new programs of gene expression that orchestrate T cell responses [94-97].

While much is known of the TCR-induced membrane-proximal signaling events that promote T cell activation, less information is available on the mechanisms by which these events are negatively-regulated. Strong candidate negative-regulators are PTPs which have the capacity to impede signaling by dephosphorylating positive-regulatory tyrosine residues in different signaling proteins. Of the approximately 65 PTPs that are expressed in T cells, several have thus far been implicated as negative-regulators of proximal TCR signaling [1,69,101]. Included amongst these is SHP-1 and PEP which have been shown to dephosphorylate and inactivate LCK (SHP-1 and PEP) and ZAP-70 (SHP-1). Studies of SHP-1- and PEP-deficient mice support the contention that both PTPs are significant negative-regulators of proximal TCR signaling [59,102,103].

Another PTP that has been proposed to function as an attenuator of early TCR signaling is PTPN3 (also known as PTPH1 in humans) [62]. PTPN3 comprises of an NH_2-terminal FERM domain, a central PDZ domain, and a COOH-terminal PTP domain. Over-expression of PTPN3 in the Jurkat T cell leukemia cell line profoundly inhibits TCR signal transduction leading to activation of the promoter for the T cell growth-promoting cytokine, IL-2 [69,70]. Furthermore, a FERM domain-deleted mutant of PTPN3 is impaired in its ability to inhibit TCR-induced IL-2 promoter activity coincident with an inability of this mutant to localize to the plasma membrane [70]. This finding suggests that PTPN3 inhibits TCR signaling in Jurkat by dephosphorylating a plasma membrane-localized substrate. A recent study indicates that one important target of PTPN3 is the TCRζ chain. In this regard, PTPN3 was identified as the only PTP from a large tested panel of recombinant PTPs that is capable of interacting physically with TCRζ and dephosphorylating TCRζ ITAMs *in vitro* [71]. In addition, using an unbiased

biochemical fractionation approach, PTPN3 and SHP-1 were identified as essentially the only PTPs expressed in Jurkat that are able to dephosphorylate TCRζ [71]. Together with the finding that PTPN3 dephosphorylates TCRζ when both are transfected into COS-7 cells, these studies have contributed to the notion that PTPN3 acts a negative-regulator of TCR signaling by dephosphorylating the TCRζ chain.

To ascertain whether PTPN3 acts as a physiological negative-regulator in T cells, we have generated two different strains of mice that do not express catalytically-active PTPN3. T cell development, activation and TCR signal transduction have each been investigated in these mice.

2.3 Materials and Methods

2.3.1 Generation of PTPN3-deficient mice

PTPN3 PTP domain-negative (PTPN3 ΔPTP) gene-trapped mice were generated from gene-trapped 129P2/Ola Hsd E14Tg2a.4 embryonic stem (ES) cell lines (RRR012, RRR573 and RRS555) purchased from BayGenomics. The position of the gene-trap within the *Ptpn3* locus was determined by sequencing of PCR products generated from genomic DNA template using *Ptpn3* and targeting vector-based primers. In all three ES cell lines, the gene-trap is located within exon 27, and for two of the ES cell lines (RRR012 and RRR573) the insertion is in the identical position (further details can be provided upon request). The three new *Ptpn3* alleles are referred to as $Ptpn3^{RRR012PdK}$, $Ptpn3^{RRR573PdK}$ and $Ptpn3^{RRS555PdK}$. ES cells were injected into C57BL/6J x (C57BL/6J x DBA/2) blastocysts to generate chimeras which were bred with C57BL/6J mice to achieve germline transmission of the trapped alleles. Experiments were performed with

littermate F2 animals generated from the intercross of C57BL/6J x 129P2 Ola Hsd$^{+/Ptpn3\ \Delta PTP}$ F1 mice.

A targeting vector for the generation of *Ptpn3* gene-targeted mice was constructed by inserting genomic DNA fragments from a *Ptpn3* genomic BAC clone into p-*loxP*-2FRT-PGKneo. Exon 27 was thus flanked by *loxP* sites, with the neomycin resistance (*NeoR*) selection cassette (flanked by *FRT* sites) inserted into intron 27 (Fig 7, further details available upon request). Linearized vector was electroporated into the Bruce4 ES cell line of C57BL/6J origin [104]. Correctly targeted ES cell clones were identified by Southern blotting and injected into C57BL/6J Tyr$^{c\text{-}2J/c\text{-}2J}$ blastocysts. Resultant chimeras were then bred to C57BL/6J Tyr$^{c\text{-}2J/c\text{-}2J}$ mice to achieve germline transmission of the targeted *Ptpn3*^{tm1PdK} allele. Heterozygotes were intercrossed to generate homozygote *Ptpn3*^{tm1PdK} animals and littermate controls.

Unless otherwise noted, all mice were 6-8 weeks of age at the time of experimentation. All experiments were performed in compliance with University of Michigan guidelines and were approved by the University Committee on the Use and Care of Animals.

2.3.2 Genotyping

Genomic DNA from ES cell clones or tail biopsies was digested overnight with restriction enzymes, run on 0.5% agarose/TAE gels and transferred to positively-charged nylon membranes (Ambion) for Southern blotting. Probes were generated by PCR from a *Ptpn3* genomic BAC and ^{32}P-labeled by random priming. Following overnight hybridization, membranes were washed under high stringency conditions and exposed to film. In some experiments, the genotype of F1 mice generated from crosses of

heterozygote *Ptpn3*^{tm1PdK} mice was determined by PCR of tail genomic DNA. Forward and reverse primers for the detection of the wild-type *Ptpn3* allele were based at the beginning of exon 27 and the end of exon 28 respectively and generate a 770 bp product from the wild-type allele (a product of greater than 3 kb might also be generated from the targeted allele under optimal conditions). Primers for the detection of the targeted allele are based within the *NeoR* gene and generate a product of 330 bp (see Fig 7).

2.3.3 Flow cytometry

Splenocytes and thymocytes were blocked with murine IgG (Sigma) and then stained with the following conjugated monoclonal antibodies (BD Biosciences): H57-597-CyChrome (TCRβ chain), RA3-6B2-PE (CD45R/B220), H1.2F3-FITC (CD69), IM7-FITC (CD44), MEL-14-biotin (CD62L), GK1.5-PE and H129.19-CyChrome (CD4), 53-6.7-CyChrome (CD8) and PC61-PE (CD25). Cell staining was analyzed by flow cytometry using a FACScan (Becton Dickinson).

2.3.4 T cell cytokine production and proliferation

Splenocytes were stimulated with varying amounts of 145-2C11 (CD3ε; eBioscience) and 0.5 μg/mL 37.51 (CD28; BD Biosciences) or with varying amounts of staphylococcal enterotoxin B (SEB) in 96 well round-bottom plates in complete medium (RPMI supplemented with 10% FCS, 25 nM β–Mercaptoethanol, 50 U/mL Penicillin, 50 mg/mL Streptomycin, and 2 mM L-glutamine). Concentrations of cytokines in culture supernatant were determined by ELISA after 24-48 h of culture. To assess T cell proliferation, splenocyte cultures were first labeled with 1 μM CFSE (Molecular Probes). After 72-96 h, CFSE fluorescence intensity was analyzed by flow cytometry.

In some experiments recently-stimulated T cells were used. For this purpose, splenocytes were first activated with 0.5 μg/mL anti-CD3 and anti-CD28 in complete medium in 6 well plates. After 48 h, recombinant human IL-2 (10 U/mL) was added and cells were cultured for a further 48 h. Flow cytometric analysis showed these cells were >98% TCRβ+. These activated T cells were then restimulated using identical conditions as above for analysis of cytokine production and proliferation.

2.3.5 Western blotting and co-immunoprecipitation

Thymocytes, lymph node (LN) T cells or recently-stimulated splenic T cells were activated by incubation on ice with anti-CD3 and anti-CD28 antibodies (each 0.2 $\mu g/10^6$ cells) followed by cross-linking with anti-Armenian hamster IgG (0.5 $\mu g/10^6$ cells; Jackson Immunoresearch) at 37^{o}C for the indicated times. Cells were then lysed in 1% NP-40, 0.5% n-Dodecyl-β-D-maltoside buffer. For analysis of protein tyrosine phosphorylation, lysates were run on SDS-PAGE gels and transferred to PVDF membranes (Perkin Elmer). Membranes were then probed with an anti-phosphotyrosine antibody (PY99; Santa Cruz) before stripping and reprobing with an ERK-2 antibody (C-14; Santa Cruz) to determine equal loading. To ascertain the extent of TCRζ phosphorylation, ZAP-70 was immunoprecipitated from lysates using a ZAP-70 antibody (99F2; Cell Signaling). Coimmunoprecipitated tyrosine-phosphorylated TCRζ was then detected by Western blotting using an anti-phosphotyrosine antibody as above.

In separate experiments, expression of PTPN3 in whole brain lysates and purified unstimulated and recently-activated splenic CD4 and CD8 T cells (purified by negative selection) was determined by Western blotting using a PTPN3 monoclonal antibody. This antibody was produced by immunization of mice with a human PTPN3 peptide

(residues 392-503) corresponding to the PDZ domain. T cell blots were reprobed with a control HePTP antibody [105].

2.4 Results

2.4.1 Generation of PTPN3 ΔPTP gene-trapped mice

Three independent *Ptpn3* gene-trapped murine ES cell clones of 129P2/Ola Hsd strain origin (RRR012, RRR573 and RRS555) were obtained from the BayGenomics gene trap resource. Data from 5' RACE experiments provided by the resource indicated that in *Ptpn3* RNA transcripts from these cell lines, *Ptpn3* exon 26 is spliced to the splice acceptor upstream of the *βgeo* sequence of the gene trap. Therefore, since exon 27 of the *Ptpn3* gene encodes the nucleophilic cysteine residue of the PTPN3 PTP domain, such transcripts would direct the expression of a PTPN3 protein that completely lacks catalytic activity (Fig 3A). Southern blotting analysis of genomic DNA prepared from the ES cell clones confirmed that in each case the gene-trap was inserted into the *Ptpn3* locus downstream of exon 26 (Fig 3B, C). To determine the precise position of the gene trap we performed PCRs upon genomic DNA using primers based within the gene trap together with primers based within the *Ptpn3* genomic locus. Sequencing of the PCR products revealed that for each cell line the gene trap was inserted within exon 27. Furthermore, for two of the cell lines (RRR012 and RRR573) the gene trap was inserted in the same position. The location of the gene trap within exon 27 (rather than intron 26) eliminates the possibility that any catalytically-active PTPN3 protein could be produced in these cell lines (or animals derived from them) as a result of RNA splicing.

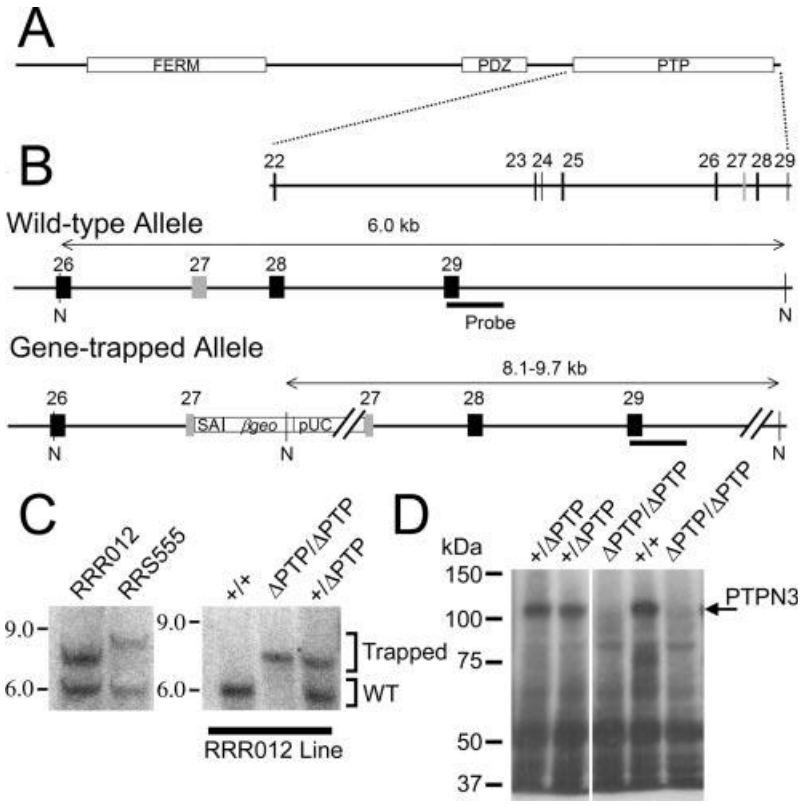

Figure 3 Generation of gene-trapped PTPN3 ΔPTP mice

A) Domain organization of PTPN3 and exon/intron organization of the *Ptpn3* locus corresponding to the PTP domain. Exon 27 encodes the nucleophilic cysteine residue of the PTP active site. B) Representation of wild-type and gene-trapped *Ptpn3* alleles showing *Nco*I (N) restriction sites and probe used in Southern blotting. Gene traps are located within exon 27 of the *Ptpn3* gene (see *Results* for details). SA, splice acceptor; β*geo*, sequence encoding a β-galactosidase-neomycin phospho-transferase fusion; pUC, cloning vector component of gene trap. C) Southern blot of *Nco*I-digested genomic DNA from two independent *Ptpn3* gene-trapped ES cell clones (*left*) and tail DNA from progeny of F_1 mice generated from one of the ES cell clones (RRR012) (*right*). Positions of bands from wild-type (WT) and gene-trapped alleles are indicated. D) Western blot of whole brain lysates from homozygote PTPN3 ΔPTP mice and littermate controls using a PTPN3 mAb. Note the absence of a 110-kDa PTPN3 Ab-reactive band in homozygotes which represents catalytically active PTPN3.

Ptpn3 gene-trapped ES cell lines were used to produce chimeric mice which were then bred with C57BL/6J mice to generate (C57BL/6 x 129P2/Ola Hsd) F1 mice that carried the gene-trapped allele (*Ptpn3*^{RRR012PdK}, *Ptpn3*^{RRR573PdK} or *Ptpn3*^{RRS555PdK}). These F1 mice were then intercrossed to generate homozygote PTPN3 ΔPTP F2 mice plus heterozygote and wild-type littermate controls (Fig. 3C). Mice of the three different genotypes were born in ratios that are in accordance with Mendelian inheritance and for

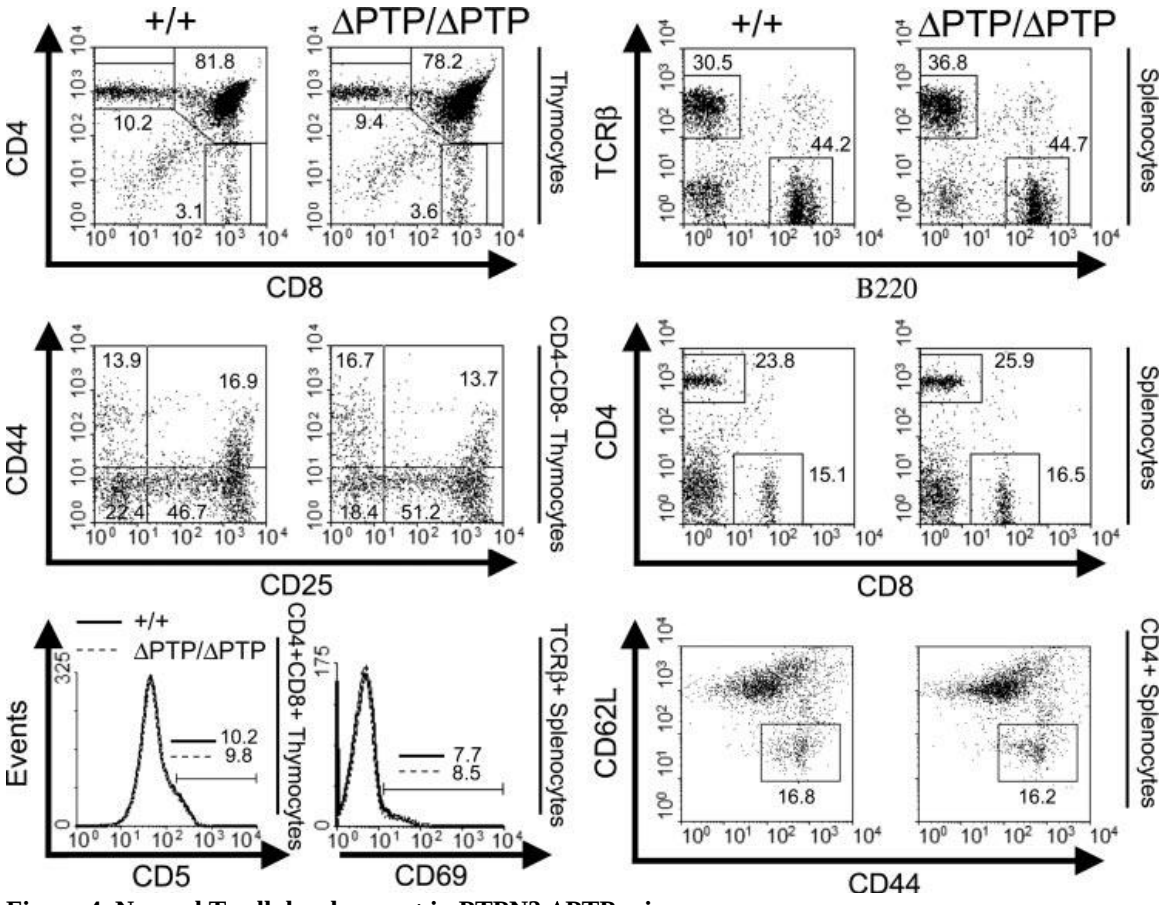

Figure 4 Normal T cell development in PTPN3 ΔPTP mice.

Depicted are flow cytometry plots of thymocytes and splenocytes from homozygote PTPN3 ΔPTP mice and littermate wild-type controls showing expression of the indicated markers on the indicated live cell populations. Percentages of cells that fall within the designated regions of dot plots and percentages of cells that are positive for marker expression in histograms are shown. In CD44/CD62L plots, the boxed population represents $CD44^{hi}CD62L^{lo}$ recently activated memory cells. Data are representative of five repeat experiments.

PTPN3 ΔPTP heterozygotes and homozygotes no obvious effects of the mutation upon growth or development were observed.

2.4.2 T cell development and homeostasis in PTPN3 ΔPTP mice

To determine if the PTPN3 ΔPTP mutation affected T cell development or peripheral T cell homeostasis, numbers and ratios of T cell subsets in thymus and secondary lymphoid organs of 6-8 week old mice were examined. In thymus, numbers and ratios of CD4- CD8- double-negative (DN), CD4+CD8+ double-positive and

CD4+CD8- or CD4-CD8+ single-positive thymocytes were similar between homozygote PTPN3 ΔPTP and wild- type mice (Fig 4 and data not shown). Furthermore, levels of expression of CD5 upon DP thymocytes were the same between the two groups of mice which is consistent with the view that there is no hyper-activation of this subset and no increase in the efficiency of positive selection. Amongst DN thymocytes, ratios of CD44+CD25- (DN1), CD44+CD25+ (DN2), $CD44^{lo}$CD25+ (DN3) and CD44-CD25- (DN4) thymocytes were the same between the two groups of mice (Fig 4). In spleen and LN, the number of T cells, their ratio to non-T cells and ratio of CD4+ to CD8+ T cells was unaffected in the homozygote PTPN3 ΔPTP mice (Fig 4 and data not shown). Also, there was no evidence of previous or ongoing spontaneous activation of peripheral T cells in homozygote PTPN3 ΔPTP mice as judged by expression of the CD44, CD62L and CD69 markers (Fig 4). Apart from T cells, numbers and ratios of other lymphoid populations including B cells, NK cells, macrophages, dendritic cells and granulocytes were all found to be normal in homozygote PTPN3 ΔPTP mice (Fig 4 and data not shown).

2.4.3 T cell cytokine production and proliferation in PTPN3 ΔPTP mice

We examined the ability of T cells from PTPN3 ΔPTP mice to synthesize cytokines and proliferate in response to TCR stimulation. Should PTPN3 normally function as a negative-regulator of TCR signaling, then it might be expected that PTPN3 ΔPTP T cells would synthesize increased quantities of cytokines and proliferate to a greater extent than wild-type T cells. To examine this, splenocytes from homozygous PTPN3 ΔPTP mice and wild-type controls were stimulated with a CD3 antibody (directed to the TCR complex) plus an antibody against the CD28 T cell costimulatory receptor *in*

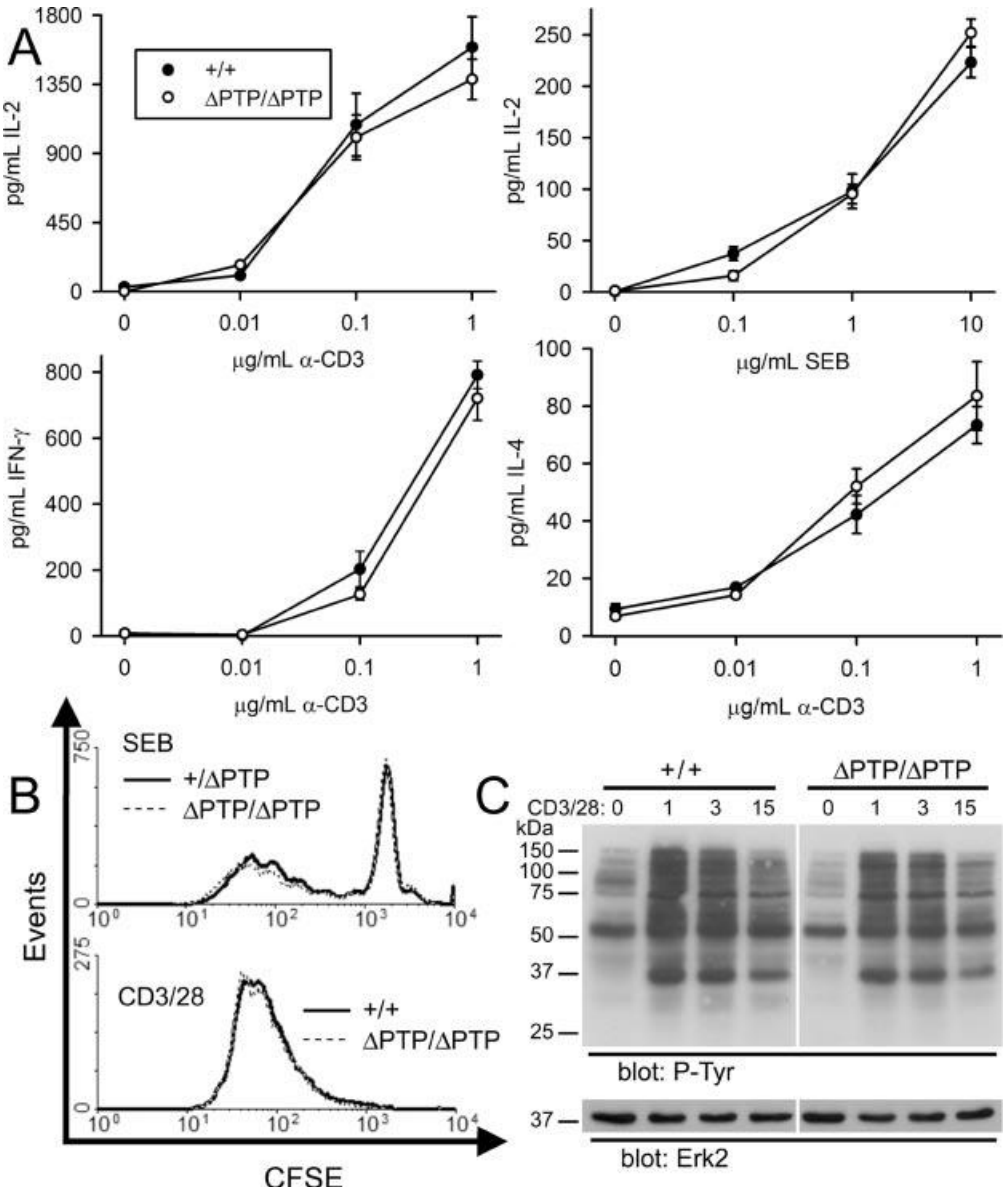

Figure 5 Normal T cell function and TCR signal transduction in PTPN3 ΔPTP mice

A) Whole splenocytes were stimulated with the indicated concentrations of CD3 Ab and 0.5 μg/ml of a CD28 Ab or with the indicated concentrations of SEB. Culture supernatant concentrations of IL-2 (at 24 and 48 h for CD3/CD28 and SEB stimulation, respectively) and IFN-γ and IL-4 (at 48 h) were determined by ELISA. Shown are means +/- 1 SD of triplicate determinations. Similar results were obtained in five repeat experiments. B) Whole splenocyte cultures were labeled with CFSE and stimulated with CD3 (1 μg/ml) and CD28 (0.5 μg/ml) Abs or with SEB (10 μg/ml). CFSE fluorescence intensity was measured after 72 h (CD3/CD28) or 96 h (SEB) by flow cytometry. Shown are representative experiments of three repeats. C) LN T cells were stimulated with CD3 and CD28 Abs for the indicated times in minutes. Protein tyrosine phosphorylation was then assessed by Western blotting of whole cell lysates using an anti-phosphotyrosine Ab. Blots were reprobed with an ERK2 Ab to verify equal loading.

vitro. Alternatively, splenocytes were stimulated with the superantigen, SEB. Concentrations of the cytokines IL-2, IFN-γ and IL-4 in culture supernatants were then determined after 1-2 days of culture. To measure T cell proliferation, similar cultures were initiated only cells were labeled with CFSE beforehand. Dilution of CFSE fluorescence after 3-4 days of culture was then assessed and taken as an indication of the extent of proliferation. As shown, T cells from homozygous PTPN3 ΔPTP mice synthesized similar quantities of IL-2, IFN-γ and IL-4 as T cells from wild-type littermate mice when stimulated with CD3/CD28 antibodies (Fig 5A). Similarly, PTPN3 ΔPTP T cells synthesized comparable amounts of IL-2 (Fig 5A) and IFN-γ and IL-4 (not shown) in response to SEB. In addition, the ability of T cells to proliferate to CD3/CD28 antibody or SEB in these *in vitro* cultures was comparable between the two groups of mice (Fig 5B).

2.4.4 T cell cytokine production and proliferation of re-stimulated PTPN3 ΔPTP T cells

Resting peripheral T cells express PTPN3 at only low levels [69,70]. However, we observed that PTPN3 was expressed at substantially higher levels in wild-type T cells after 2-3 days stimulation with CD3/CD28 antibodies and that these elevated levels of expression were maintained following several days of culture in IL-2 (Fig 6). Therefore, we considered the possibility that PTPN3 may function as a more significant negative-regulator in recently-stimulated T cells. To examine this, CD3/CD28-activated splenic T cells were grown in IL-2 for 2 days and then re-stimulated with CD3 and CD28 antibodies. Cytokine secretion and proliferation was then measured as before. However, despite the elevated expression levels of PTPN3, recently-stimulated T cells from PTPN3

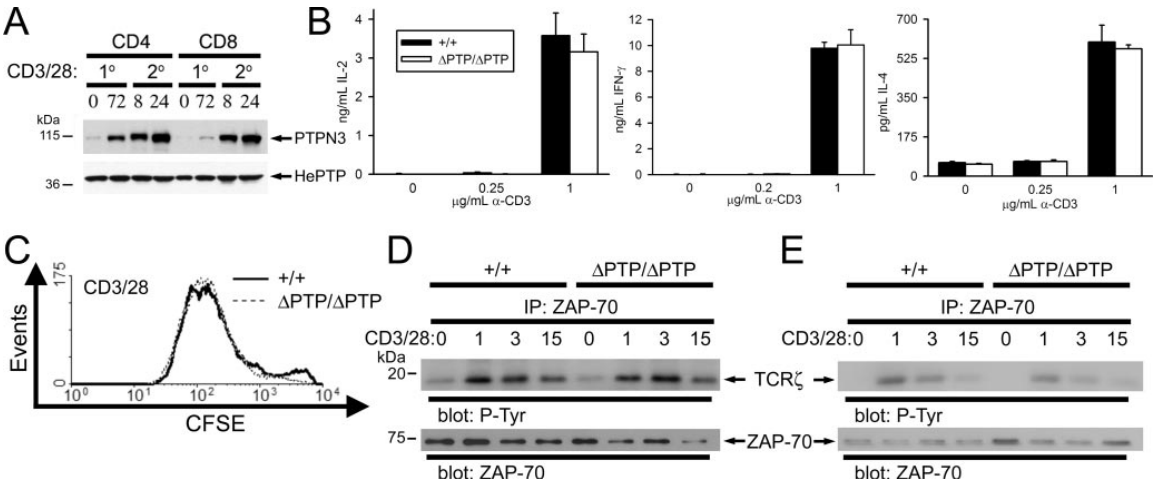

Figure 6 Normal cytokine synthesis, proliferation, and TCR signal transduction in restimulated PTPN3 ΔPTP T cells

A) Purified CD4 and CD8 splenic T cells from C57BL/6 wild-type mice were stimulated with CD3/CD28 Abs (1°) for 72 h and then cultured in IL-2 for a further 48 h. T cells were then restimulated with CD3/CD28 Abs (2°). Aliquots were taken from CD3/CD28-stimulated cultures at the indicated time points (h) and lysed. Expression of PTPN3 was then determined by Western blotting. Blots were stripped and reprobed with a HePTP Ab to show equal loading. B-C) CD3/CD28-induced cytokine synthesis and proliferation of recently activated T cells from homozygote PTPN3 ΔPTP mice and littermate wild-type controls (stimulated with CD3/CD28 Abs for 48 h and IL-2 propagated for a further 48 h) was determined as in Fig 5. Shown are results of representative experiments from five repeats. D) Recently activated T cells were stimulated with Abs to CD3 and CD28 for the indicated times (min) and lysed. Zap70 was then immunoprecipitated from lysates and coimmunoprecipitated tyrosine-phosphorylated TCRζ was detected by Western blotting using a phosphotyrosine Ab. Blots were reprobed with a Zap70 Ab to show equivalent immunoprecipitation of Zap70. E) TCRζ phosphorylation in PTPN3 ΔPTP and littermate control wild-type thymocytes was determined as in D.

ΔPTP mice did not synthesize any greater amounts of IL-2, IFN-γ or IL-4 or proliferate more in response to re-stimulation with CD3/CD28 antibodies compared to recently-stimulated T cells from wild-type mice (Fig 6A-B).

2.4.5 TCR signaling in PTPN3 ΔPTP T cells

PTPN3 has been proposed to function at an early step in the TCR signal transduction cascade acting to dephosphorylate the TCRζ chain [71]. As such it would be predicted that in T cells from PTPN3 ΔPTP mice a number of signaling proteins should become hyper-phosphorylated on tyrosine residues in response to CD3/CD28 stimulation. We examined this by Western blotting using a protein phosphotyrosine-specific antibody. In T cells that had not been recently-stimulated, no increased protein tyrosine

phosphorylation was observed (Fig 5C). Likewise, no increased tyrosine phosphorylation was observed when the same experiments were performed using recently-stimulated T cells (not shown). Using recently-stimulated T cells, we examined TCRζ chain tyrosine-phosphorylation directly. For this purpose, we immunoprecipitated ZAP-70 from T cell lysates and then detected any coimmunoprecipitated tyrosine-phosphorylated TCRζ by Western blotting using a phosphotyrosine antibody as previously described [106]. Results from these experiments showed that TCRζ is tyrosine-phosphorylated and associates with ZAP-70 to a similar degree in homozygote PTPN3 ΔPTP and wild-type T cells (Fig 6D). Similar results were also obtained with thymocytes (Fig 6E).

2.4.6 Generation of PTPN3 gene-targeted mice

To guard against the potential of early embryonic lethality of homozygote PTPN3 ΔPTP mice, we also embarked upon the production of conditional PTPN3 ΔPTP mutant mice. To this end, we used the technique of homologous recombination to generate *Ptpn3* gene-targeted clones in the Bruce4 ES cell line of C57BL/6J origin (Fig 5*A*). Several correctly-targeted clones were produced in which exon 27 of the *Ptpn3* gene was flanked by *loxP* sequences and a Neo^R cassette flanked by *FRT* sequences remained within intron 27 (Fig 7A-B). Chimeric mice were produced from two such targeted clones (4D4 and 4E4) and were bred with C57BL/6J mice to generate heterozygote $Ptpn3^{tm1PdK}$ mice. The Neo^R cassette of the targeted allele contains a strong cryptic splice acceptor sequence. Therefore, if the Neo^R cassette is allowed to remain within a targeted intron then this commonly results in a null allele as upstream exons are spliced to the Neo^R cassette in RNA transcripts [107]. For the $Ptpn3^{tm1PdK}$ targeted allele, if exon 27 or any upstream exon were to splice to the Neo^R cassette, then transcripts would direct the

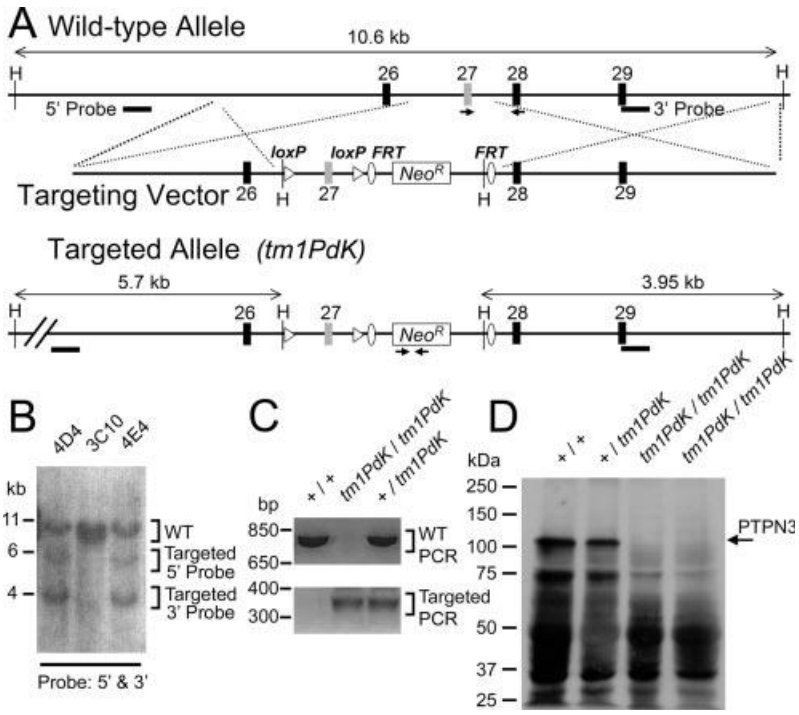

Figure 7 Generation of *Ptpn3*^{tm1PdK} mice

A) Shown is part of the wild-type genomic Ptpn3 locus with targeting vector and expected organization of the targeted allele. Positions of HindIII (H) restriction sites and probes used in Southern blotting are indicated. B) Southern blots of HindIII-digested genomic DNA from different ES cell clones probed with 5' and 3' probes. Positions of bands from wild-type and targeted alleles are shown. C) Tail DNA from progeny of F1 mice generated from one of the ES lines (4E4) was used as a template in PCRs with primers that detect wild-type or targeted alleles (positions indicated by arrows in A. Mouse genotypes are indicated at top. D) Western blot of whole brain lysates from homozygote Ptpn3tm1PdK mice and littermate controls using a PTPN3 mAb. Note the absence of wild-type PTPN3 at 110 kDa in the homozygote Ptpn3tm1PdK mice.

expression of a catalytically-inactive PTPN3 protein since an in frame stop codon would be encountered within the *Neo*^{R} cassette which would prevent the translation of the majority of the PTP domain. Based on these considerations, therefore, heterozygote *Ptpn3*^{tm1PdK} mice were not immediately crossed with Flp recombinase transgenic mice (to delete the *Neo*^{R} cassette) but instead were intercrossed to generate homozygous *Ptpn3*^{tm1PdK} mice and littermate heterozygote *Ptpn3*^{tm1PdK} and wild-type controls (Fig 7C). This approach would allow a ready means to examine the influence of loss of catalytically-active PTPN3 on a pure-bred C57BL/6J genetic background.

Homozygote *Ptpn3*^{tm1PdK}, heterozygote *Ptpn3*^{tm1PdK} and wild-type mice were born in expected Mendelian ratios. Furthermore, as with gene-trapped PTPN3 mice, there were no obvious defects in growth or development of homozygote or heterozygote *Ptpn3*^{tm1PdK} mice. To confirm loss of normal PTPN3 protein expression in homozygous *Ptpn3*^{tm1PdK} mice, brain lysates were analyzed by Western blotting using a PTPN3 monoclonal antibody (Fig 7D). As shown, full-length catalytically-active PTPN3 protein at 110 kDa could not be detected in the *Ptpn3*^{tm1PdK} homozygotes. Furthermore, no additional reactive bands at lower molecular weight could be detected in heterozygote or homozygote *Ptpn3*^{tm1PdK} mice compared to wild-type mice even upon long exposure. Since the PTPN3 antibody used reacts with the PDZ domain of the phosphatase this indicates that if any PTPN3 proteins are produced in these mice then they either lack the PDZ domain as well as the PTP domain or, if they contain the PDZ domain, are expressed at very low undetectable levels (note that the expected molecular weight of a FERM plus PDZ domain-containing protein is at least 50 kDa).

2.4.7 T cell development and function in PTPN3 gene-targeted mice

Analysis of T cell development and function was performed using Ptpn3tm1PdK mice and control mice generated from one of the targeted ES cell lines (4E4). Numbers and ratios of T cell subsets to one another and to other leukocytes were determined in thymus and peripheral lymphoid organs of 6-8 week old mice as before. In thymus, no differences in the number or ratio of DN (DN 1-4), double-positive and single-positive thymocytes were noted between wild-type, heterozygote and homozygote *Ptpn3*^{tm1PdK} mice (Fig 8A and data not shown). Similarly, the number and ratio of TCR+, CD4+ and CD8+ T cells in spleen and LN was comparable between the three groups of mice (Fig

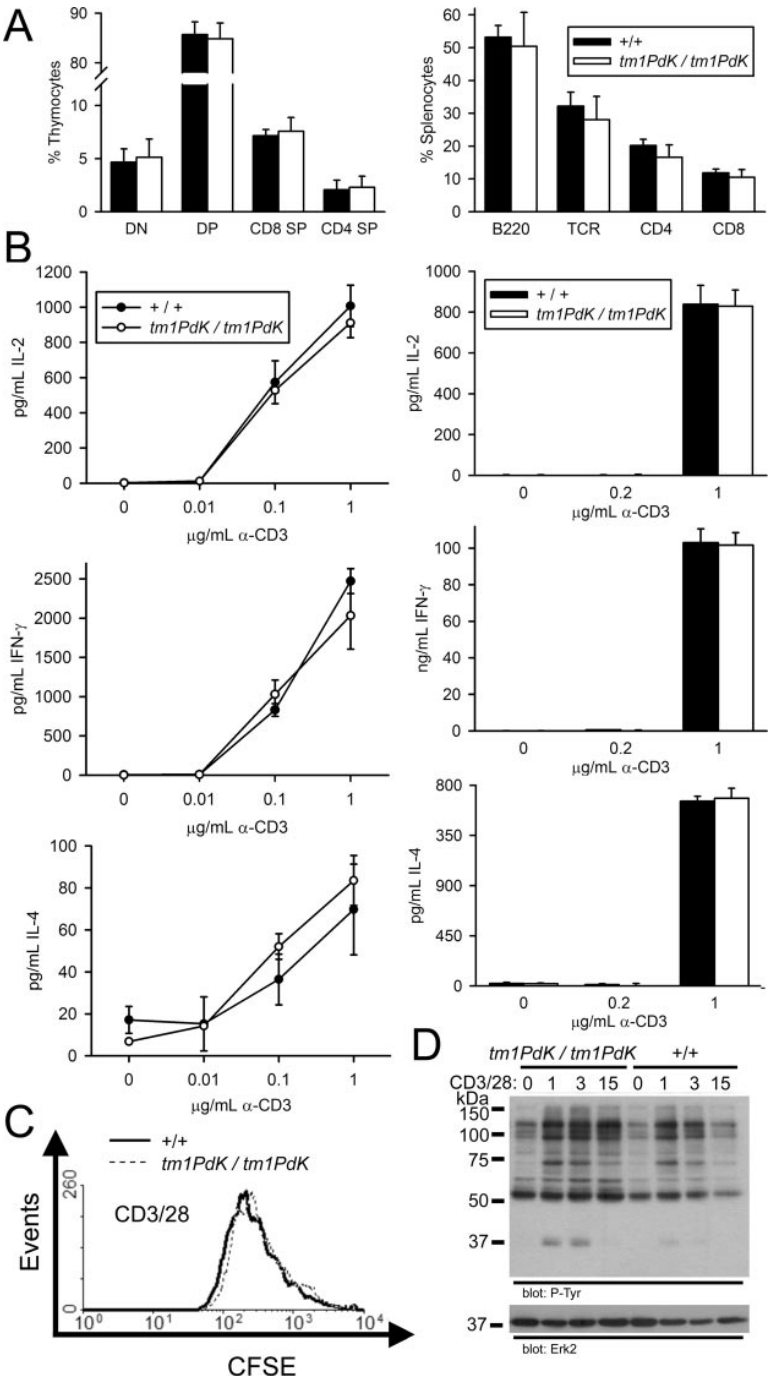

Figure 8 Normal T cell development, function, and TCR signal transduction in Ptpn3^{tm1PdK} mice

A) Percentages of the indicated thymocyte (left) and splenocyte populations (right) in homozygote Ptpn3^{tm1PdK} and littermate wild-type mice were determined by flow cytometry. Data are represented as mean percentage plus 1 SD and are derived from four mice of each genotype. B) Synthesis of cytokines by quiescent (left panels) and recently stimulated (as in Fig 6) (right panels) splenic T cells was determined as in Fig 5 and 6. Data are representative of three repeat experiments. C) Proliferation of quiescent splenic T cells was determined by dilution of CFSE fluorescence as in Fig 5. The same results were obtained in three repeat experiments. D) The CD3/CD28-induced protein tyrosine phosphorylation response of quiescent splenic T cells was determined by Western blotting as in Fig 5. Any small differences in the phosphotyrosine signal are seen to correlate with the amount of protein loaded.

8A and data not shown). All other examined leukocyte populations were also present in lymphoid organs in expected numbers and ratios (not shown).

We next examined CD3/CD28-induced T cell cytokine synthesis in *Ptpn3*^{tm1PdK} mice (Fig 8B). As with homozygote *Ptpn3* gene-trapped mice, T cells from homozygote *Ptpn3*^{tm1PdK} mice synthesized similar quantities of IL-2, IFN-γ and IL-4 in response to CD3/CD28 as wild-type littermates. Furthermore, when recently-stimulated T cells from the two groups of mice were examined there was also no apparent difference in the quantity of cytokines that were synthesized. Consistent with these results, T cells from homozygote *Ptpn3*^{tm1PdK} mice proliferated normally in response to CD3/CD28 and showed a similar CD3/CD28-induced protein tyrosine phosphorylation response as T cells from wild-type mice (Fig 8C-D).

2.4.8 T cell numbers and function in aged gene-trapped PTPN3 ΔPTP mice

Mice with defects in T cell negative-regulatory pathways commonly accumulate large numbers of activated T cells in peripheral lymphoid organs with age [35,38,108,109]. Furthermore, this lymphoid hyperplasia is frequently associated with the development of systemic autoimmune disease [14,108,110]. Therefore, we examined older gene-trapped PTPN3 ΔPTP mice (up to 1 year of age) for any evidence of T cell disregulation or generalized autoimmunity. No such signs were observed. In peripheral lymphoid organs, numbers and ratios of T cell subsets were normal and there was no altered expression of CD44, CD62L or CD69 activation markers (Fig 9). T cell production of cytokines in response to CD3/CD28 stimulation was also normal (data not shown). Mice remained healthy and there was no morphological, histological or serological evidence of autoimmunity (data not shown).

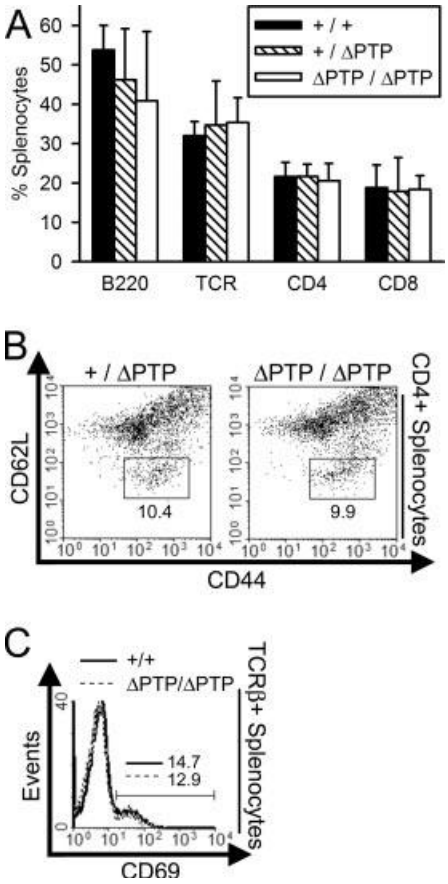

Figure 9 Phenotypic analysis of splenocytes from aged gene-trapped PTPN3 ΔPTP mice

A) Percentage representation of the indicated splenocyte populations from aged mice (10.5 to 12 mo) was determined by flow cytometry. Data are represented as means plus 1 SD from analyses of six mice of each genotype. B-C) Expression of CD44/CD62L and CD69 upon $CD4^+$ or $TCR\beta^+$ splenic T cells from aged mice was determined by flow cytometry. Shown are representative histograms from four repeat experiments.

2.5 Discussion

PTPN3 has been suggested to function as an important negative-regulator of TCR signal transduction acting to dephosphorylate the TCRζ chain [69-71]. However, this conclusion has been based upon studies which have examined the effect of over-expression of PTPN3 in the Jurkat T leukemia cell line and upon biochemical characterization of PTPN3 activity *in vitro*. Therefore, we sought to determine if PTPN3 acts as a physiological negative-regulator of TCR signaling in primary T cells. For this purpose, we produced two independent strains of PTPN3 mutant mice. One strain carries

a gene-trapped *Ptpn3* allele and other contains a gene-targeted *Ptpn3* allele. Catalytically-active PTPN3 is not expressed in either strain of mice. Both strains of mice were viable and fertile and exhibited normal growth and development showing that catalytically-active PTPN3 is dispensable in these regards. More pertinent to the current study, T cell development, T cell activation in the periphery and TCR signal transduction were unaffected in both strains. Thus, catalytically-active PTPN3 does not appear to have an essential function as a negative-regulator of TCR signal transduction in primary T cells.

One potential explanation for the lack of a requirement for catalytically-active PTPN3 in negative regulation of TCR signaling is functional redundancy with a closely-related PTP known as PTPMEG1 (PTPN4) [63]. Like PTPN3, PTPMEG1 comprises of a FERM domain, a PDZ domain and a PTP domain and shows 50% overall sequence identity with PTPN3. Moreover, PTPMEG1 is well expressed in T cells and similar to PTPN3 is able to inhibit TCR-induced IL-2 promoter activation when over-expressed in Jurkat [69]. Therefore, in T cells, as well as in other cell types, loss of catalytically-active PTPN3 may be compensated for by PTPMEG1. To address this issue of redundancy, it will be necessary to generate PTPMEG1-deficient mice and PTPN3/PTPMEG1-double-deficient mice. Of course, as an alternative explanation for the lack of an apparent influence of the loss of catalytically-active PTPN3, we cannot exclude the possibility that PTPN3 performs some scaffolding function in T cells independent of the catalytic domain. However, since PTP domain-negative PTPN3 variants are at best expressed at very low levels in mutant mice this possibility seems unlikely.

Apart from early TCR signal transduction, PTPN3 has also been implicated as a regulator of other cellular signaling processes. Notably, PTPN3 has been described to

interact physically with the cytoplasmic domain of tumor necrosis factor (TNF) α-convertase (TACE) [111]. TACE is a metalloprotease-disintegrin involved in ectodomain shedding of several proteins including not only TNFα but also transforming growth factor-α, L-selectin, TNF receptors I and II and interleukin-1 receptor II [112,113]. In co-transfection experiments performed in COS-7 cells, PTPN3 was shown to inhibit cell surface expression of TACE in a manner that was dependent upon PTPN3 catalytic activity. As a consequence, PTPN3 inhibited phorbol ester-induced secretion of TNFα when co-expressed with TACE in COS-7 [111]. The inference is that PTPN3 functions as a physiologic negative-regulator of TACE and ectodomain shedding of the afore-mentioned proteins. However, we have not observed any increased or accelerated loss of L-selectin from the surface of T cells from PTPN3 PTP domain-negative mice when stimulated with CD3/CD28 antibodies *in vitro* (data not shown). This finding argues against a role for PTPN3 in regulating TACE expression levels in primary cells.

Another function that has been ascribed to PTPN3 is dephosphorylation of the ubiquitously-expressed molecular chaperone, Valosin-containing protein (VCP). VCP was originally identified as a ligand of the PTPN3 PTP domain by a substrate-trapping technique [114]. Later, PTPN3-mediated dephosphorylation of VCP was shown to promote the formation of transitional endoplasmic reticulum formation *in vitro* [115] . However, while we cannot exclude a role for PTPN3 in transitional endoplasmic reticulum formation *per se*, in T cells at least we have not observed any altered tyrosine-phosphorylation of VCP either prior to or after activation with CD3 and CD28 antibodies (data not shown). This demonstrates that catalytically-active PTPN3 is not an essential regulator of VCP tyrosine phosphorylation in this cell type.

Finally, in a recent study, PTPN3 was identified as one of six PTPs out of all eighty-seven that are encoded in the human genome to be frequently mutated in colorectal cancer cell lines [116]. Interestingly, of the other five PTPs, one, PTPL1/FAP-1 (PTPN13), also contains FERM and PDZ domains and another, PTP36/PEZ (PTPN14), contains a FERM domain. Thus, of the only five PTPs that contain FERM domains, three are found to be mutated in colorectal cancer cell lines. This finding implies that PTPN3 (as well as the other two FERM domain-containing PTPs) may function as important tumor suppressors in colorectal cancer. Thus far, we have not observed spontaneous intestinal tumors in PTPN3 PTP domain-negative mice up to one year of age. However, it will be important to determine if loss of catalytically-active PTPN3 accelerates or enhances tumor formation in established murine colorectal cancer models such as the $APC^{Min/+}$ mouse. Such studies are ongoing in the laboratory.

Chapter 3: The FERM and PDZ Domain-containing PTP, PTPN4 and PTPN3, are both Dispensable for T Cell Receptor Signal Transduction

3.1 Abstract

PTPN3 and PTPN4 are two closely-related non-receptor PTP that, in addition to a PTP domain, contain FERM and PDZ domains. Both PTP have been implicated as negative-regulators of early signal transduction through the TCR, acting to dephosphorylate the TCRζ chain, a component of the TCR complex. Previously, we reported upon the production and characterization of PTPN3-deficient mice which show normal TCR signal transduction and T cell function. To address if the lack of a T cell phenotype in PTPN3-deficient mice can be explained by functional redundancy of PTPN3 with PTPN4, we generated PTPN4-deficient and PTPN4/PTPN3 double-deficient mice. As in PTPN3 mutants, T cell development and homeostasis and TCR-induced cytokine synthesis and proliferation were found to be normal in PTPN4-deficient and PTPN4/PTPN3 double-deficient mice. PTPN13 is another FERM and PDZ domain-containing non-receptor PTP that is distantly-related to PTPN3 and PTPN4 and which has been shown to function as a negative-regulator of T helper-1 (Th1) and Th2 differentiation. Therefore, to determine if PTPN13 might compensate for the loss of PTPN3 and PTPN4 in T cells, we generated mice that lack functional forms of all three

PTP. T cells from triple-mutant mice developed normally and showed normal cytokine secretion and proliferative responses to TCR stimulation. Furthermore, T cell differentiation along the Th1, Th2 and Th17 lineages was largely unaffected in triple-mutants. We conclude that PTPN3 and PTPN4 are dispensable for TCR signal transduction.

3.2 Introduction

A common event in cellular signal transduction is the phosphorylation of proteins on tyrosine residues which results in diverse cellular outcomes. This phosphorylation is mediated by PTK. By contrast, PTP remove phosphate groups from protein tyrosyl residues and thus oppose the actions of PTK. The mammalian genome encodes 38 classical PTP that can be subdivided into receptor-like and non-transmembrane PTP [4,6,31]. The non-transmembrane PTP family consists of 17 members, of which 14 are expressed in T lymphocytes of the immune system [39].

T cells become activated subsequent to MHC-peptide recognition mediated by the clonally distributed, cell surface expressed TCR [7]. One of the first events in the now well-established TCR signaling cascade is the phosphorylation and activation of the SrcFK, LCK and FYN [9]. These PTK phosphorylate ITAMs present within the cytoplasmic tails of invariant CD3 and TCRζ proteins that form part of the TCR complex [11]. Subsequently, the Syk-family kinase, ZAP-70, is recruited to the complex by the recognition of phosphorylated ITAMs, and, in turn, is activated via SrcFK-mediated phosphorylation. Activated ZAP-70 phosphorylates the transmembrane adapter protein LAT [12]. LAT further propagates the signal, leading to membrane recruitment

of additional signaling intermediates that ultimately result in the nuclear mobilization of the transcription factors NFAT, NF-κB, and AP-1 [13]. These transcription factors drive the expression of new genes that result in cytokine secretion, cytokine receptor expression, cell division, and effector cell differentiation.

While the role of PTK in TCR signal transduction has been extensively studied, the identity of PTP that negatively-regulate this pathway is less clear. PTP that are established physiological negative-regulators of proximal TCR signaling are SHP-1 and PEP. These PTP dephosphorylate and inactivate LCK, FYN, and ZAP-70 [40,54,59]. Other PTP that have been implicated in negative regulation of TCR signal transduction are PTPN3 and PTPN4 [62,63]. In mice, these PTP are 50% identical and 67% homologous at the amino acid level. They consist of an NH_2-terminal FERM domain, a central PDZ domain, and a COOH-terminal PTP domain. FERM and PDZ domains bind the cytosolic domain of transmembrane proteins [54-56]. Both domains have also been shown to bind directly to the phospholipid $PI(4,5)P_2$ [57,58]. The FERM domains of PTPN3 and PTPN4 are required for PTP membrane localization in T cells [69]. A screen in the Jurkat T cell leukemia line seeking to identify candidate negative regulators of TCR signal transduction revealed that over-expression of PTPN3 and PTPN4 resulted in an approximate 75% and 40% reduction, respectively, of TCR-induced activation of the promoter for the T cell growth-promoting cytokine, IL-2 [70]. Mutation of the catalytic cysteine residue or deletion of the FERM domain from these PTP abrogated this inhibitory effect, illustrating the importance of these domains for negative regulation [59,60]. In a separate study, PTPN3 was shown to both bind and dephosphorylate TCRζ

in vitro and when over-expressed in COS fibroblasts [61]. Recently, PTPN4 has also been shown to dephosphorylate TCRζ [62].

The third member of the FERM and PDZ domain-containing PTP family is PTPN13, also known as PTP-Bas, PTP-BL, and FAP-1 [117]. PTPN13 is a large protein that in addition to a PTP domain contains one FERM domain, five PDZ domains and a non-catalytic C-lobe domain. Mice that express a PTP domain-deleted form of PTPN13 exhibit impaired motor nerve repair and axon branching, and retinal ganglion cell neurite initiation and survival [118,119]. This suggests a role for PTPN13 in neural cell growth and survival, especially following injury. Additionally, *in vitro*, T cells from PTPN13-deficient mice demonstrated increased differentiation into T helper-1 (Th1) and T helper-2 (Th2) subsets that synthesize the cytokines interferon-γ (IFN-γ) and IL-4 respectively [120]. Ostensibly, this is associated with increased phosphorylation of signal transducer and activator of transcription (STAT) proteins which mediate cytokine signal transduction.

We have previously shown that mice lacking PTPN3 exhibit normal T cell development and function [74]. We hypothesized that the lack of apparent function of PTPN3 in T cells can be explained on the grounds that PTPN4 can substitute for the function of PTPN3 in this cell type. To address this we have generated PTPN4-deficient mice and PTPN4/PTPN3 double-deficient mice. Furthermore, to address the possibility that PTPN13 can substitute for the function of both PTPN4 and PTPN3 in T cells, we have additionally generated PTPN4/PTPN3/PTPN13 triple-mutant mice. The function of T cells in these different mice has been examined.

3.3 Materials and Methods

3.3.1 Mice

The ES cell line, OST146128 (of 129 Sv/Ev origin), which contains a gene trap cassette within intron 2 of the *ptpn4* locus, was purchased from Lexicon Genetics (The Woodlands, TX). ES cells were injected into C57BL/6J x (C57BL/6J x DBA/2) blastocysts to generate chimeras, which were bred to C57BL/6 mice to achieve germline transmission of the trapped *ptpn4* allele. F1 progeny were then intercrossed to generate PTPN4-deficient mice for experiments. To generate PTPN4/PTPN3 double-deficient mice, PTPN4 F1 mice were crossed to *ptpn3* $^{tm1PdK/tm1PdK}$ mice (C57BL/6 background) described in Chapter 2 [74]. Resulting PTPN4/PTPN3 double heterozygotes were then intercrossed to generate double-deficient animals for experiments, or were crossed to *ptpn13* $^{\Delta PTP/\Delta PTP}$ (C57BL/6 background) mice described previously [118]. In the latter case, progeny were intercrossed twice to concentrate the targeted alleles, and then intercrossed again to generate PTPN4/PTPN3-deficient PTPN13 ΔPTP/ΔPTP triple-mutant mice. Unless otherwise noted, all mice were 6-8 weeks of age at the time of experimentation. All experiments were performed in compliance with University of Michigan guidelines and were approved by the University Committee on the Use and Care of Animals.

3.3.2 PCR

To confirm loss of PTPN4 expression in PTPN4 gene-trapped mice, RNA was purified from splenocytes using Trizol (Invitrogen) and analyzed by RT-PCR (Superscript One-Step kit; Invitrogen) using a forward primer based in exon 2 and a

reverse primer based in exon 8 of the *ptpn4* gene. βActin transcripts were also amplified to control for the quantity and quality of RNA preparations.

Relative expression levels of PTPN4 in different tissues of wild-type mice were determined by quantitative PCR of cDNA samples from a Tissue Scan RT kit (Origene). Amounts of cDNA used in reactions were normalized to expression levels of GAPDH in each tissue. SYBR Green mastermix (Eurogentec) was used with a forward primer based in exon 2 and a reverse primer based in exon 3 of the *ptpn4* gene and reactions were performed in an MX3000p quantitative real-time PCR machine (Stratagene). Cycle threshold values were used to calculate the relative abundance of PTPN4 transcripts in tissues. Results were normalized to the amount of PTPN4 transcript detected in muscle, which was arbitrarily given a value of one.

3.3.3 Flow cytometry

Thymocytes, splenocytes, and lymph node (LN) cells were blocked with murine IgG (Sigma) and stained with the following conjugated monoclonal antibodies (BD Biosciences): H57-597-APC (TCRβ chain), RA3-6B2-APC-Cy7 (CD45R/B220), IM7-FITC (CD44), GK1.5-APC-Cy7 (CD4), 53-6.7-PerCP (CD8) and PC61-PE (CD25). Cell staining was analyzed by flow cytometry using a FACSCanto (Becton Dickinson).

3.3.4 T cell cytokine synthesis and proliferation

LN cells were stimulated with varying concentrations of 145-2C11 (CD3ε; eBioscience) and 37.51 (CD28; BD Biosciences) in 96 well round-bottom plates in complete medium (RPMI supplemented with 10% FCS, 25 nM β–mercaptoethanol, 50 U/mL Penicillin, 50 mg/mL Streptomycin, 2 mM L-glutamine, 10 mM HEPES, and 1 mM sodium pyruvate). Concentrations of cytokines in supernatants were determined by

ELISA after 24 h (IL-2) or 48 h (IFN-γ and IL-4) of culture. To assess T cell proliferation, splenocyte cultures were first labeled with 1 μM carboxyfluorescein succinimidyl ester (CFSE; Molecular Probes), and stimulated as above. After 72 h stimulation, CFSE fluorescence intensity was analyzed by flow cytometry.

In some experiments T cells were induced to differentiate into Th1, Th2, or Th17 cells. For this purpose, splenic CD4+ T cells were purified by negative selection and were stimulated with immobilized anti-CD3 (3 μg/mL for coating) and soluble (1 μg/mL) anti-CD28 antibodies plus recombinant human IL-2 (50 U/mL) in complete medium. For Th1 and Th2 and differentiation, IL-12 (3.5 ng/mL) /anti-IL-4 antibody (11B11; 10 μg/mL) or IL-4 (10 ng/mL)/anti-IFN-γ antibody (R4-6A2; 10 μg/mL), respectively, were added to the cultures. To induce Th17 cell differentiation, anti-IFN-γ (10 μg/mL), anti-IL-4 (10 μg/mL), IL-23 (20 ng/mL), IL-6 (10 ng/mL), and TGFβ (5 ng/mL) were added to media. After 72 h, cells were recultured in complete medium supplemented with IL-2 for Th1 and Th2 polarized cultures or anti-IL-4/anti-IFN-γ/IL-23/IL-6 for Th17 polarized cultures as above. After a further 48 h, cells were restimulated with immobilized CD3 antibody (1 μg/mL for coating), and supernatants were harvested after 24 h for quantitation of cytokine secretion by ELISA. All cytokines and blocking antibodies were purchased from PeproTech and BD Biosciences, respectively.

3.3.5 Statistical analysis

Statistical significance of differences in cell population representation or in cytokine secretion between test and control mice was assessed using a paired or unpaired Student's T-test as indicated.

In T cell polarization studies, in order to compile data from a number of independent experiments, cytokine secretion by different PTP mutant T cells was first normalized to that observed with control T cells to derive a fold increase in cytokine secretion as follows: (PTP mutant secretion – control secretion)/control secretion (in the case of increased secretion by mutant; assigned a positive value) or (control secretion – PTP mutant secretion)/PTP mutant secretion (in the case of decreased secretion by mutant; assigned a negative value). Mean fold increase in cytokine secretion relative to wild-type secretion was then calculated for several repeat experiments (Fig 16). Statistical significance of differences in cytokine secretion between PTP mutant and control cells was determined with the use of a paired Students T-test.

3.3.6 Western blotting

Splenocytes were lysed in a buffer containing 1% NP-40, run on SDS-PAGE gels and transferred to PVDF membranes (Perkin Elmer). Membranes were then probed with an anti-PTPN3 mAb [74], before stripping and reprobing with a GAPDH antibody (FL-335; Santa Cruz) to determine the amount of total protein loaded in each lane.

3.4 Results

3.4.1 Generation of PTPN4-deficient mice

PTPN4 is a member of the non-transmembrane PTP family that contains both a FERM and PDZ domain. A previous report had indicated that PTPN4 is strongly expressed in testis [121]. To analyze which other tissues also expressed PTPN4, we performed quantitative PCR upon a panel of normalized mouse tissue cDNA samples using PTPN4-specific primers (Fig 10A). As shown, PTPN4 transcript levels were indeed

highest in male reproductive organs. In addition, however, PTPN4 was also expressed in most other examined tissues including thymus and spleen.

To study the role of PTPN4 in T cells, we generated PTPN4-deficient mice. For this purpose, we obtained an ES cell line that contained a gene trap inserted within the *ptpn4* locus. This ES cell line was used to generate chimeric founder mice which were crossed to wild-type mice to achieve germline transmission of the trapped allele. Heterozygote PTPN4 mice were then intercrossed to generate homozygous PTPN4 mutants. Homozygote mutants were born in the expected Mendelian ratios and displayed no abnormalities in growth or development. Both male and female mice were fertile. The PTPN4 gene trap is contained within intron 2 of the *ptpn4* locus, downstream of exon 2 that contains the translation initiation codon (Fig 10B). Consequently, in primary transcripts produced from the gene-trapped allele, exon 2 would be spliced to the gene trap which contains a strong splice acceptor at its 5'end. This would result in extinction of PTPN4 protein expression since read through of exon 2 to exon 3 would not occur. To confirm loss of PTPN4 expression, we performed RTPCR upon splenic RNA from heterozygote and homozygote gene-trapped mice using a forward primer based in exon 2 and a reverse primer based in exon 8 of the *ptpn4* gene (Figure 10C). As shown, PTPN4 amplicons of the expected size were readily detected in heterozygote mice but were completely absent from homozygote mice. Thus, homozygous PTPN4 gene-trapped mice are PTPN4 null and cannot express PTPN4 protein.

3.4.2 Intact immune compartments in PTPN4-deficient mice

In order to investigate a potential role for PTPN4 in immune cell development, we examined the numbers and ratios of leukocytes in primary and secondary lymphoid

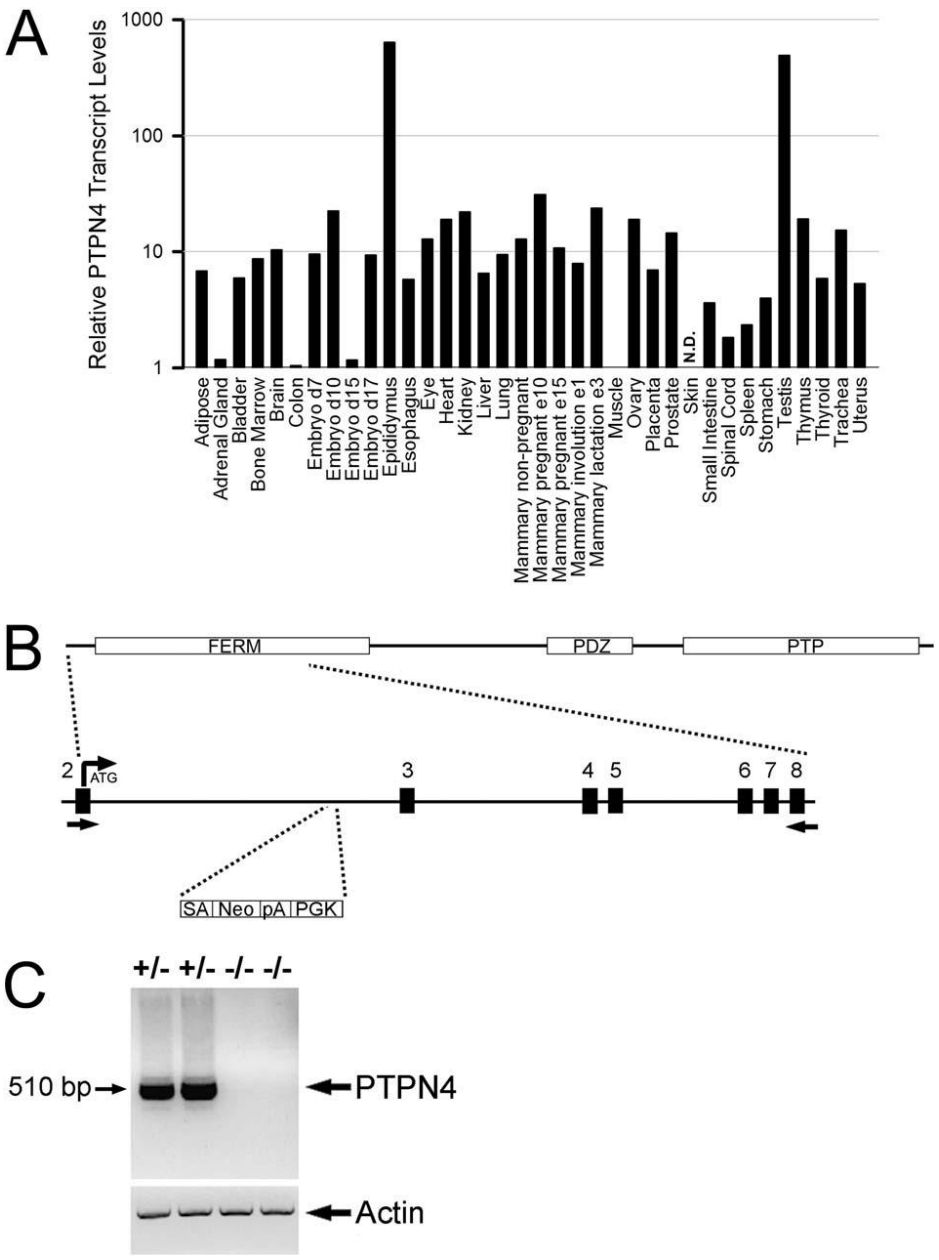

Figure 10 Generation of PTPN4-deficient mice

A) Relative PTPN4 expression levels were determined by quantitative PCR of different tissue cDNA samples using PTPN4-specific primers. For each tissue, expression levels are normalized to muscle, arbitrarily given a value of 1. N.D., not detected. B) Top, Domain organization of PTPN4, showing the location of the FERM, PDZ, and PTP domains. Bottom, Exon/intron organization of the 5' end of the ptpn4 gene encoding part of the PTPN4 FERM domain. The location of the gene-trapping cassette within intron 2 is shown. Note that exon 2 contains the translation initiation site. Arrows indicate positions of PCR primers used in panel C. SA, splice acceptor; Neo, sequence encoding neomycin phosphotransferase; pA, polyadenylation sequence; PGK, cloning vector component of gene trap. C) RTPCR was performed upon RNA isolated from splenocytes from mice heterozygous and homozygous for the gene-trapped allele using PTPN4 primers shown in B or control β-actin primers. Note the complete absence of PTPN4 transcripts in the homozygous mice.

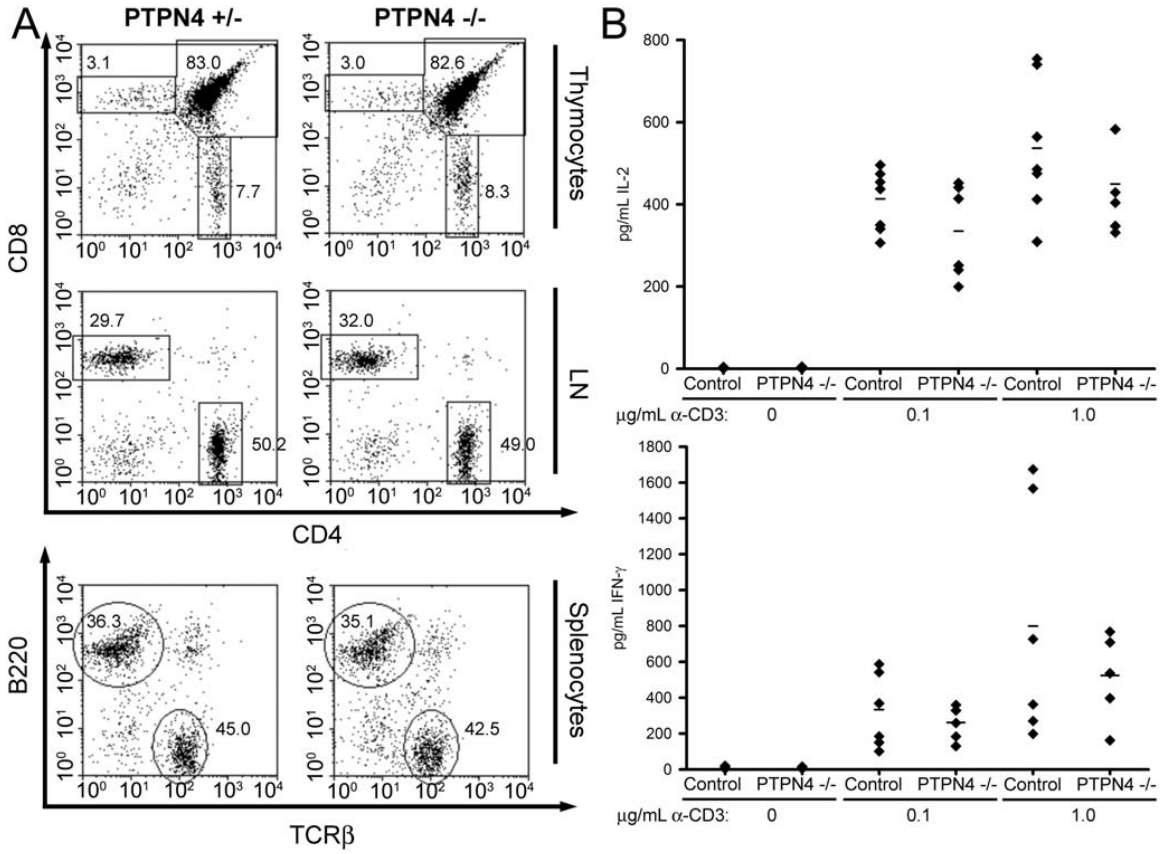

Figure 11 Normal T cell development and function in PTPN4-deficient mice

A) Flow cytometry plots of thymocytes, LN cells, and splenocytes from PTPN4-deficient mice and littermate controls showing expression of the indicated markers on live cell populations. Percentages of cells that fall within the indicated regions are shown. Data are representative of three repeat experiments. B) LN T cells were stimulated with the indicated concentrations of CD3 antibody and 0.5 μg/mL CD28 antibody. Concentrations of cytokines in supernatants were determined by ELISA. Each symbol represents the mean of triplicate determinations from a single mouse. Bars represent the mean cytokine secretion. Differences between PTPN4-deficient and control mice are not statistically significant (Paired Student's T test).

organs of PTPN4-deficient mice by flow cytometry (Fig 11A). With regards T cell development in the thymus, no differences were observed in the number or ratio of CD4-CD8- double-negative (DN), CD4+CD8+ double-positive (DP) or CD4+CD8- or CD4-CD8+ single-positive (SP) thymocytes compared to controls. Likewise, no differences in the number or ratio of CD4+ or CD8+ T cells were observed in LN or spleen. All other examined leukocytic populations including B cells, macrophages, dendritic cells, granulocytes and NK cells were also normally represented in secondary lymphoid organs as well as bone marrow of PTPN4-deficient mice (Fig 11A and not shown).

3.4.3 T cell activation and function in PTPN4-deficient mice

We next examined the ability of PTPN4-deficient T cells to synthesize cytokines in response to TCR stimulation. LN cells from PTPN4-deficient and control mice were thus stimulated with CD3 antibodies (directed to the TCR complex) and antibodies against the CD28 T cell costimulatory receptor. Secretion of cytokines into culture supernatants was then measured by ELISA. No significant differences in the synthesis of the T cell growth factor, IL-2, or the hallmark Th1 and Th2 cytokines, IFN-γ and IL-4, respectively, were apparent in these experiments (Fig 11B and data not shown). Thus, PTPN4 appears to be dispensable for TCR-induced synthesis of these cytokines.

3.4.4 T cell development and function in PTPN4/PTPN3 double-deficient mice

We hypothesized that the apparent lack of a T cell phenotype in PTPN4-deficient mice can be explained by a functional redundancy of PTPN4 with PTPN3 and vice versa. Analysis of the expression of PTPN3 in PTPN4-deficient mice and of PTPN4 in PTPN3-deficient mice indicated that loss of expression of one PTP did not result in a compensatory increase in expression of the other PTP (Figure 12A-B). Nonetheless, the possibility of functional redundancy still existed. Therefore, PTPN4-deficient mice were crossed with PTPN3-deficient mice and progeny were then intercrossed to generate PTPN4/PTPN3 double-deficient mutants.

Like single PTP-deficient mice, PTPN4/PTPN3-double-deficient mice were born in expected Mendelian ratios and showed normal growth and development. With regards T cell development, no abnormalities were apparent (Fig 12C). Numbers and ratios of DN, DP and SP thymocyte subpopulations were normal and among DN cells, the representation of CD44+CD25- (DN1), CD44+CD25+ (DN2), $CD44^{lo}$CD25+ (DN3) and

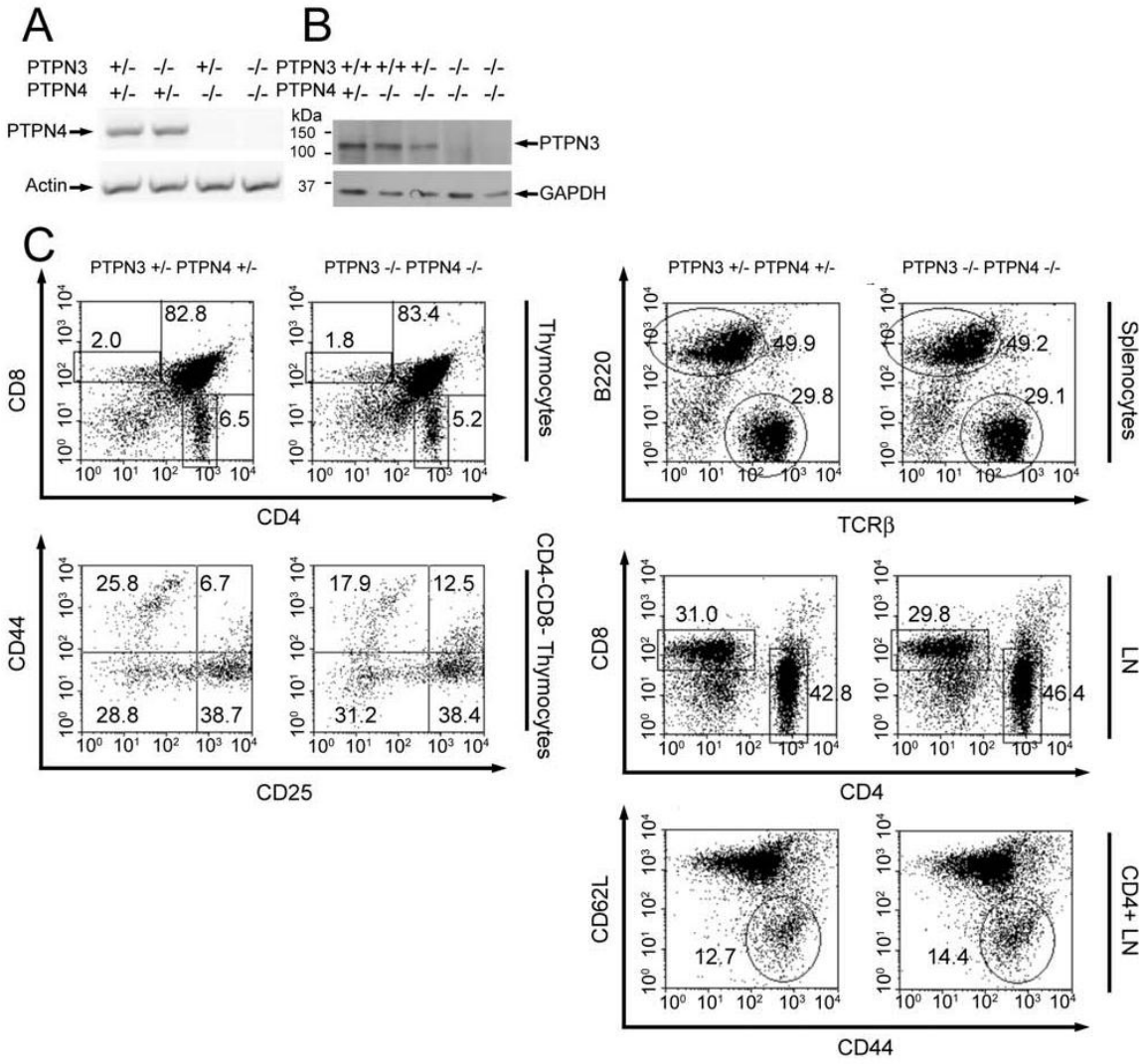

Figure 12 PTPN4/PTPN3 double-deficient mice show normal T cell development

A) Expression of PTPN4 in mice of the indicated genotypes (top) determined by RTPCR. B) Expression of PTPN3 in mice of the indicated genotypes (top) determined by Western blotting. Blots were stripped and reprobed with GAPDH antibodies to confirm equivalent protein loading. C) Flow cytometry plots of thymocytes and peripheral immune cells from PTPN4 -/- PTPN3 -/- mice and littermate controls showing expression of the indicated markers on live cell populations. In CD44/CD62L plots, the gated population represents recently activated memory T cells. Data are representative of six repeat experiments.

CD44-CD25- (DN4) subsets was unaffected in the double-mutants. Similarly, in secondary lymphoid organs, numbers and ratios of CD4+ and CD8+ T cells were normal. In addition, there was no evidence of any increased previous or ongoing T cell activation as judged by an increase in the frequency of cells that express the CD44 memory cell marker or a decrease in the frequency of cells that express CD62L, respectively.

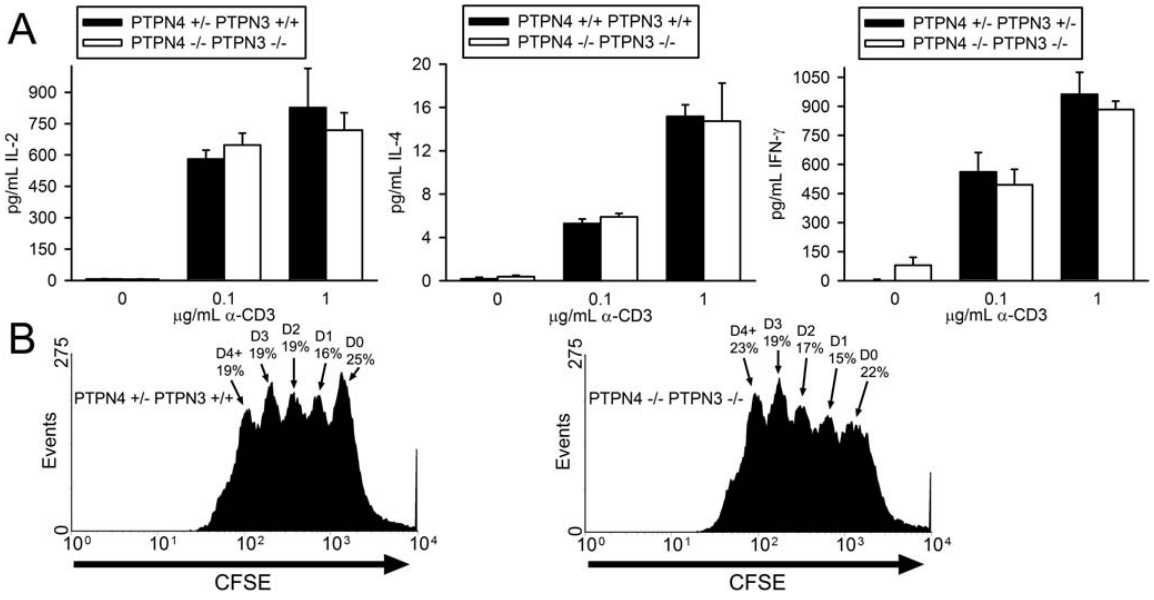

Figure 13 T cell cytokine synthesis and proliferation in PTPN4/PTPN3 double-deficient mice

A) LN T cells were stimulated with the indicated concentrations of CD3 antibody and 0.75 μg/mL CD28 antibody. Concentrations of cytokines in supernatants were determined as in Figure 2. Each bar represents the mean plus one standard deviation of triplicate determinations from one mouse. Differences between mice are not statistically significant (Student's T-test). Data are representative of six repeat experiments. B) Splenic T cells were labeled with CFSE and stimulated with 0.1 μg/mL CD3 antibody and 0.75 μg/mL CD28 antibody. After 72 h, CFSE dye intensity was measured by flow cytometry. The percentage of live cells that have undergone the indicated number of cell divisions is shown. Data are representative of three repeat experiments.

To examine the influence of loss of expression of PTPN4 and PTPN3 upon T cell function, we examined both T cell cytokine synthesis and T cell proliferation in PTPN4/PTPN3 double-deficient mice. Synthesis of IL-2, IFN-γ and IL-4 in response to CD3/CD28 antibody stimulation was determined as before (Figure 13A). As shown, T cells from PTPN4/PTPN3 double-deficient mice secreted similar quantities of these cytokines in these assays as T cells from control mice. To assess division, T cells were labeled with CFSE and dilution of CFSE was determined 72 h post-CD3/CD28 stimulation (Figure 13B). These analyses revealed that PTPN4/PTPN3 double-deficient T cells proliferate comparably to control T cells *in vitro*.

3.4.5 Generation and characterization of PTPN4/PTPN3 double-deficient PTPN13 ΔPTP/ΔPTP mice

The remaining PTP in the mouse and human genomes that contains both FERM and PDZ domains is PTPN13. Although the degree of homology between PTPN13 and PTPN4 or PTPN3 is much less than that between PTPN4 and PTPN3, the possibility that PTPN13 might compensate functionally for the loss of PTPN4 and PTPN3 in T cells existed. Moreover, recent studies of PTPN13-deficient mice indicated that this PTP regulates T helper cell differentiation through function as a negative-regulator of the phosphorylation of STAT-4 and STAT-6. Therefore, we asked if a role for PTPN4 and PTPN3 in T cells might be revealed in mice that do not express functional PTPN13. To examine this, PTPN4/PTPN3 double-deficient mice were crossed with mice that express a PTP domain-deleted PTPN13 protein (PTPN13 ΔPTP) to generate PTPN4/PTPN3-double-deficient PTPN13 ΔPTP/ΔPTP mutant mice [107]. As with single PTP and PTP double-deficient mutants, PTPN4/PTPN3 double-deficient PTPN13 ΔPTP/ΔPTP mice were born in normal Mendelian ratios and showed normal growth and development. With regards T cell development, analysis of the numbers and ratios of T cell subsets in thymus and peripheral lymphoid organs showed that this was also normal in triple-mutant mice (Figure 14). In addition, peripheral T cells from triple-mutants were found to secrete similar amounts of cytokines and proliferated to the same extent in response to CD3/CD28-stimulation as T cells from control mice (Figure 15).

Given the reported role of PTPN13 in control of T helper cell differentiation, we examined this directly in the triple-mutants. T cells from wild-type, PTPN13 ΔPTP/ΔPTP, PTPN4/PTPN3 double-deficient, and PTPN4/PTPN3 double-deficient

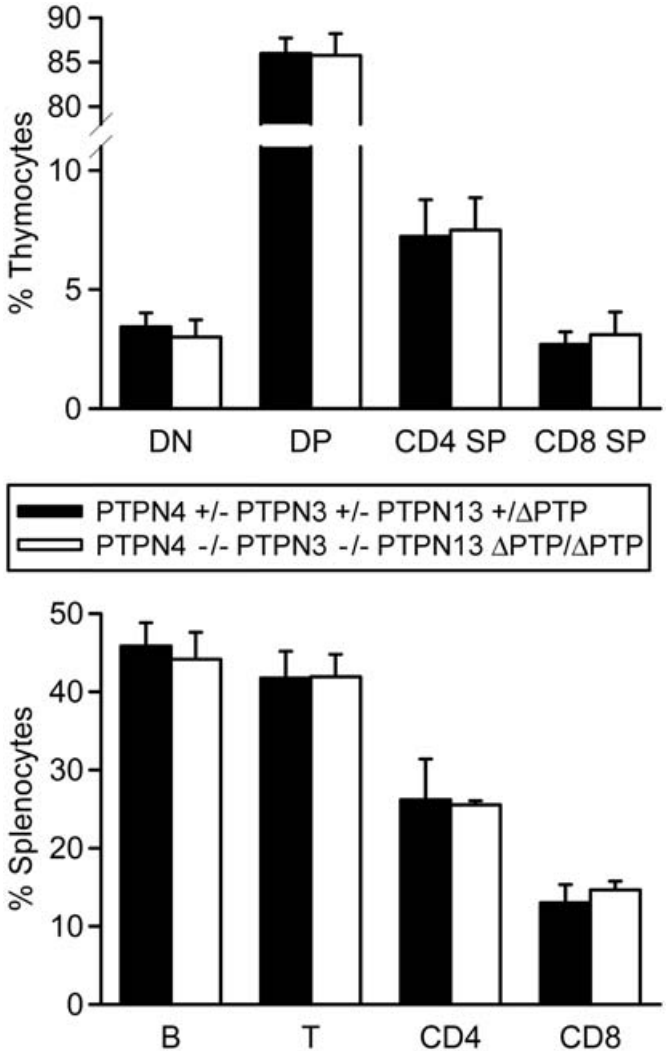

Figure 14 Normal T cell development in PTPN4/PTPN3 double-deficient PTPN13 ΔPTP/ΔPTP mice

Thymocytes and splenocytes from mice of the indicated genotypes were analyzed by flow cytometry for expression of T cell and B cell markers. Shown is the mean percentage representation plus one standard deviation of the indicated subpopulations among total live cells (n = 4 mice of each genotype). Differences between mice are not statistically significant.

PTPN13ΔPTP/ΔPTP mice were thus induced to differentiate along Th1, Th2 or Th17 lineages (see Materials and Methods). To examine the extent of differentiation, cells were then re-stimulated with CD3 antibody and secretion of IFN-γ, IL-4 and IL-17, respectively, was determined by ELISA (Figure 16). Results of these analyses showed that T cells from PTPN3/PTPN4-double-deficient mice were able to differentiate along the Th1, Th2 and Th17 lineages to an extent comparable to that observed with T cells

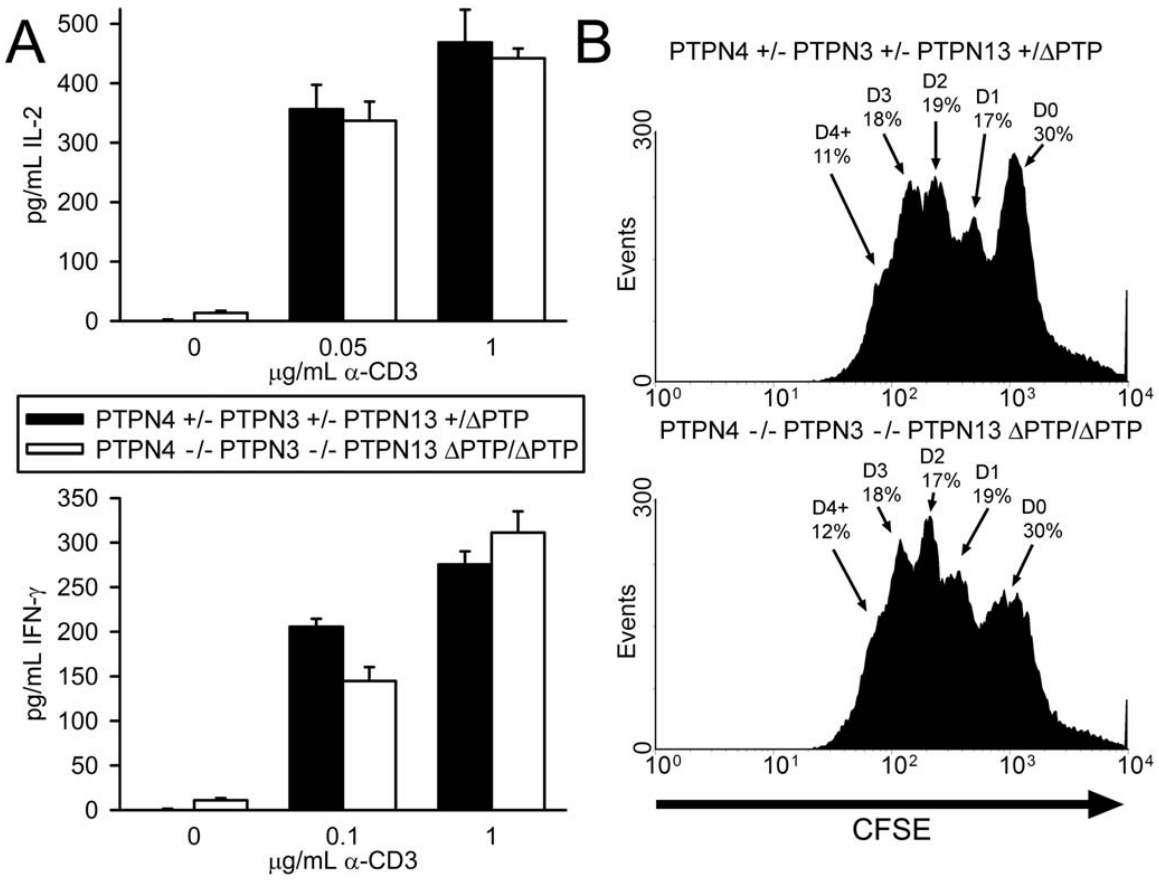

Figure 15 Function of PTPN4/PTPN3 double-deficient PTPN13 ΔPTP/ΔPTP T cells

A) LN T cells were stimulated with the indicated concentrations of CD3 antibody and 0.5 μg/mL CD28 antibody. Concentrations of cytokines in supernatants were determined as in Figure 2. Differences between mice are not statistically significant, excepting IFN-γ secretion at low dose anti-CD3 which is not a reproducible finding over four repeat experiments. B) Splenic T cells were labeled with CFSE and stimulated with 0.1 μg/mL CD3 antibody and 0.5 μg/mL CD28 antibody. After 72 h, CFSE dye intensity was measured by flow cytometry. Data are representative of four mice of each genotype.

from wild-type mice. Similarly, T cells from PTPN13 ΔPTP/ΔPTP mice showed the same extent of differentiation into Th1 and Th17 cells as T cells from wild-type mice, although showed increased differentiation along the Th2 cell lineage. These last results, therefore, differ from previous findings where increased Th1 differentiation as well as increased Th2 differentiation was reported in PTPN13-deficient mice. Finally, and importantly, T cells from PTPN4/PTPN3 double-deficient PTPN13 ΔPTP/ΔPTP mice behaved similarly to T cells from PTPN13 ΔPTP/ΔPTP mice in so much that they showed normal differentiation into Th1 and Th17 cells and somewhat increased differentiation along the

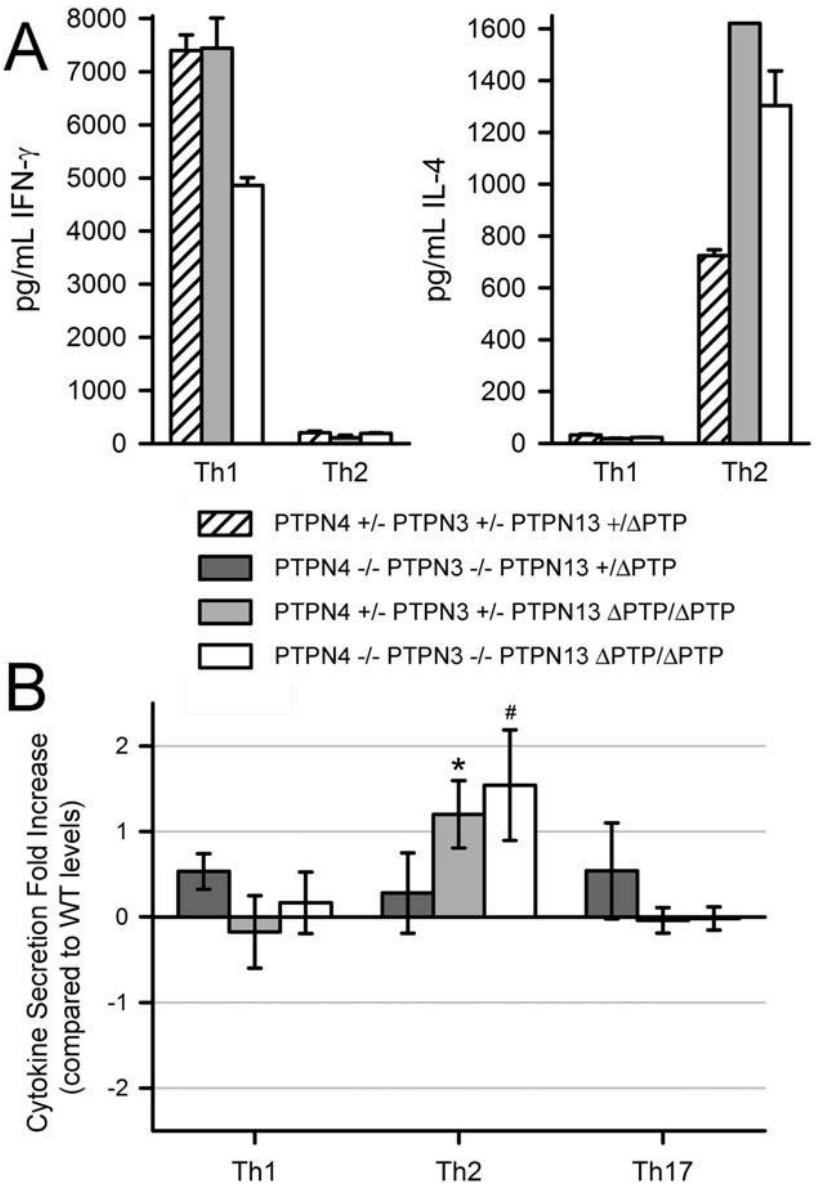

Figure 16 PTPN4 and PTPN3 are not required for CD4+ T cell differentiation

Purified CD4+ T cells were cultured under Th1-, Th2-, or Th17-inducing conditions. T cells were re-stimulated with CD3 antibodies and concentrations of IFN-γ, IL-4, and IL-17, respectively, in culture supernatants was determined by ELISA. A) Shown are results of a representative Th1/Th2 polarization experiment comparing control, PTPN13 ΔPTP/ΔPTP and PTPN4/PTPN3 double-deficient PTPN13 ΔPTP/ΔPTP T cells. Shown is mean cytokine secretion plus 1 standard deviation of triplicate determinations from single littermate mice. Conditions of polarization are indicated on the x-axis. B) Several repeat experiments of the type indicated in A) were performed. In each experiment, a fold increase in IFN-γ, IL-4 or IL-17 expression under conditions of Th1, Th2 or Th17 polarization respectively was calculated for mutant T cells relative to wild-type T cells (see Materials and Methods). Shown is the mean fold increase +/- one standard error (PTPN4 -/- PTPN3 -/- PTPN13 +/ΔPTP, n = 8; PTPN4 +/-PTPN3 +/- PTPN13 ΔPTP/ΔPTP, n = 5; PTPN4 -/- PTPN3-/- PTPN13 ΔPTP/ΔPTP, n = 4). Note that a 0 value fold increase indicates no change in cytokine secretion relative to wild-type. * differences relative to wild-type responses are statistically significant as determined in a paired Student's T-test comparing raw data (see Materials and Methods). All other differences relative to wild-type cells are not statistically significant. # p=0.07.

Th2 lineage (albeit not reaching statistical significance, $p<0.07$). In summary, these results show that PTPN3 and PTPN4 are dispensable for T cell function, even in the absence of functional PTPN13.

3.5 Discussion

The non-receptor PTP, SHP-1 and PEP, are established physiological negative-regulators of TCR signal transduction that act by dephosphorylating PTK that become activated at an early point in the TCR signaling cascade [40,54,59]. However, the identity of PTP which dephosphorylate other tyrosine-phosphorylated proteins in this cascade, and which may thus also function as negative-regulators of TCR signaling, has remained elusive. In this regard, there has been considerable interest in two closely related PTP, PTPN3 and PTPN4, as potential novel negative-regulators of TCR signal transduction. Both PTP are able to dephosphorylate the TCRζ chain *in vitro* and in cell lines [71,72]. In addition, when over-expressed in the Jurkat T leukemia cell line, both PTP inhibit TCR-induced activation of the IL-2 promoter, an effect that requires an intact FERM domain necessary for translocation of these PTP to the plasma membrane [69,70].

To address if PTPN3 functions as a physiological negative-regulator of TCR signal transduction, we recently generated PTPN3-deficient mice (Chapter 2). However, no abnormalities in T cell development or function were apparent in these mice. We hypothesized that the lack of a T cell phenotype could be explained by a functional redundancy of PTPN3 with PTPN4, since both PTP are expressed in T cells. Hence, in the current study, we generated PTPN4-deficient and PTPN3/PTPN4 double-deficient mice. Consistent with a recent report, T cell development and function was found to be

normal in PTPN4-deficient mice [62]. Moreover, there was no apparent T cell phenotype in PTPN3/PTPN4 double-deficient mice either. Thus, PTPN4 does not compensate for the loss of PTPN3 in T cells and vice versa.

We further asked if the absence of a T cell phenotype in PTPN3/PTPN4 double-deficient mice could be explained by functional redundancy with PTPN13, which also contains FERM and PDZ domains, albeit that this PTP shows a low degree of homology to PTPN3 and PTPN4. Therefore, we generated PTPN4/PTPN3 double-deficient PTPN13 ΔPTP/ΔPTP mice that lack functional forms of all three PTP. Once again, T cell development and TCR-induced cytokine secretion and proliferation were found to be normal in these mice. In addition, since PTPN13 has previously been shown to inhibit Th1 and Th2 differentiation through dephosphorylation of STAT proteins, we examined T helper cell polarization in triple-mutants [109]. In comparison to T cells from control mice, T cells from triple-mutant mice showed normal differentiation into Th1 and Th17 cells. An increased (not statistically significant) propensity of T cells to differentiate into Th2 cells was observed in triple-mutants. However, this increased Th2 differentiation was no greater in magnitude than that observed with PTPN13 ΔPTP/ΔPTP T cells. Thus, in conclusion, we have found no evidence for the notion that PTPN3 and PTPN4 function as negative-regulators of TCR signal transduction.

Functions for PTPN3 and PTPN4 outside of the immune system have been proposed. PTPN3 has been shown to dephosphorylate the growth hormone receptor (GHR) and one other group reported an increased weight gain amongst male PTPN3-deficient mice [122,123]. These findings suggest a role for PTPN3 as a negative-regulator of GHR signal transduction and body mass. However, counter to this, in our colony, we

have not observed any increased growth of male or female PTPN3-deficient mice up to 18 months of age. Similarly, we have not observed any increased body mass of PTPN4-deficient or PTPN4/PTPN3 double-deficient mice in comparison with littermate controls (not shown). It is possible that this discrepancy can be explained in terms of differences in genetic background or the precise nature of genetic disruptions in PTPN3 mutant strains. With regards strain differences, PTPN3 mutant mice that we have studied include PTPN3 gene-trapped mice on a 129P2/Ola Hsd background and PTPN3 gene-targeted mice on a C57BL/6 background (neither show growth abnormalities) [74]. By contrast, in the study in which an increased weight gain was reported for PTPN3-deficient males, mice were on a mixed 129 SvEv X C57BL/6 genetic background [112]. Concerning differences in the precise nature of disruptions, of the two PTPN3 mutant mice that were generated in our laboratory, we established by Western blotting that expression of PTPN3 protein was extinguished. By contrast, in the third PTPN3 mutant strain, although the nature of the genetic mutation precludes expression of catalytically-active PTPN3 protein, whether or not these mice express truncated forms of PTPN3 that contain only modular binding domains remains to be established.

Aside from growth, PTPN3 and PTPN4 have both been ascribed functions within the central nervous system. PTPN4 interacts with glutamate receptor subunits, which are required for neural development and function [124]. Consistent with a neural role, PTPN4-deficient mice were shown to have impaired cerebellar function, including defective motor learning [125]. In a recent report, PTPN3-deficient mice were also shown to have impaired memory function and motor learning, albeit that significant differences compared to controls were detected only in females [126]. Furthermore, in *Drosophila*,

loss of expression of PTPMEG (the single homologue of PTPN3 and PTPN4 in this species) results in defective axon growth associated with impaired development of mushroom bodies [127]. Therefore, given these reports, we examined motor learning function in our own PTPN4 and PTPN3 single-deficient mice and in PTPN4/PTPN3 double-deficient mice. In an accelerated rotarod test, no difference in motor learning was noted in comparison with controls (not shown). For PTPN3, discrepancies might again be explained by differences in background strain or the precise nature of genetic disruptions. For PTPN4, only strain differences could be invoked to account for the discrepant findings. Thus, the PTPN4-deficient mice reported here are on a mixed 129 SvEv X C57BL/6 background whereas the PTPN4-deficient mice that were reported to exhibit motor learning defects are on a 129SvJ background [90]. In both types of PTPN4 mutant, although the precise nature of the genetic mutation differs, PTPN4 gene expression was shown to be extinguished.

In summary, we have thus far been unable to observe any phenotypic abnormalities in PTPN4-deficient, PTPN3-deficient or PTPN4/PTPN3 double-deficient mice either within or outside of the immune system. Thus, a physiological function for these PTP that can be consistently demonstrated awaits discovery. In considering potential other roles, it is of interest that human papillomaviruses specifically target FERM and PDZ domain-containing PTP for degradation during infection and transformation [128-130]. One possible explanation for this finding is that FERM and PDZ domain-containing PTP play a role in defense against this type of virus. Notwithstanding the fact that human papillomaviruses do not infect murine cells,

discovery of the function of these PTP in papillomavirus infection could provide important clues as to their role in normal cellular physiology.

Chapter 4: The role of SHP-2 in adult animals: HSC and Tissue Remodeling

4.1 Abstract

SHP-2 (PTPN11) is essential for signaling from multiple classes of cell surface receptors. Mice deficient in SHP-2 expression exhibit defective gastrulation and fail to survive, which has precluded the use of non-conditional SHP-2 deficient mice to examine the role of SHP-2 in mature animals. To study this, we have used a conditional SHP-2 deficient mutant together with an ubiquitin promoter-driven ERT2-Cre transgene to mediate drug inducible deletion of SHP-2 in multiple tissues in adult mice. Using this model, we have determined that induced deletion of SHP-2 results in lethality preceded by weight loss. Epidermal acanthosis, anemia and premature thymic involution were also observed in these mice. Roles for SHP-2 in the homeostasis of the skeletal system are further demonstrated by the striking bone and cartilage remodeling defects resulting from the loss of SHP-2 in this model.

4.2 Introduction

The ubiquitously expressed PTP SHP-2 contains tandem NH_2-terminal SH2 domains and a COOH-terminal PTP domain. Humans with mutations of *Ptpn11*, the gene encoding SHP-2, exhibit one of two related syndromes. Autosomal dominant gain-

of-function SHP-2 mutations result in Noonan's Syndrome (NS) [131,132]. NS mutations are localized throughout the SHP-2 protein coding sequence, but are concentrated in the NH_2-terminal SH2 domain. The intramolecular fold-mediated inhibition of the PTP domain is disrupted by NS-associated mutations, resulting in increased activity of the mutant enzyme [133,134]. Alternatively, distinct SHP-2 mutations result in LEOPARD (multiple Lentigines, Electrocardiographic conduction abnormalities, Ocular hypertelorism, Pulmonary stenosis, Abnormal genitalia, Retardation of growth, sensorineural Deafness) syndrome (LS) [135,136]. LS patients exhibit mutations in the PTP domain, including the highly-conserved PTP signature motif, which lead to decreased SHP-2 catalytic activity [137,138]. It has been proposed that LS mutations result in dominant-negative inhibition of SHP-2 activity, since LS is dominantly inherited, no missense or frameshift mutations have been detected in LS patients, and SHP-2 haploinsufficiency does not result in disease in mice [139].

Interestingly, despite increased SHP-2 enzymatic activity in NS and decreased SHP-2 enzymatic activity in LS, these syndromes present similarly in the clinic [140,141]. NS patients exhibit facial dysmorphia, heart defects, and short stature. LS patients are characterized by hyperpigmented skin lesions in addition to facial dysmorphia, cardiac abnormalities, and short stature. It is unknown how mutations resulting in opposing changes to the catalytic activity of SHP-2 result in comparable phenotypes. It has been hypothesized, although not yet been formally shown, that NS and LS are the result of SHP-2-mediated misregulation of Ras-MAPK signal transduction. The recent discovery that patients afflicted with two disorders that present similarly in the clinic to NS and LS, namely cardio-facio-cutaneous syndrome and

Costello syndrome, harbor mutations in Ras-MAPK pathway genes supports this model [142].

A role for SHP-2 as a positive regulator of Ras-MAPK signal transduction from growth factor receptors has been definitively shown in mice. SHP-2 deficient mice fail to survive beyond embryonic day 10 due to defective gastrulation, at least partially as a result of a reduced level and duration of FGF-induced MAPK activation [75]. More recently, a floxed (fl) allele of SHP-2 was generated to circumvent the embryonic lethality of SHP-2 deficiency [76]. Roles for SHP-2 in Ras-MAPK activation in FGF signal transduction in neural stem cells, the IGF-1 and EGF pathways in cardiac myocytes, and EGF and hepatocyte growth factor signaling in liver regeneration, have been shown in tissue-specific SHP-2 deficient mice [77-79]. In addition to growth factor receptors, signal transduction from receptor tyrosine kinases in cytokine and hormone receptor signaling pathways has also been shown to require SHP-2 for appropriate activation of ERK [40,76]. Despite clear roles for SHP-2 in many cellular signaling events utilizing the Ras-MAPK pathway, the precise molecular mechanism of SHP-2 regulation of this pathway remains unclear [143].

A definitive role for SHP-2 has remained elusive in T lymphocytes; however, SHP-2 has been proposed to be the effector molecule of inhibitory surface receptors and has recently been implicated in positive regulation of TCR signal transduction. SHP-2 has been shown to associate with a number of T cell inhibitory receptors, including CTLA-4, PD-1, BTLA-1, CEACAM-1, and CD31 [40,82-84]. Coimmunoprecipitation studies revealed a SHP-2-CTLA-4-TCRζ complex, which led to the hypothesis that SHP-2 is the effector molecule of CTLA-4, functioning to dephosphorylate the ITAMs of

TCRζ [82,88-90]. Overexpression experiments and coimmunoprecipitation of SHP-2 with killer-inhibitory receptors in NK cell lines have further suggested an additional role for SHP-2 in inhibitory receptor signal transduction in NK cells [144,145].

The recently generated conditional SHP-2 allele permits T cell-restricted SHP-2 ablation to test the hypothesis that SHP-2 is the effector molecule for inhibitory receptors like CTLA-4 and PD-1. Gen-Sheng Feng's laboratory, using T cell-specific SHP-2 deletion mediated by LCK-Cre, reported a role for SHP-2 as a positive regulator of pre-TCR signaling, with no evidence that SHP-2 deficiency resulted in altered inhibitory receptor signaling [91]. SHP-2 fl/fl LCK-Cre mice exhibit decreased total numbers of thymocytes, of which a higher percentage are at the DN stage of development. Altered ratios of DN3 to DN4 thymocytes indicate that SHP-2 is required for optimal pre-TCR signal transduction at the DN3-DN4 checkpoint. Reduced ERK phosphorylation in SHP-2 deficient thymocytes was shown in response to CD3/CD28 antibody stimulation. Studies of mature peripheral T cells isolated from these mice suggest that SHP-2 is additionally a positive regulator of TCR signal transduction in mature T cells. However these experiments remain inconclusive, due to the possibility that altered thymic development results in this peripheral T cell phenotype.

To determine if SHP-2 functions in positive and negative selection, SHP-2 fl/fl mice were crossed with TCR transgenic animals. The use of SHP-2 fl/fl TCR transgenic mice permits the examination of a population of T cells that express a monoclonal TCR to reveal thymic selection abnormalities that might not be apparent in a polyclonal population. The timing of SHP-2 deletion is critical to the interpretation of these experiments, since a role for SHP-2 in pre-TCR signaling has been shown, and therefore

the DP stage thymocytes in SHP-2 fl/fl LCK-Cre mice might represent an abnormal population of thymocytes that is not physiologically representative. Consequently, experiments revealing a function for SHP-2 in positive and negative selection in SHP-2 fl/fl LCK-Cre mice would be inconclusive. Conversely, in SHP-2 fl/fl CD4-Cre mice, SHP-2 function is retained in pre-TCR signaling events, producing an intact DN3-DN4 transition [146]. Subsequent advancement of thymocytes into the DP stage of development then results in Cre-mediated loss of SHP-2 expression. This enables the examination of these hitherto wild-type thymocytes to progress through the positive and negative selection checkpoints in the absence of SHP-2. Despite these considerations, however, we have been unable to demonstrate a consistent reduction of SHP-2 protein levels in SHP-2 fl/fl CD4-Cre DP thymocytes. Therefore, a definitive role for SHP-2 in thymic positive and/or negative selection remains undefined.

We next sought to determine the role of SHP-2 in mature T cells. Although peripheral T cells from SHP-2 fl/fl LCK-Cre mice have been characterized, the functions ascribed to SHP-2 in mature T cells as a result of these experiments may instead reflect the altered thymic development of these T cells. To definitively test a role for SHP-2 in mature T cells, we crossed SHP-2 fl/fl and ERT2-Cre transgenic mice. In ERT2-Cre mice, the Cre recombinase is expressed from the ubiquitin promoter as a fusion protein with a mutated form of estrogen receptor (ERT2), which binds tamoxifen but not estrogen [92]. The ubiquitously expressed ERT2-Cre is retained in the cytoplasm, preventing DNA recombination. Upon tamoxifen binding, translocation of the fusion protein to the nucleus permits recombination of the floxed allele and *de novo* SHP-2 deletion. *In vitro* tamoxifen treatment did not result in the reduction of SHP-2 protein

levels from mature T cells. We next injected adult mice with tamoxifen, with the expectation that SHP-2 would be deleted from not only peripheral T cells, but all tissues. In the course of these experiments, we have identified a variety of unexpected phenotypes, including a block in hematopoiesis, skin dysplasia, and skeletal malformations.

4.3 Methods

4.3.1 Mice

SHP-2 fl/fl mice were obtained from Gen-Sheng Feng (Burnham Institute) [76]. Mice containing the ubiquitin promoter-driven ERT2-Cre transgene were obtained from Eric J Brown (University of Pennsylvania) [92]. SHP-2 fl/fl ERT2-Cre adult mice (6-8 weeks old) were injected intraperitoneally on two successive days with tamoxifen (200μg/g body weight in corn oil). Animal health was monitored by observed activity level and weekly weighing, and mice were sacrificed when moribund. Littermate and gender-matched control mice, of genotypes SHP-2 +/+, SHP-2 fl/+, SHP-2 fl/+ ERT2-Cre and SHP-2 fl/fl, were similarly injected with tamoxifen. Mice of these genotypes are collectively referred to as "control" in experiments involving multiple mice as no haploinsufficiency of SHP-2 was observed. This research was performed in compliance with University of Michigan guidelines and was approved by the University Committee on the Use and Care of Animals.

4.3.2 Flow cytometry

Single cell suspensions of thymocytes, splenocytes, and hind limb-derived bone marrow cells were blocked with murine IgG (Sigma). Cells were stained with

monoclonal antibodies from BD Biosciences and cell staining was analyzed on a FacsCanto (BD). Antibodies to TCRβ, B220, CD11b, GR-1, and Ter119 were used to define lineage-positive cells in the bone marrow.

4.3.3 Tissue lysates and Western blotting

To prepare tissue lysates, organs were crushed and lysed in a buffer containing 1% NP-40. Lysates were run on SDS-PAGE gels and transferred to PVDF membranes for Western blotting. Membranes were probed with anti-SHP-2 rabbit polyclonal antibody (Cell Signaling) before stripping and reprobing with anti-GAPDH (Santa Cruz) as a loading control.

4.3.4 Clinical chemistry and histology

Spin hematocrit and methylene blue reticulocyte counts were performed on heparinized blood. Serum clinical chemistries were analyzed on a Vettest Chemistry Analyzer Model 8008 (Idexx). For histology, tissues were fixed in 10% buffered formalin, transferred to 70% ethanol, embedded in paraffin, and 5μm sections were stained with hematoxylin and eosin. Bone samples were decalcified over a period of two weeks in 10% EDTA-Ammonium Hydroxide pH 7.2 on a rocking platform prior to embedding, and were sectioned at a thickness of 8μm.

4.3.5 X-ray and microCT

Bones were carefully dissected and imaged on a Faxitron Corp (Wheeling, IL) microradiography machine. Microcomputed tomography (microCT) scanning was performed using a cone beam MicroCT system (GE Healthcare Biosciences, London, Ontario). Image reconstruction was performed on 25μm voxels, a threshold was generated to define mineralized tissue, and regions of interest were defined for trabecular

and cortical parameters using the MicroView Analysis program (GE Healthcare Biosciences).

4.4 Results

4.4.1 Induced deletion of SHP-2 from adult mice

Interbreeding of SHP-2 exon 4 fl/fl mice with ERT2-Cre transgenic mice enables the examination of the roles of SHP-2 in adult tissues by temporal ERT2-Cre-mediated deletion of this PTP. SHP-2 fl/fl ERT2-Cre mice begin to die 10 days following tamoxifen administration. By three weeks post-injection, we observed 50% mortality of SHP-2 fl/fl ERT2-Cre mice, with 100% mortality by 14 weeks (Fig 17A). SHP-2 fl/fl ERT2-Cre mice exhibit severe weight loss prior to death (Fig 17B). This could be detected as early as 11 weeks before euthanization, although typically weight loss was more precipitous and resulted in morbidity within two weeks. Visual inspection during postmortem analysis revealed that SHP-2 fl/fl ERT2-Cre mice exhibited a near complete absence of subcutaneous fat. To determine the efficiency of SHP-2 deletion, organ lysates from SHP-2 fl/fl ERT2-Cre and littermate controls were prepared and revealed a reduction of SHP-2 protein levels in a variety of tissues (Fig 17C).

4.4.2 Pathology of SHP-2 fl/fl ERT2-Cre mice

Considering the high frequency of cardiac defects in NS and LS patients, hearts from SHP-2 fl/fl ERT2-Cre mice were histologically examined for lesions. No defects in cardiac valves or walls were seen in these mice (data not shown). A further broad pathological examination of moribund induced SHP-2 deficient mice failed to reveal an obvious cause of disease, however we did observe marked epidermal hyperplasia

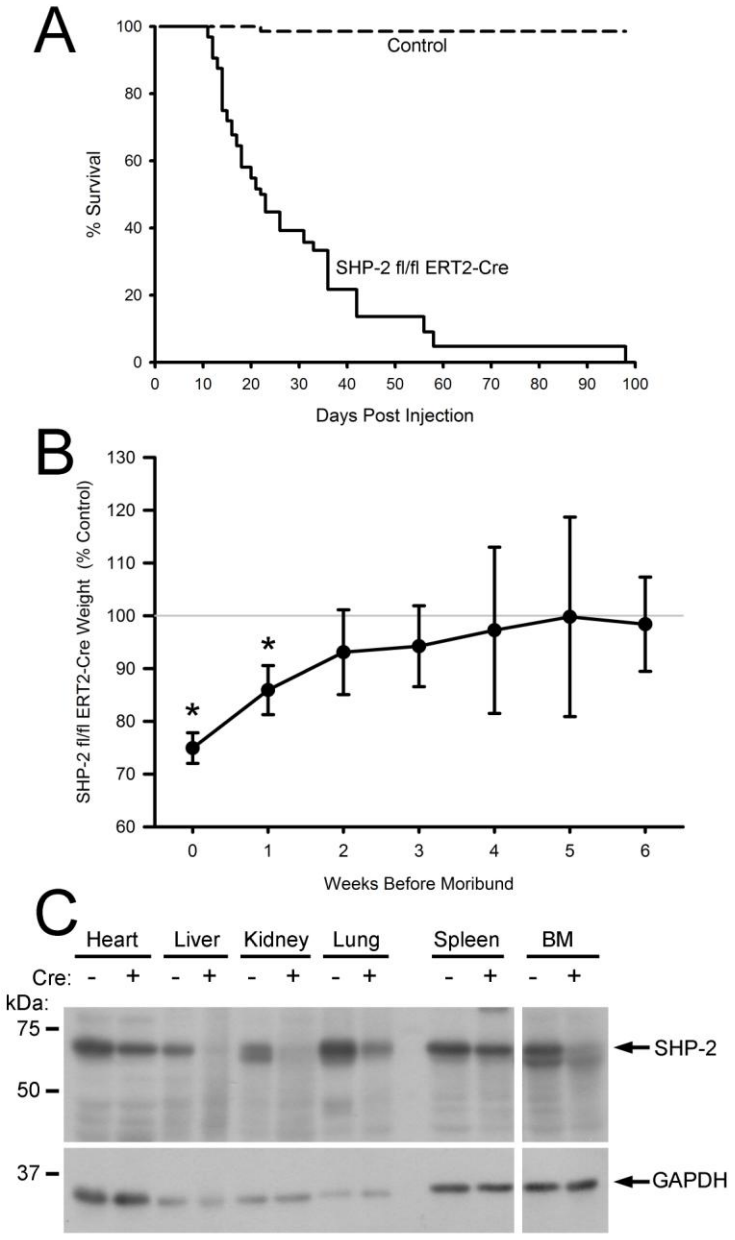

Figure 17 Induced SHP-2 deficiency in adult mice results in weight loss and rapid mortality

A) Kaplan-Meier plot depicting the survival of SHP-2 fl/fl ERT2-Cre mice (n=32) and SHP-2 sufficient control mice (n=70) following tamoxifen injection. B) SHP-2 fl/fl ERT2-Cre mice and littermate control weights were recorded weekly following tamoxifen injection. Depicted is the normalized weight of SHP-2 fl/fl ERT2-Cre mice (total n=14), shown as a percent of littermate controls (total n=32). Euthanization of moribund SHP-2 fl/fl ERT2-Cre mice precludes all data points from representing the total number of animals. *, p<.0005. as determined by paired Student's T-test. C) Lysates from a SHP-2 fl/fl ERT2-Cre and littermate control SHP-2 fl/fl mouse prepared 15 days post tamoxifen injection were blotted with an anti-SHP-2 antibody and then stripped and reprobed with anti-GAPDH to demonstrate equal loading. At this early time point post tamoxifen injection, absence of SHP-2 from individual tissues, with a reduction in other tissues is apparent. The shown experiment is representative of three repeats.

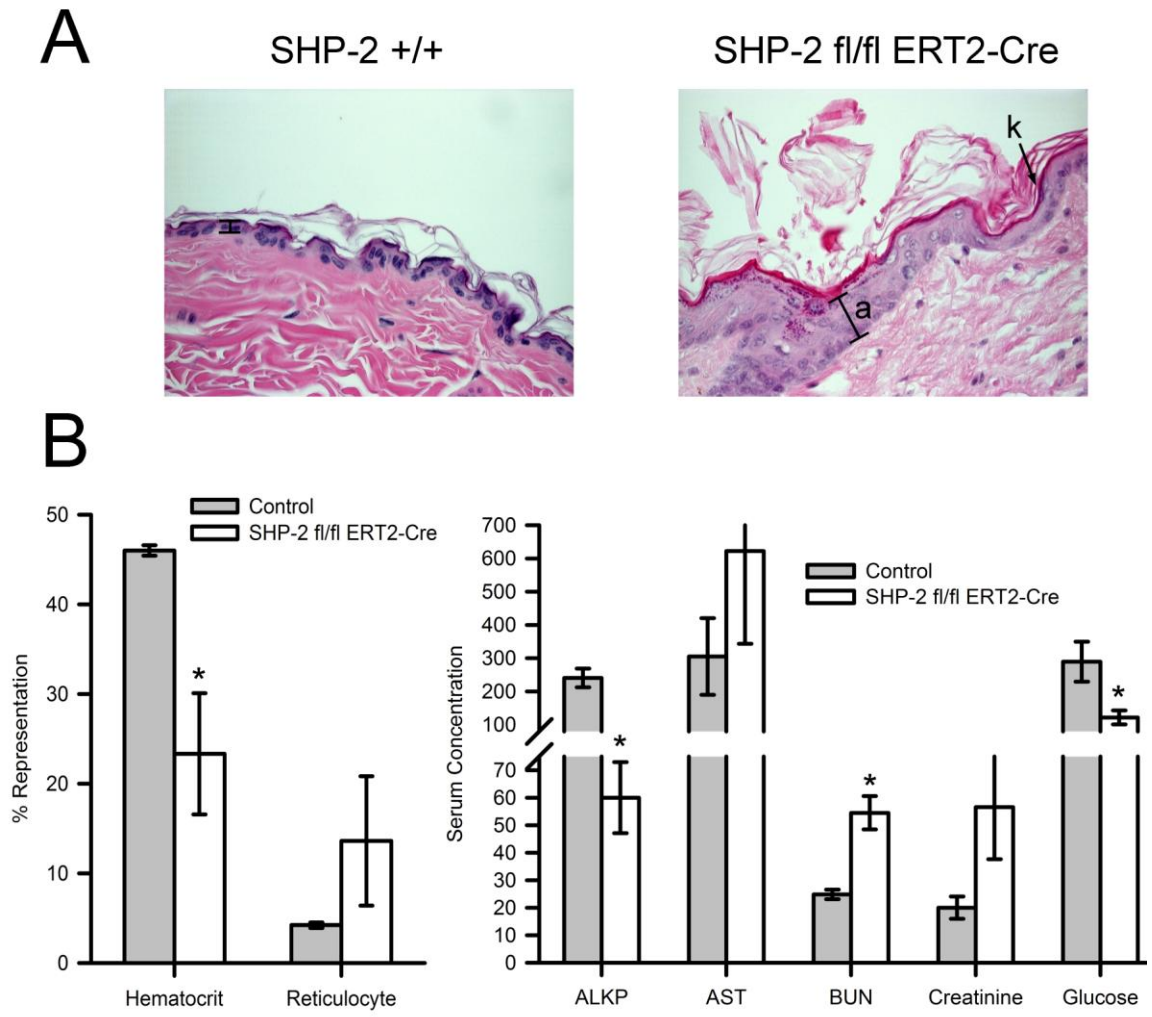

Figure 18 Pathology of induced SHP-2 deficient mice

A) Skin sections stained by H&E reveal hyperkeratosis (k) and acanthosis (a) in moribund induced SHP-2 deficient mice. B) Spin hematocrits and reticulocyte counts were performed on heparinized whole blood from moribund SHP-2 fl/fl ERT2-Cre mice and littermate controls. The concentrations of a panel of metabolites were determined from serum. Hematocrit is represented as percent blood volume, and reticulocytes are shown as percent blood cells. Clinical chemistries are represented as U/L (ALKP, AST), μg/mL (BUN, glucose), or ng/mL (creatinine). The mean from SHP-2 fl/fl ERT2-Cre mice (n=3) and littermate controls (n=3) are depicted +/- one standard error. *, $p<.05$ determined by paired Student's T-test.

(acanthosis) and thickening of the outermost layer of dead keratinocytes (hyperkeratosis) in the skin of SHP-2 fl/fl ERT2-Cre mice (Fig 18A).

We next tested the serum levels of a variety of metabolites in moribund mice to better understand the disease in these induced SHP-2 deficient animals (Fig 18B). Serum glucose levels in SHP-2 fl/fl ERT2-Cre mice were decreased compared to littermate

control mice. We also observed elevated blood urea nitrogen (BUN) and creatinine levels in SHP2 fl/fl ERT2-Cre mice. Elevated serum BUN and creatinine levels are associated with kidney dysfunction, which could not be detected at a gross pathological level. Reduced serum alkaline phosphatase (ALKP) and a trend towards increased aspartate transaminase (AST) suggest functional liver abnormalities in SHP-2 fl/fl ERT2-Cre mice. Similarly, no pathological lesions could be seen in the livers from these mice.

Induced SHP-2 deficient mice exhibit severe anemia concomitant with the onset of weight loss (Fig 18B). Elevated numbers of reticulocytes are also detected in the serum following weight loss in SHP-2 fl/fl ERT2-Cre mice.

4.4.3 Impaired hematopoiesis in SHP-2 fl/fl ERT2-Cre mice

The severe anemia in induced SHP-2-deficient mice led us to more closely examine hematopoiesis in these mice. Strikingly, thymii isolated from SHP-2 fl/fl ERT2-Cre mice are exceptionally small, and contain almost no DP thymocytes (Fig 19A). The few cells recovered from the thymus are early thymic progenitors and single positive T cells. In contrast, the numbers and ratios of lymphocyte subsets in lymph nodes were not significantly altered in SHP-2 fl/fl ERT2-Cre mice (data not shown). However, a bimodal distribution of splenic cellularity was observed upon comparison of SHP-2 fl/fl ERT2-Cre to littermate control mice. A subset of SHP-2 fl/fl ERT2-Cre spleens exhibited reduced cellularity, yet retained a normal proportion of T cells, B cells, macrophages, neutrophils (Fig 19B). In contrast, the remaining induced SHP-2 deficient spleens were grossly enlarged as a result of increased numbers of macrophages and Ter119+ cells, despite decreases in T cell and B cell numbers. The presence of large

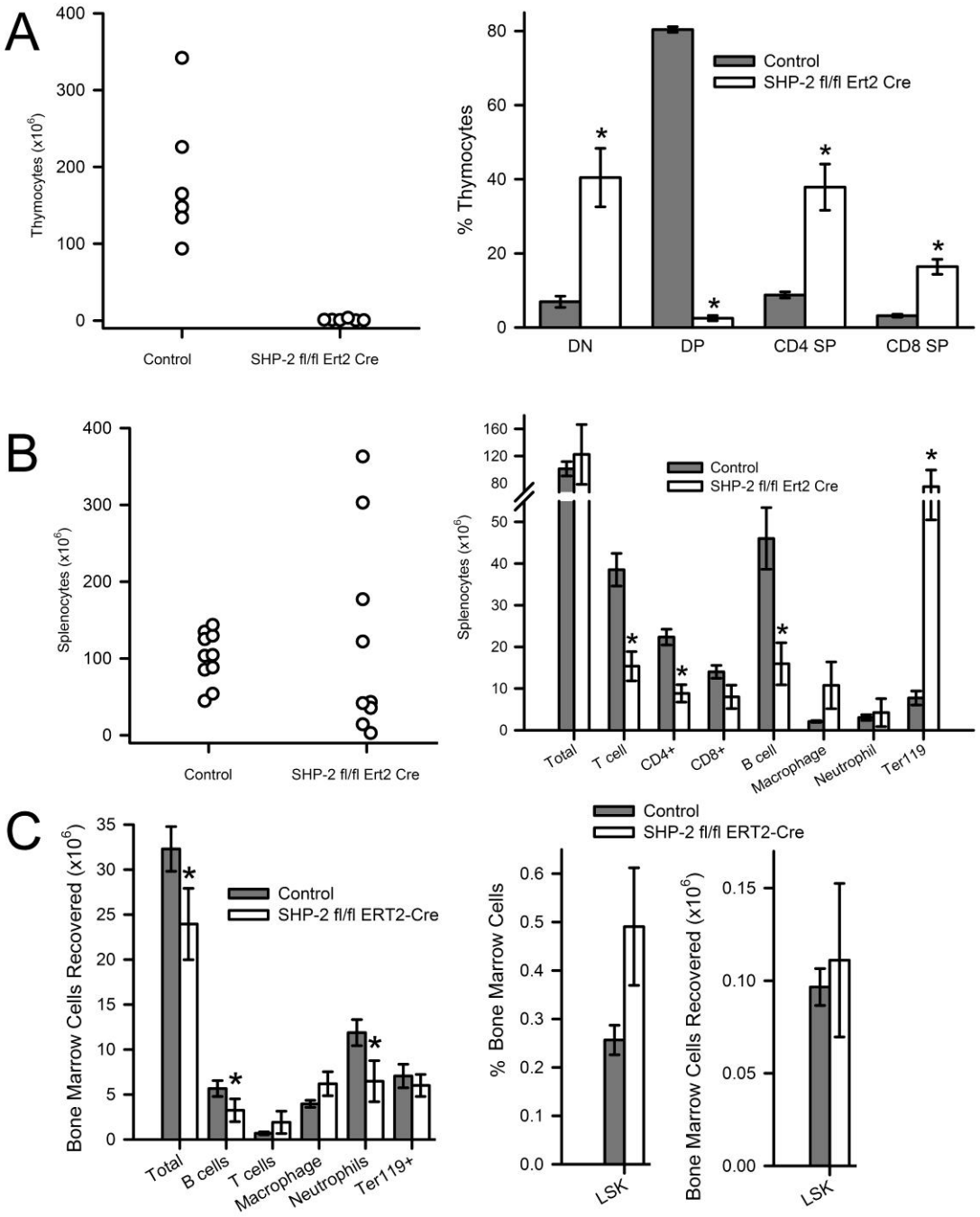

Figure 19 Impaired hematopoiesis in SHP-2 fl/fl ERT2-Cre mice

A) (Left) Thymic cellularity and (right) percent representation of double negative (DN), double positive (DP) and single positive (SP) thymocytes isolated from moribund SHP-2 fl/fl ERT2-Cre mice (n=6) and littermate controls (n=6). B) (Left) Splenic cellularity and (Right) populations of leukocyte subsets and developing erythrocytes were enumerated following flow cytometric staining from control (n=10) and moribund induced SHP-2 deficient mice (n=9). C) (Left) Cellularity of the bone marrow compartment, determined as in B. (Middle) Populations and (right) numbers of $Lin^{-}c\text{-}Kit^{+}sca\text{-}1^{+}$ cells, which are enriched for HSC, were determined by flow cytometry (n=3 for contol and induced SHP-2 animals). In scatter plots, each symbol represents an individual mouse. In bar graphs, the means +/- one standard error are depicted. *, $p<.05$ as determined by paired Student's T-test.

numbers of Ter119+ cells, which are late-stage developing erythrocytes, in the spleen are evidence of extramedullary hematopoiesis (EMH).

The reduced thymic size and EMH in the spleen led us to further examine the cellularity of the bone marrow compartment. A significant decrease in the number of cells recovered from bone marrow was reproducibly observed (Fig 19C). Diminished numbers and percentages of B cells and neutrophils were seen, and increases of the cellularity and percentage representation of T cells and macrophages were observed. We next determined whether a decrease in the number of hematopoietic stem cells (HSC) could account for the near complete absence of thymocytes and splenic EMH in SHP-2 fl/fl ERT2-Cre mice. Total numbers of $Lin^{-}Sca\text{-}1^{+}c\text{-}kit^{+}$ (LSK) cells, a population enriched in HSC, isolated from the hind limbs of SHP-2 fl/fl ERT2-Cre mice and littermate controls however remain unchanged (Fig 19C). Therefore, the thymic involution and splenic EMH are not the result of a collapse of HSC renewal in the bone marrow.

4.4.4 Development of severe spinal curvature in the absence of SHP-2

The most striking phenotype exhibited by SHP-2 fl/fl ERT2-Cre mice is the rapid development of altered spinal morphology. Beginning four weeks following tamoxifen treatment, SHP-2 fl/fl ERT2-Cre mice show evidence of a pronounced dorsal curvature of the spine. X-ray analysis of these spines confirmed induced SHP-2 deficient mice exhibit significantly increased kyphosis compared to littermate control animals (Fig 20A). Although less apparent during visual inspection of live animals, necropsy additionally revealed scoliosis of SHP-2 fl/fl ERT2-Cre spinal columns. Analysis of X-ray images showed increased radiodensity of the vertebral bodies in induced SHP-2

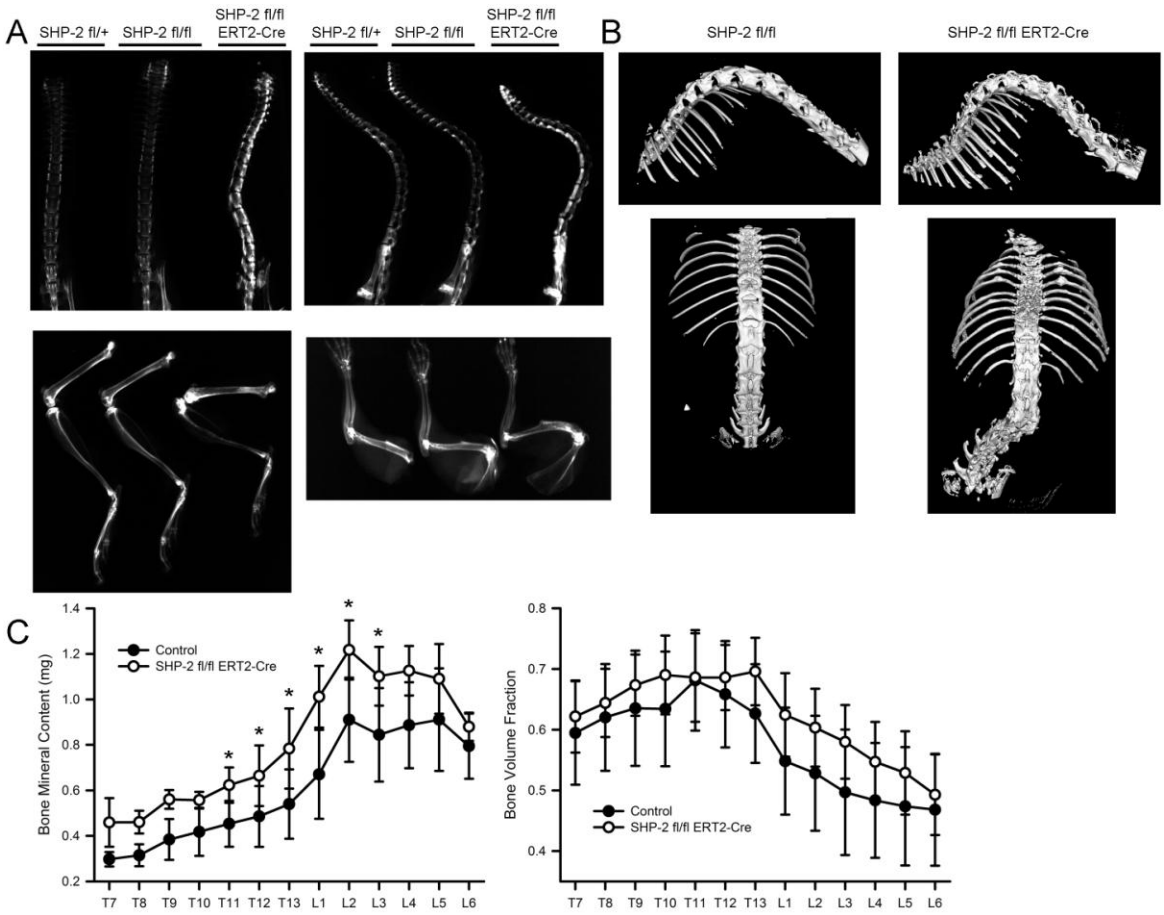

Figure 20 Spinal curvature and increased bone mineral content in SHP-2 fl/fl ERT2-Cre mice

A) X-rays of SHP-2 fl/fl ERT2-Cre mice reveals scoliosis and kyphosis compared to littermate controls. X-rays further demonstrate increased radiodensity in vertebral bodies and in the femur and humerus from mice that survive at least six weeks post tamoxifen injection. B) Visualizations of the isosurfaces generated by microCT confirms spinal curvature in induced SHP-2 deficient animals. C) Quantification of bone mineral content and bone volume fraction from microCT analysis of individual thoracic (T) and lumbar (L) vertebrae reveals trends towards increased and more mineralized bone in SHP-2 fl/fl ERT2-Cre mice, with statistical significance in some individual vertebral bodies. *, $p<.05$ determined by paired Student's T-test.

deficient mice. Furthermore, increased lifespan following tamoxifen injection correlated to accumulation of radiodensity in SHP-2 fl/fl ERT2-Cre humeri and femora. To quantitate the increased bone in SHP-2 fl/fl ERT2-Cre spines, a cohort of mice which survived five weeks post tamoxifen injection were analyzed by microCT (Fig 20B). SHP-2 fl/fl ERT2-Cre mice exhibit increased bone mineral content in some vertebrae and a trend towards a higher bone volume fraction in vertebral bodies (Fig 20C). These

results are especially apparent in the lower thoracic and lumbar vertebrae, which are most affected by scoliosis.

4.4.5 Bone and cartilage homeostasis defects in induced SHP-2 deficient mice

To investigate the mechanism underlying the altered spinal morphology in SHP-2 fl/fl ERT2-Cre deficient mice, we analyzed histological sections of vertebral bodies. Consistent with previous results, induced SHP-2 deficient vertebrae exhibited increased trabecular bone (Fig 21). The metaphyses of femora and humeri from SHP-2 fl/fl ERT2-Cre mice show similarly increased trabecular bone. The organization of cortical bone layers is also disrupted in SHP-2 fl/fl ERT2-Cre long bones. Cartilaginous growth plates from induced SHP-2 deficient mice exhibited disorganization and the absence of columnar morphology of differentiating chondrocytes. Ectopic cartilage was also observed in both vertebrae and long bones of SHP-2 fl/fl ERT2-Cre mice (Fig 21).

4.5 Discussion

To determine the role of SHP-2 in mature animals, SHP-2 fl/fl mice were crossed with ERT2-Cre transgenic mice to mediate the temporal deletion of SHP-2. Weight loss and rapid death are seen in these induced SHP-2 deficient mice. Cardiac abnormalities observed in human patients with SHP-2 mutations are absent from SHP-2 fl/fl ERT2-Cre mice. We report severe anemia in induced SHP-2 deficient mice. These data may support previous results suggesting SHP-2 association with the erythropoietin receptor is required for full proliferative activity of developing erythrocytes [147]. Elevated reticulocyte numbers in response to the anemia of SHP-2 fl/fl ERT2-Cre mice however suggest that all but the latest stage of erythropoiesis remains grossly intact. An additional

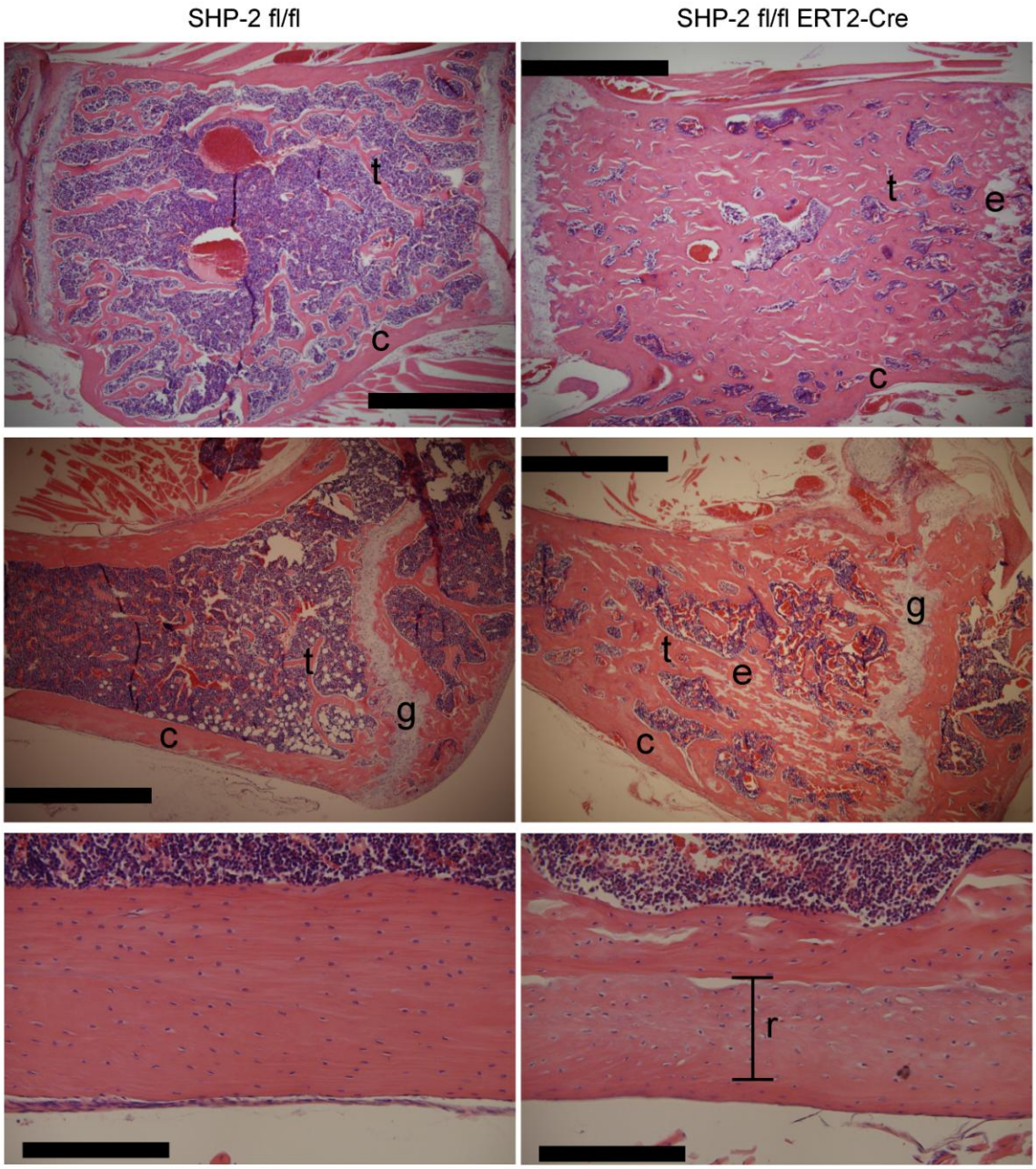

Figure 21 Increased and disorganized cartilage and bone in SHP-2 fl/fl ERT2-Cre mice

H&E stained sections of L4 vertebrae (top) and femora (middle and bottom) from induced SHP-2 deficient mice and littermate controls. In these sections, bone is stained pink, cartilage is lavender and bone marrow stains violet. Trabecular bone (t) is greatly increased in SHP-2 fl/fl ERT2-Cre mice. Cortical bone (c) thickness is similar between induced SHP-2 deficient and control mice, while remodeled (r) cortical bone exhibits a disorganized structure in SHP-2 fl/fl ERT2-Cre mice. Cartilaginous growth plates (g) are disorganized in induced SHP-2 deficient mice. These mice also have ectopic cartilage (e) in both vertebral bodies and femora. Scale bars: Top, Middle: 1mm. Bottom: 200μm.

role for SHP-2 in the maturation of erythrocytes from reticulocytes could explain the anemia in these mice, or the anemia might not be an erythryocyte cell-autonomous effect. Furthermore the anemic state of induced SHP-2 deficient mice may be the cause of the metabolite results that suggest altered kidney and liver function. Decreased serum glucose levels in SHP-2 fl/fl ERT-2 Cre mice may reflect the well known role of SHP-2 as a positive regulator of growth hormone signal transduction, as growth hormone increases serum glucose levels [148].

The homeostatic maintenance of many tissues, including the epidermal and skeletal systems, requires balance between proliferation and post-mitotic differentiation. SHP-2 mediated regulation of both the Ras-MAPK and PI3K-AKT pathways has been widely reported and would be consistent with a role for SHP-2 in proliferation/differentiation decisions in precursor cells. Increased Ras-MAPK signaling results in the terminal differentiation and inhibition of proliferation of keratinocytes [149,150]. Therefore the absence of the positive regulator SHP-2 in Ras-MAPK signal transduction could be predicted to result in increased proliferation, which is likely to account for acanthosis in SHP-2 ERT2-Cre mice. However, the published literature on Ras-MAPK signaling in promotion versus inhibition of proliferation in keratinocytes is controversial [151].

Diminished precursor cell differentiation rates may be similarly responsible for the collapse of thymic development despite similar numbers of HSC isolated from induced SHP-2 deficient hind limbs compared to littermate control animals. There is precedence for a role for SHP-2 in these proliferation/differentiation decisions, as SHP-2 deficient embryonic stem cells exhibit reduced differentiation and undergo increased self-

renewal [152]. A role for SHP-2 in hematopoiesis has been previously reported by a number of laboratories. However, these experiments examine the development of hematopoietic precursors from SHP-2 deficient ES cells. As ES cell differentiation to mesoderm and mesoderm differentiation to hemangioblast cells both require SHP-2, specific roles for SHP-2 in the generation of lymphoid, myeloid, or erythroid cells from HSCs has not been previously shown [152,153].

Alternatively, the hematopoiesis deficiencies in induced SHP-2 deficient mice might instead reveal a role for this PTP in signal transduction pathways that control the fate of precursor cells that are committed to differentiation. Accordingly the absence of SHP-2 might promote the differentiation of common myeloid progenitors (CMP) at the expense of common lymphoid progenitors (CLP), which could account for the reduced T cell and B cell populations in the periphery of SHP-2 fl/fl ERT2-Cre mice. Similarly, increased granulocyte-monocyte precursor (GMP) differentiation into macrophages with corresponding reduced neutrophil (and osteoclast) differentiation could be explained by such a function for SHP-2 in differentiation fate decisions. Experiments enumerating these precursor cells in the bone marrow of SHP-2 fl/fl ERT2-Cre mice to test this hypothesis are ongoing in the laboratory.

The cartilage and bone remodeling defects of SHP-2 deficient mice, resulting in increased and disordered bone and disorganized and ectopic cartilage, is particularly striking due to the severity of disease. Increased time to death following tamoxifen injection correlates with further severity of each of these phenotypes, as would be expected due to altered cartilage and bone homeostasis. Curved spinal morphology is seen in NS patients, 10-15% of whom have been anecdotally estimated to exhibit spinal

curvature [142]. Recently, the first study to specifically enumerate the frequency of scoliosis and kyphosis in NS patients revealed that 18 of 60 (30%) Korean NS patients are affected [154]. Skeletal defects in humans with SHP-2 mutations are not confined to the spinal column, as chest deformity in the form of pectus carnatum or pectus excavatum is observed in both NS and LS patients [155,156].

In contrast to our findings reported here, mice deficient in signal transduction through the SHP-2-Ras-MAPK pathway downstream of the cytokine receptor gp130 ($gp130^{Y757F}$) are osteopenic [157]. Elevated bone turnover was observed, with high levels of both bone formation and bone resorption. Increased numbers of osteoclasts were seen in these mice, and furthermore osteoclasts isolated from $gp130^{Y757F}$ mice exhibited increased bone resorptive properties. Interestingly, cartilaginous defects were not reported in these mice. Although the $gp130^{Y757F}$ knock-in mouse findings appear to contradict the results reported here, the discrepancies likely reflect a role for SHP-2 in multiple signaling pathways that affect bone turnover, which in SHP-2 fl/fl ERT2-Cre mice results in a net gain of bone. Alternatively, $gp130^{Y757}$ might additionally signal through a SHP-2 independent pathway that exerts a dominant effect on bone homeostasis. Another possibility is that these data might reflect differing roles for SHP-2 in bone development as compared to bone homeostasis, since SHP-2 fl/fl ERT2-Cre mice have normal bone development whereas $gp130^{Y757F}$ mice are deficient in SHP-2 signaling from the initiation of embryogenesis.

A requirement for the Ras-MAPK pathway in signal transduction from cell surface receptors in osteoclastogenesis is known. RANKL, M-CSF, and TNF-α, the former two of which are together necessary and sufficient for the generation of

osteoclasts from monocyte-like precursors, have been shown to signal through the Ras-MAPK pathway in osteoclastogenesis [158-160]. Roles for SHP-2 in potentiating signals from RANK and the M-CSF receptor to promote osteoclastogenesis might be dominant to the inhibition of osteoclast development via a gp130 signal. Additional previously described roles for the Ras-MAPK pathway in osteoclast survival would further reduce the numbers of osteoclasts present in these mice [161].

We hypothesize that the osteopetrosis in SHP-2 fl/fl ERT2-Cre mice might reflect both osteoclast and osteoblast-based roles for SHP-2. The increased bone formation and turnover rate in gp130^{Y757F} mice suggests that SHP-2 fl/fl ERT2-Cre mice might exhibit similar deficiencies. Independent roles for SHP-2 in Ras-MAPK signal transduction from RANK and M-CSF receptors in osteoclastogenesis would result in suboptimal osteoclast generation in SHP-2 fl/fl ERT2-Cre mice. The possibility of deleting SHP-2 expression *in vitro* as well as *in vivo* will allow further dissection of the roles for SHP-2 in the generation of osteo- and chondro-blasts/clasts and the interplay between these cells that result in defective bone and cartilage homeostasis. Such studies are currently ongoing in the laboratory.

Chapter 5: Conclusion

PTP are important signaling molecules implicated in many signal transduction pathways that serve to direct appropriate cellular responses to received stimuli. For the majority of the 107 genes encoding PTP in the human and mouse genomes, the physiological functions of the protein products of these genes remain to be defined. The work herein initially focused on the roles of the related PTPN3 and PTPN4 in T cells, the cell type in which these PTP had been hypothesized to play an important role. We have definitively shown that neither PTPN3 nor PTPN4 dephosphorylate TCRζ or otherwise regulate TCR signal transduction. We next sought to test the hypothesis that the PTP SHP-2 dephosphorylates TCRζ in mature T cells. Our investigations into the role of SHP-2 in adult animals describe functions for SHP-2 in hematopoiesis and bone and cartilage homeostasis. These results are summarized and discussed below.

5.1 Analysis of the Function of PTPN3 and PTPN4

Prior to the initiation of our studies on PTPN3 and PTPN4, there was considerable interest over the functions of these PTP as negative regulators of TCR signal transduction. In chapter 2, we generated PTPN3 knockout mice by two independent methods, gene-targeting and gene-trap technology. The gene-trapped ES cell was of

strain 129 origin; these ES cells are known to be easily germline transmitted. Gene-targeting by engineering *loxp* sites into the genome permits the tissue-specific deletion of PTPN3 in the event that PTPN3 had been required for embryogenesis. The gene-targeting was performed in C56BL/6 ES cells, which rendered unnecessary the time-intensive backcrossing to an immunologically-defined strain normally associated with knockout mouse characterization. Upon demonstration that PTPN3 was dispensable for TCR signal transduction, we suspected overlapping function between PTPN4 and PTPN3. PTPN4-deficient mice were generated from ES cells with a gene-trapping cassette integrated into the PTPN4 locus. As T cells from PTPN3-PTPN4 double-deficient mice are indistinguishable from wild-type T cells, we disproved the hypothesis that PTPN3 and PTPN4 have overlapping function. We further investigated whether PTPN13, the remaining member of the FERM- and PDZ-domain containing PTP family, could functionally compensate for the loss of PTPN3 and PTPN4 in T cells. Niether proximal TCR signal transduction nor differentiation of T-helper subsets indicated overlapping function between PTPN3, PTPN4, and PTPN13.

The identity of the physiologically-relevant TCRζ-dephosphorylating PTP remains unclear. A screen using substrate trapping mutants of PTP to pull down TCRζ did not reveal any other PTP besides PTPN3 and PTPN4 that could interact with TCRζ [71]. Biochemical fractionation of Jurkat cells indicated SHP-1 and PTPN3 were present in TCRζ-dephosphorylating fractions. SHP-1 expression is restricted to the hematopoietic system, and this PTP is recruited to the TCR complex in activated T cells. Since SHP-1 is known to dephosphorylate and thereby inactivate LCK and ZAP-70, this PTP is therefore active in the subcellular compartment where a TCRζ-dephosphorylating

PTP would function. As yet there is no biochemical evidence that SHP-1 can associate with or dephosphorylate TCRζ. Furthermore, experiments separating a physiological role for SHP-1 in the dephosphorylation of TCRζ from LCK and ZAP-70 dephosphorylation remain technically challenging. Nevertheless, the aforementioned localization of SHP-1 makes this PTP perhaps the most enticing candidate TCRζ-dephosphorylating enzyme. It remains possible that SHP-2 functions to dephosphorylate TCRζ, as our experiments were not able to test such a role for SHP-2 (see below).

Although the regulation of TCR signal transduction was the most cited role for PTPN3 and PTPN4, other functions for these gene products have been proposed. PTPN3 has been reported to negatively regulate growth hormone receptor signal transduction via dephosphorylation of the receptor. However, mice in our PTPN3-deficient and PTPN3-PTPN4 double-deficient colonies do not exhibit increased weight as would be predicted of such a role. PTPN4 has been reported to interact with the glutamate receptor GluRδ2, and signals from GluRδ2 are required for cerebellar long-term depression (CLTD). Learning and coordination require CLTD, and accordingly roles for PTPN4 and PTPN3 in motor learning have been proposed. In *Drosophila*, deficiency of PTPMEG, the single homologue of PTPN4 and PTPN3 in this species, results in defective axon growth. These flies often become trapped alive in their food, suggesting impaired balance and coordination. However, accelerated rotorod experiments revealed intact motor learning in our PTPN3-PTPN4 double-deficient mice.

After examining additional proposed roles for PTPN3 and PTPN4 from the literature not discussed here, we sought proteins that interact with the modular domains of these PTP to suggest previously undefined functions. Yeast 3-hybrid screens, which

included a promiscuous PTK domain to phosphorylate potential PTP binding partners, did generate new potential interaction partners for PTPN3. To determine PTPN4-binding proteins, constructs of single or multiple domains of PTPN4 were used to pull-down interacting proteins from Jurkat lysates which were identified by mass spectrometry. For neither PTPN3 nor PTPN4 were specific classes of proteins or well-defined molecules in known cellular signal transduction cascades identified that could suggest a role for PTPN3 or PTPN4 in any cell type.

While our experiments have not revealed a function for PTPN3 and PTPN4 in T cells, the physiological role of these PTP in mice or humans remains unknown. Previously proposed functions for these PTP originated in cell line overexpression studies. While these types of studies can be invaluable in defining novel roles for gene products, the definitive method of determining the role of a molecule is to characterize the phenotype of knockout animals. A further example of the limitation of studies using cell lines is the initial excitement generated by the detection of multiple PTP-encoding genes mutated in colorectal cancer cell lines, including PTPN3 and PTPN13 [116]. However, a follow-up study did not find any of the same nonreceptor PTP genes mutated in colorectal cancer biopsies [162].

Overlapping function between the family of PTP that encode FERM domains (PTPN3, PTPN4, PTPN13, PTPN14, PTPN21) might explain the apparent lack of a role for PTPN3 and PTPN4 in all experimental systems tested thus far; alternatively it is possible that these two PTP are redundant and not functionally required in mammals. Unlike prokaryotes, genomic size in higher eukaryotes is not regulated by intense selective pressures, thus the presence of PTPN3 and PTPN4 in the genome may be an

evolutionary artifact. However, the absence of mutations in the coding sequence of PTPN3 or PTPN4 that would result in defective splicing, premature translation termination, or ablation of domain structure argues against the notion that these genes have not been retained by natural selection. A more likely explanation is that our experiments have not yet examined the specific setting in which these PTP are required, in the immune system or otherwise. For example, the functions of the immune system of inbred mouse strains in a specific pathogen-free laboratory setting is significantly different than that required by wild mice in the natural environment. Furthermore, the majority of our experiments have utilized non-physiological stimulation of the immune system. Experiments of this type exhibit suboptimal sensitivity, which may preclude the detection of a more subtle role for these PTP. The strains developed in this work will be important to validate future hypotheses regarding the physiological role of PTPN3 and PTPN4 in mice.

5.2 SHP-2 Function in T cells

Roles for SHP-2 in multiple signaling pathways in many cell types have been reported. Targeted deletion of SHP-2 exon 2 or exon 3 in mice results in embryonic lethality by day 10.5. This requirement for SHP-2 in embryogenesis had precluded definitive studies on the physiological function of this ubiquitously expressed PTP in mature animals. Roles for SHP-2 in the differentiation of ES cells to many cells types including the earliest hematopoietic and limb bud precursors were shown using SHP-2 exon3 -/- ES cells [163,164]. However, the interpretation of these experiments is complicated by expression of a truncated SHP-2 protein in SHP-2 exon3 -/- mice [40].

The exon 3 -/- SHP-2 protein has a nonfunctional NH_2-terminal SH2 domain, and thus exhibits increased activity and altered intracellular targeting. Attempts to circumvent the lethality associated with SHP-2 deficient embryos included the overexpression of catalytically inactive SHP-2^{C459S} in a tissue-restricted manner [165]. SHP-2^{C459S} overexpressing T cells develop normally but exhibit increased secretion of T_H2-specific cytokines.

The recently described SHP-2 exon 4 fl/fl mice exhibit SHP-2 deficiency in Cre-targeted tissues and represent the definitive method by which the function of SHP-2 can be described in various cell types. Deletion of SHP-2 mediated by LCK-Cre revealed a role for SHP-2 in pre-TCR signal transduction. The discrepancy of results between SHP-2^{C459S} and SHP-2 deficient thymocytes may represent the general limitation of overexpression studies in mice using dominant negative mutants. However, in our experiments, we were unable to demonstrate deletion of SHP-2 protein from peripheral T cells or thymocytes using multiple Cre transgenes. The ERT2-Cre system mediates successful recombination of the SHP-2 allele in many tissues (Fig 17), and furthermore our laboratory has shown that this Cre is able to recombine other floxed alleles in T cells. The observation that the SHP-2 locus is resistant to Cre-mediated recombination in T cells has also been made by other laboratories [165]. The unexplained resistance of mature T cells to Cre-mediated recombination, possibly due to a compact chromatin structure which renders the locus inaccessible, represents a significant challenge to the definitive characterization of the role of SHP-2 in this cell type.

5.3 SHP-2 in Proliferation/Differentiation Cell Fate Decisions

The homeostatic maintenance of many tissues, including the hematopoietic, epidermal and skeletal systems, requires balance between proliferation and post-mitotic differentiation. SHP-2 mediated regulation of both the Ras-MAPK and PI3K-AKT pathways has been widely reported and would explain a possible function for SHP-2 in proliferation/differentiation decisions in multipotent cells.

We hypothesize that a role for SHP-2 in these fate decisions may connect the phenotypes we see in SHP-2 fl/fl ERT2-Cre mice. Acanthosis is caused by hyperproliferation of keratinocytes, a process which would also be expected to result in the hyperkeratosis we observe in these mice. Inhibition of differentiation at the reticulocyte stage of erythrogenesis might be the cause of the anemia observed in SHP-2 fl/fl ERT2-Cre mice. Increased turnover of HSC, or skewed differentiation of HSC toward CMP at the expense of CLP, could be envisaged to result in premature thymic involution. Alternatively, the thymic phenotype might be potentially explained by the loss of a hematopoietic niche due to increasing bone density. While at the pathological level we cannot observe increased bone density until four weeks post tamoxifen injection, changes in the niche microenvironment could take place much sooner.

Bone marrow chimeras might aid in the determination of whether SHP-2 fl/fl ERT2-Cre mice have primary or bone architecture-mediated secondary hematopoietic defects. However, osteoclasts and chondroclasts are hematopoietic in origin and this would complicate the interpretation of results. Accordingly, while normal hematopoietic compartments in experiments where SHP-2 deficient bone marrow is transferred into lethally irradiated wild-type mice would demonstrate a non-cellautonomous cause for

thymic involution and anemia, defective hematopoietic development in these bone marrow chimeras would not be interpretable.

The striking bone and cartilage homeostasis defects require further experimentation to determine the mechanism by which this altered remodeling occurs. We hypothesize that SHP-2 fl/fl ERT2-Cre mice exhibit independent bone and cartilage homeostasis deficiencies. A trend towards increased bone density in induced SHP-2 deficient calvarial bone, which ossifies and is maintained without a cartilaginous matrix, indicates a primary bone defect. Ectopic surface cartilage in the joint spaces of SHP-2 fl/fl ERT2-Cre mice is unrelated to bone alterations and indicates a primary cartilage defect. Cartilaginous matrix-specific staining using alcian blue will be performed to further understand the cartilage defect in induced SHP-2 deficient mice. Subsequent stains for markers of cell proliferation (Ki67) or apoptosis (TUNEL) will provide additional data to characterize the disorganized and ectopic cartilage observed in these mice.

In regards increased bone in SHP-2 fl/fl ERT2-Cre mice, we would predict an imbalance in the ratio of osteoblasts to osteoclasts or their respective activities. Ennumeration of osteoclast numbers in osteopetrotic tissue sections is in progress, and the quantification of osteoclasts normalized to the amount of bone surface will be important to determine if reduced numbers of osteoclasts result in the increased bone in SHP-2 fl/fl ERT2-Cre mice. This mechanism would be predicted at least partially responsible for the osteopetrotic bone, since the Ras-MAPK and PI3K/AKT pathways are required for signal transduction from RANK in osteoclastogenesis [159]. At least three causes of reduced osteoclast numbers beyond diminished RANK signal transduction can

be envisaged. The first might be that SHP-2 is required for expression of RANKL on osteoblasts, which itself is required for osteoclast development. Second, diminished Ras-MAPK activation can result in decreased osteoclast survival in the asbsence of SHP-2 [161]. Thirdly, decreased osteoclast numbers might be secondary to altered differentiation of GMP that favors macrophage development at the expense of osteoclastogenesis.

Regardless of the size of the osteoclast population, osteoclast activity might be reduced in SHP-2 fl/fl ERT2-Cre mice. Haploinsufficiency in mice of the Ras GTPase activating protein NF1, an established Ras-MAPK negative regulator, results in increased osteoclast numbers. These $NF1^{+/-}$ osteoclasts further demonstrate increased bone resorption associated with increased ERK and PI3K/AKT activation [166,167]. These data suggest that Ras-MAPK signals stimulate bone resorption; therefore in SHP-2 deficient mice, we might predict reduced osteoclast activity.

Alternatively, increased trabecular bone in SHP-2 fl/fl ERT2-Cre mice might be the result of increased osteoblast numbers or activity. Roles for Ras-MAPK in osteogenesis are controversial with evidence for both promotion and inhibition of osteoblast development in cell line experiments [168]. However, human NF1 patients exhibit osteopenia and osteoprogenitors from NF1-heterozygous mice possess reduced osteogenic potential, which suggests that physiologically the Ras-MAPK pathway antagonizes osteogenesis [169,170]. We might therefore predict that in SHP-2 fl/fl ERT2-Cre mesenchymal stem cells reduced Ras-MAPK signals promote osteogenesis. This hypothesis can be tested by examining the *in vitro* expansion of osteoblasts from mesenchymal stem cells. A role for SHP-2 in osteoclasts or osteoblasts is not mutually

exclusive. The severity of osteopetrosis might suggest disregulation of both cell types in induced SHP-2 deficient animals.

The importance of SHP-2 regulation of the Ras-MAPK pathway or alternative pathways like the PI3K/AKT pathway in bone and cartilage homeostasis in SHP-2 fl/fl ERT2-Cre mice can be definitively addressed once the responsible cell type(s) have been described. Initial experiments will examine the requirement for SHP-2 in the development of these cell types. The ability to delete SHP-2 in a temporal fashion in SHP-2 fl/fl ERT2-Cre mice permits the isolation of SHP-2 sufficient cells that have undergone normal differentiation and allows their functions to be tested in the absence of this PTP. Further characterization of the role for SHP-2 in bone homeostasis might result in a novel treatment for osteoporosis if transient inhibitors of SHP-2 activity could be specifically targeted to the skeletal system.

References

1. Alonso A, Sasin J, Bottini N, Friedberg I, Osterman A, Godzik A, Hunter T, Dixon J, Mustelin T (2004) Protein tyrosine phosphatases in the human genome. Cell 117: 699-711.
2. Tiganis T, Bennett AM (2007) Protein tyrosine phosphatase function: the substrate perspective. Biochem J 402: 1-15.
3. Andersen JN, Mortensen OH, Peters GH, Drake PG, Iversen LF, Olsen OH, Jansen PG, Andersen HS, Tonks NK, Moller NP (2001) Structural and evolutionary relationships among protein tyrosine phosphatase domains. Mol Cell Biol 21: 7117-7136.
4. Tonks NK (2006) Protein tyrosine phosphatases: from genes, to function, to disease. Nat Rev Mol Cell Biol 7: 833-846.
5. Andersen JN, Jansen PG, Echwald SM, Mortensen OH, Fukada T, Del Vecchio R, Tonks NK, Moller NP (2004) A genomic perspective on protein tyrosine phosphatases: gene structure, pseudogenes, and genetic disease linkage. FASEB J 18: 8-30.
6. Tonks NK, Neel BG (2001) Combinatorial control of the specificity of protein tyrosine phosphatases. Curr Opin Cell Biol 13: 182-195.
7. Kenneth M. Murphy PT, Mark Walport (2007) Janeway's Immunobiology, 7th Edition. New York: Garland Science.
8. Bluestone JA (1995) New perspectives of CD28-B7-mediated T cell costimulation. Immunity 2: 555-559.
9. Palacios EH, Weiss A (2004) Function of the Src-family kinases, Lck and Fyn, in T-cell development and activation. Oncogene 23: 7990-8000.
10. Veillette A, Bookman MA, Horak EM, Bolen JB (1988) The CD4 and CD8 T cell surface antigens are associated with the internal membrane tyrosine-protein kinase p56lck. Cell 55: 301-308.
11. Pitcher LA, van Oers NS (2003) T-cell receptor signal transmission: who gives an ITAM? Trends Immunol 24: 554-560.
12. Chu DH, Morita CT, Weiss A (1998) The Syk family of protein tyrosine kinases in T-cell activation and development. Immunol Rev 165: 167-180.
13. Sommers CL, Samelson LE, Love PE (2004) LAT: a T lymphocyte adapter protein that couples the antigen receptor to downstream signaling pathways. Bioessays 26: 61-67.
14. Ohashi PS (2002) T-cell signalling and autoimmunity: molecular mechanisms of disease. Nat Rev Immunol 2: 427-438.

15. Fisher GH, Rosenberg FJ, Straus SE, Dale JK, Middleton LA, Lin AY, Strober W, Lenardo MJ, Puck JM (1995) Dominant interfering Fas gene mutations impair apoptosis in a human autoimmune lymphoproliferative syndrome. Cell 81: 935-946.
16. Takahashi T, Tanaka M, Brannan CI, Jenkins NA, Copeland NG, Suda T, Nagata S (1994) Generalized lymphoproliferative disease in mice, caused by a point mutation in the Fas ligand. Cell 76: 969-976.
17. Watanabe-Fukunaga R, Brannan CI, Copeland NG, Jenkins NA, Nagata S (1992) Lymphoproliferation disorder in mice explained by defects in Fas antigen that mediates apoptosis. Nature 356: 314-317.
18. Rieux-Laucat F, Le Deist F, Hivroz C, Roberts IA, Debatin KM, Fischer A, de Villartay JP (1995) Mutations in Fas associated with human lymphoproliferative syndrome and autoimmunity. Science 268: 1347-1349.
19. Bouillet P, Metcalf D, Huang DC, Tarlinton DM, Kay TW, Kontgen F, Adams JM, Strasser A (1999) Proapoptotic Bcl-2 relative Bim required for certain apoptotic responses, leukocyte homeostasis, and to preclude autoimmunity. Science 286: 1735-1738.
20. Benoist C, Mathis D (2001) Autoimmunity provoked by infection: how good is the case for T cell epitope mimicry? Nat Immunol 2: 797-801.
21. Ohashi PS, Oehen S, Buerki K, Pircher H, Ohashi CT, Odermatt B, Malissen B, Zinkernagel RM, Hengartner H (1991) Ablation of "tolerance" and induction of diabetes by virus infection in viral antigen transgenic mice. Cell 65: 305-317.
22. Oldstone MB, Nerenberg M, Southern P, Price J, Lewicki H (1991) Virus infection triggers insulin-dependent diabetes mellitus in a transgenic model: role of anti-self (virus) immune response. Cell 65: 319-331.
23. Parsons MJ, Jones RG, Tsao MS, Odermatt B, Ohashi PS, Woodgett JR (2001) Expression of active protein kinase B in T cells perturbs both T and B cell homeostasis and promotes inflammation. J Immunol 167: 42-48.
24. Goldrath AW, Bogatzki LY, Bevan MJ (2000) Naive T cells transiently acquire a memory-like phenotype during homeostasis-driven proliferation. J Exp Med 192: 557-564.
25. Brunkow ME, Jeffery EW, Hjerrild KA, Paeper B, Clark LB, Yasayko SA, Wilkinson JE, Galas D, Ziegler SF, Ramsdell F (2001) Disruption of a new forkhead/winged-helix protein, scurfin, results in the fatal lymphoproliferative disorder of the scurfy mouse. Nat Genet 27: 68-73.
26. Chatila TA, Blaeser F, Ho N, Lederman HM, Voulgaropoulos C, Helms C, Bowcock AM (2000) JM2, encoding a fork head-related protein, is mutated in X-linked autoimmunity-allergic disregulation syndrome. J Clin Invest 106: R75-81.
27. Fontenot JD, Gavin MA, Rudensky AY (2003) Foxp3 programs the development and function of CD4+CD25+ regulatory T cells. Nat Immunol 4: 330-336.
28. Khattri R, Cox T, Yasayko SA, Ramsdell F (2003) An essential role for Scurfin in CD4+CD25+ T regulatory cells. Nat Immunol 4: 337-342.
29. Hori S, Nomura T, Sakaguchi S (2003) Control of regulatory T cell development by the transcription factor Foxp3. Science 299: 1057-1061.
30. Ochs HD, Ziegler SF, Torgerson TR (2005) FOXP3 acts as a rheostat of the immune response. Immunol Rev 203: 156-164.

31. Hendriks WJ, Elson A, Harroch S, Stoker AW (2008) Protein tyrosine phosphatases: functional inferences from mouse models and human diseases. FEBS J 275: 816-830.
32. Kane LP, Weiss A (2003) The PI-3 kinase/Akt pathway and T cell activation: pleiotropic pathways downstream of PIP3. Immunol Rev 192: 7-20.
33. Song J, Lei FT, Xiong X, Haque R (2008) Intracellular signals of T cell costimulation. Cell Mol Immunol 5: 239-247.
34. Di Cristofano A, Kotsi P, Peng YF, Cordon-Cardo C, Elkon KB, Pandolfi PP (1999) Impaired Fas response and autoimmunity in Pten+/- mice. Science 285: 2122-2125.
35. Suzuki A, Yamaguchi MT, Ohteki T, Sasaki T, Kaisho T, Kimura Y, Yoshida R, Wakeham A, Higuchi T, Fukumoto M, et al. (2001) T cell-specific loss of Pten leads to defects in central and peripheral tolerance. Immunity 14: 523-534.
36. Moody JL, Jirik FR (2004) Compound heterozygosity for Pten and SHIP augments T-dependent humoral immune responses and cytokine production by CD(4+) T cells. Immunology 112: 404-412.
37. Chiang YJ, Kole HK, Brown K, Naramura M, Fukuhara S, Hu RJ, Jang IK, Gutkind JS, Shevach E, Gu H (2000) Cbl-b regulates the CD28 dependence of T-cell activation. Nature 403: 216-220.
38. Bachmaier K, Krawczyk C, Kozieradzki I, Kong YY, Sasaki T, Oliveira-dos-Santos A, Mariathasan S, Bouchard D, Wakeham A, Itie A, et al. (2000) Negative regulation of lymphocyte activation and autoimmunity by the molecular adaptor Cbl-b. Nature 403: 211-216.
39. Mustelin T, Vang T, Bottini N (2005) Protein tyrosine phosphatases and the immune response. Nat Rev Immunol 5: 43-57.
40. Pao LI, Badour K, Siminovitch KA, Neel BG (2007) Nonreceptor protein-tyrosine phosphatases in immune cell signaling. Annu Rev Immunol 25: 473-523.
41. Ostergaard HL, Shackelford DA, Hurley TR, Johnson P, Hyman R, Sefton BM, Trowbridge IS (1989) Expression of CD45 alters phosphorylation of the lck-encoded tyrosine protein kinase in murine lymphoma T-cell lines. Proc Natl Acad Sci U S A 86: 8959-8963.
42. Sieh M, Bolen JB, Weiss A (1993) CD45 specifically modulates binding of Lck to a phosphopeptide encompassing the negative regulatory tyrosine of Lck. Embo J 12: 315-321.
43. Sicheri F, Moarefi I, Kuriyan J (1997) Crystal structure of the Src family tyrosine kinase Hck. Nature 385: 602-609.
44. Xu W, Harrison SC, Eck MJ (1997) Three-dimensional structure of the tyrosine kinase c-Src. Nature 385: 595-602.
45. Trowbridge IS, Thomas ML (1994) CD45: an emerging role as a protein tyrosine phosphatase required for lymphocyte activation and development. Annu Rev Immunol 12: 85-116.
46. Byth KF, Conroy LA, Howlett S, Smith AJ, May J, Alexander DR, Holmes N (1996) CD45-null transgenic mice reveal a positive regulatory role for CD45 in early thymocyte development, in the selection of CD4+CD8+ thymocytes, and B cell maturation. J Exp Med 183: 1707-1718.

47. Mee PJ, Turner M, Basson MA, Costello PS, Zamoyska R, Tybulewicz VL (1999) Greatly reduced efficiency of both positive and negative selection of thymocytes in CD45 tyrosine phosphatase-deficient mice. Eur J Immunol 29: 2923-2933.
48. Tchilian EZ, Wallace DL, Wells RS, Flower DR, Morgan G, Beverley PC (2001) A deletion in the gene encoding the CD45 antigen in a patient with SCID. J Immunol 166: 1308-1313.
49. Kung C, Pingel JT, Heikinheimo M, Klemola T, Varkila K, Yoo LI, Vuopala K, Poyhonen M, Uhari M, Rogers M, et al. (2000) Mutations in the tyrosine phosphatase CD45 gene in a child with severe combined immunodeficiency disease. Nat Med 6: 343-345.
50. Majeti R, Xu Z, Parslow TG, Olson JL, Daikh DI, Killeen N, Weiss A (2000) An inactivating point mutation in the inhibitory wedge of CD45 causes lymphoproliferation and autoimmunity. Cell 103: 1059-1070.
51. Majeti R, Bilwes AM, Noel JP, Hunter T, Weiss A (1998) Dimerization-induced inhibition of receptor protein tyrosine phosphatase function through an inhibitory wedge. Science 279: 88-91.
52. Tsui HW, Siminovitch KA, de Souza L, Tsui FW (1993) Motheaten and viable motheaten mice have mutations in the haematopoietic cell phosphatase gene. Nat Genet 4: 124-129.
53. Shultz LD, Coman DR, Bailey CL, Beamer WG, Sidman CL (1984) "Viable motheaten," a new allele at the motheaten locus. I. Pathology. Am J Pathol 116: 179-192.
54. Lorenz U, Ravichandran KS, Burakoff SJ, Neel BG (1996) Lack of SHPTP1 results in src-family kinase hyperactivation and thymocyte hyperresponsiveness. Proc Natl Acad Sci U S A 93: 9624-9629.
55. Kamata T, Yamashita M, Kimura M, Murata K, Inami M, Shimizu C, Sugaya K, Wang CR, Taniguchi M, Nakayama T (2003) src homology 2 domain-containing tyrosine phosphatase SHP-1 controls the development of allergic airway inflammation. J Clin Invest 111: 109-119.
56. Zhang J, Somani AK, Siminovitch KA (2000) Roles of the SHP-1 tyrosine phosphatase in the negative regulation of cell signalling. Semin Immunol 12: 361-378.
57. Cloutier JF, Veillette A (1996) Association of inhibitory tyrosine protein kinase p50csk with protein tyrosine phosphatase PEP in T cells and other hemopoietic cells. EMBO J 15: 4909-4918.
58. Cloutier JF, Veillette A (1999) Cooperative inhibition of T-cell antigen receptor signaling by a complex between a kinase and a phosphatase. J Exp Med 189: 111-121.
59. Hasegawa K, Martin F, Huang G, Tumas D, Diehl L, Chan AC (2004) PEST domain-enriched tyrosine phosphatase (PEP) regulation of effector/memory T cells. Science 303: 685-689.
60. Vang T, Congia M, Macis MD, Musumeci L, Orru V, Zavattari P, Nika K, Tautz L, Tasken K, Cucca F, et al. (2005) Autoimmune-associated lymphoid tyrosine phosphatase is a gain-of-function variant. Nat Genet 37: 1317-1319.
61. Vang T, Miletic AV, Bottini N, Mustelin T (2007) Protein tyrosine phosphatase PTPN22 in human autoimmunity. Autoimmunity 40: 453-461.

62. Yang Q, Tonks NK (1991) Isolation of a cDNA clone encoding a human protein-tyrosine phosphatase with homology to the cytoskeletal-associated proteins band 4.1, ezrin, and talin. Proc Natl Acad Sci U S A 88: 5949-5953.
63. Gu MX, York JD, Warshawsky I, Majerus PW (1991) Identification, cloning, and expression of a cytosolic megakaryocyte protein-tyrosine-phosphatase with sequence homology to cytoskeletal protein 4.1. Proc Natl Acad Sci U S A 88: 5867-5871.
64. Algrain M, Turunen O, Vaheri A, Louvard D, Arpin M (1993) Ezrin contains cytoskeleton and membrane binding domains accounting for its proposed role as a membrane-cytoskeletal linker. J Cell Biol 120: 129-139.
65. Kim E, Niethammer M, Rothschild A, Jan YN, Sheng M (1995) Clustering of Shaker-type K+ channels by interaction with a family of membrane-associated guanylate kinases. Nature 378: 85-88.
66. Sato T, Irie S, Kitada S, Reed JC (1995) FAP-1: a protein tyrosine phosphatase that associates with Fas. Science 268: 411-415.
67. Zimmermann P, Meerschaert K, Reekmans G, Leenaerts I, Small JV, Vandekerckhove J, David G, Gettemans J (2002) PIP(2)-PDZ domain binding controls the association of syntenin with the plasma membrane. Mol Cell 9: 1215-1225.
68. Bompard G, Martin M, Roy C, Vignon F, Freiss G (2003) Membrane targeting of protein tyrosine phosphatase PTPL1 through its FERM domain via binding to phosphatidylinositol 4,5-biphosphate. J Cell Sci 116: 2519-2530.
69. Gjorloff-Wingren A, Saxena M, Han S, Wang X, Alonso A, Renedo M, Oh P, Williams S, Schnitzer J, Mustelin T (2000) Subcellular localization of intracellular protein tyrosine phosphatases in T cells. Eur J Immunol 30: 2412-2421.
70. Han S, Williams S, Mustelin T (2000) Cytoskeletal protein tyrosine phosphatase PTPH1 reduces T cell antigen receptor signaling. Eur J Immunol 30: 1318-1325.
71. Sozio MS, Mathis MA, Young JA, Walchli S, Pitcher LA, Wrage PC, Bartok B, Campbell A, Watts JD, Aebersold R, et al. (2004) PTPH1 is a predominant protein-tyrosine phosphatase capable of interacting with and dephosphorylating the T cell receptor zeta subunit. J Biol Chem 279: 7760-7769.
72. Young JA, Becker AM, Medeiros JJ, Shapiro VS, Wang A, Farrar JD, Quill TA, van Huijsduijnen RH, van Oers NS (2008) The protein tyrosine phosphatase PTPN4/PTP-MEG1, an enzyme capable of dephosphorylating the TCR ITAMs and regulating NF-kappaB, is dispensable for T cell development and/or T cell effector functions. Mol Immunol 45: 3756-3766.
73. Bauler TJ, Hendriks WJ, King PD (2008) The FERM and PDZ domain-containing protein tyrosine phosphatases, PTPN4 and PTPN3, are both dispensable for T cell receptor signal transduction. PLoS ONE 3: e4014.
74. Bauler TJ, Hughes ED, Arimura Y, Mustelin T, Saunders TL, King PD (2007) Normal TCR signal transduction in mice that lack catalytically active PTPN3 protein tyrosine phosphatase. J Immunol 178: 3680-3687.
75. Saxton TM, Henkemeyer M, Gasca S, Shen R, Rossi DJ, Shalaby F, Feng GS, Pawson T (1997) Abnormal mesoderm patterning in mouse embryos mutant for the SH2 tyrosine phosphatase Shp-2. EMBO J 16: 2352-2364.

76. Zhang EE, Chapeau E, Hagihara K, Feng GS (2004) Neuronal Shp2 tyrosine phosphatase controls energy balance and metabolism. Proc Natl Acad Sci U S A 101: 16064-16069.
77. Ke Y, Zhang EE, Hagihara K, Wu D, Pang Y, Klein R, Curran T, Ranscht B, Feng GS (2007) Deletion of Shp2 in the brain leads to defective proliferation and differentiation in neural stem cells and early postnatal lethality. Mol Cell Biol 27: 6706-6717.
78. Kontaridis MI, Yang W, Bence KK, Cullen D, Wang B, Bodyak N, Ke Q, Hinek A, Kang PM, Liao R, et al. (2008) Deletion of Ptpn11 (Shp2) in cardiomyocytes causes dilated cardiomyopathy via effects on the extracellular signal-regulated kinase/mitogen-activated protein kinase and RhoA signaling pathways. Circulation 117: 1423-1435.
79. Bard-Chapeau EA, Yuan J, Droin N, Long S, Zhang EE, Nguyen TV, Feng GS (2006) Concerted functions of Gab1 and Shp2 in liver regeneration and hepatoprotection. Mol Cell Biol 26: 4664-4674.
80. Ke Y, Lesperance J, Zhang EE, Bard-Chapeau EA, Oshima RG, Muller WJ, Feng GS (2006) Conditional deletion of Shp2 in the mammary gland leads to impaired lobulo-alveolar outgrowth and attenuated Stat5 activation. J Biol Chem 281: 34374-34380.
81. Princen F, Bard E, Sheikh F, Zhang SS, Wang J, Zago WM, Wu D, Trelles RD, Bailly-Maitre B, Kahn CR, et al. (2009) Deletion of Shp2 tyrosine phosphatase in muscle leads to dilated cardiomyopathy, insulin resistance, and premature death. Mol Cell Biol 29: 378-388.
82. Marengere LE, Waterhouse P, Duncan GS, Mittrucker HW, Feng GS, Mak TW (1996) Regulation of T cell receptor signaling by tyrosine phosphatase SYP association with CTLA-4. Science 272: 1170-1173.
83. Chemnitz JM, Parry RV, Nichols KE, June CH, Riley JL (2004) SHP-1 and SHP-2 associate with immunoreceptor tyrosine-based switch motif of programmed death 1 upon primary human T cell stimulation, but only receptor ligation prevents T cell activation. J Immunol 173: 945-954.
84. Gavrieli M, Watanabe N, Loftin SK, Murphy TL, Murphy KM (2003) Characterization of phosphotyrosine binding motifs in the cytoplasmic domain of B and T lymphocyte attenuator required for association with protein tyrosine phosphatases SHP-1 and SHP-2. Biochem Biophys Res Commun 312: 1236-1243.
85. Scalapino KJ, Daikh DI (2008) CTLA-4: a key regulatory point in the control of autoimmune disease. Immunol Rev 223: 143-155.
86. Tivol EA, Borriello F, Schweitzer AN, Lynch WP, Bluestone JA, Sharpe AH (1995) Loss of CTLA-4 leads to massive lymphoproliferation and fatal multiorgan tissue destruction, revealing a critical negative regulatory role of CTLA-4. Immunity 3: 541-547.
87. Waterhouse P, Penninger JM, Timms E, Wakeham A, Shahinian A, Lee KP, Thompson CB, Griesser H, Mak TW (1995) Lymphoproliferative disorders with early lethality in mice deficient in Ctla-4. Science 270: 985-988.

88. Lee KM, Chuang E, Griffin M, Khattri R, Hong DK, Zhang W, Straus D, Samelson LE, Thompson CB, Bluestone JA (1998) Molecular basis of T cell inactivation by CTLA-4. Science 282: 2263-2266.
89. Masteller EL, Chuang E, Mullen AC, Reiner SL, Thompson CB (2000) Structural analysis of CTLA-4 function in vivo. J Immunol 164: 5319-5327.
90. Chambers CA, Allison JP (1996) The role of tyrosine phosphorylation and PTP-1C in CTLA-4 signal transduction. Eur J Immunol 26: 3224-3229.
91. Nguyen TV, Ke Y, Zhang EE, Feng GS (2006) Conditional deletion of Shp2 tyrosine phosphatase in thymocytes suppresses both pre-TCR and TCR signals. J Immunol 177: 5990-5996.
92. Ruzankina Y, Pinzon-Guzman C, Asare A, Ong T, Pontano L, Cotsarelis G, Zediak VP, Velez M, Bhandoola A, Brown EJ (2007) Deletion of the developmentally essential gene ATR in adult mice leads to age-related phenotypes and stem cell loss. Cell Stem Cell 1: 113-126.
93. Janeway C, Travers P, Walport M, Shlomchik M (2005) Immunobiology 6 : the immune system in health and disease. New York: Garland Pub.
94. Cantrell DA (1996) T cell antigen receptor signal transduction pathways. Cancer Surv 27: 165-175.
95. Samelson LE (2002) Signal transduction mediated by the T cell antigen receptor: the role of adapter proteins. Annu Rev Immunol 20: 371-394.
96. Werlen G, Palmer E (2002) The T-cell receptor signalosome: a dynamic structure with expanding complexity. Curr Opin Immunol 14: 299-305.
97. Mustelin T, Tasken K (2003) Positive and negative regulation of T-cell activation through kinases and phosphatases. Biochem J 371: 15-27.
98. Hermiston ML, Xu Z, Weiss A (2003) CD45: a critical regulator of signaling thresholds in immune cells. Annu Rev Immunol 21: 107-137.
99. Gorska MM, Stafford SJ, Cen O, Sur S, Alam R (2004) Unc119, a novel activator of Lck/Fyn, is essential for T cell activation. J Exp Med 199: 369-379.
100. Marti F, Garcia GG, Lapinski PE, MacGregor JN, King PD (2006) Essential role of the T cell-specific adapter protein in the activation of LCK in peripheral T cells. J Exp Med 203: 281-287.
101. Mustelin T, Rahmouni S, Bottini N, Alonso A (2003) Role of protein tyrosine phosphatases in T cell activation. Immunol Rev 191: 139-147.
102. Pani G, Fischer KD, Mlinaric-Rascan I, Siminovitch KA (1996) Signaling capacity of the T cell antigen receptor is negatively regulated by the PTP1C tyrosine phosphatase. J Exp Med 184: 839-852.
103. Brockdorff J, Williams S, Couture C, Mustelin T (1999) Dephosphorylation of ZAP-70 and inhibition of T cell activation by activated SHP1. Eur J Immunol 29: 2539-2550.
104. Kontgen F, Suss G, Stewart C, Steinmetz M, Bluethmann H (1993) Targeted disruption of the MHC class II Aa gene in C57BL/6 mice. Int Immunol 5: 957-964.
105. Nika K, Hyunh H, Williams S, Paul S, Bottini N, Tasken K, Lombroso PJ, Mustelin T (2004) Haematopoietic protein tyrosine phosphatase (HePTP) phosphorylation by cAMP-dependent protein kinase in T-cells: dynamics and subcellular location. Biochem J 378: 335-342.

106. Itoh Y, Wang Z, Ishida H, Eichelberg K, Fujimoto N, Makino J, Ogasawara K, Germain RN (2005) Decreased CD4 expression by polarized T helper 2 cells contributes to suboptimal TCR-induced phosphorylation and reduced Ca2+ signaling. Eur J Immunol 35: 3187-3195.
107. Meyers EN, Lewandoski M, Martin GR (1998) An Fgf8 mutant allelic series generated by Cre- and Flp-mediated recombination. Nat Genet 18: 136-141.
108. Cohen PL, Eisenberg RA (1991) Lpr and gld: single gene models of systemic autoimmunity and lymphoproliferative disease. Annu Rev Immunol 9: 243-269.
109. Layer K, Lin G, Nencioni A, Hu W, Schmucker A, Antov AN, Li X, Takamatsu S, Chevassut T, Dower NA, et al. (2003) Autoimmunity as the consequence of a spontaneous mutation in Rasgrp1. Immunity 19: 243-255.
110. King PD (2004) Lupus-like autoimmunity caused by defects in T-cell signal transduction. Curr Opin Investig Drugs 5: 517-523.
111. Zheng Y, Schlondorff J, Blobel CP (2002) Evidence for regulation of the tumor necrosis factor alpha-convertase (TACE) by protein-tyrosine phosphatase PTPH1. J Biol Chem 277: 42463-42470.
112. Schlondorff J, Blobel CP (1999) Metalloprotease-disintegrins: modular proteins capable of promoting cell-cell interactions and triggering signals by protein-ectodomain shedding. J Cell Sci 112 (Pt 21): 3603-3617.
113. Primakoff P, Myles DG (2000) The ADAM gene family: surface proteins with adhesion and protease activity. Trends Genet 16: 83-87.
114. Zhang SH, Liu J, Kobayashi R, Tonks NK (1999) Identification of the cell cycle regulator VCP (p97/CDC48) as a substrate of the band 4.1-related protein-tyrosine phosphatase PTPH1. J Biol Chem 274: 17806-17812.
115. Lavoie C, Chevet E, Roy L, Tonks NK, Fazel A, Posner BI, Paiement J, Bergeron JJ (2000) Tyrosine phosphorylation of p97 regulates transitional endoplasmic reticulum assembly in vitro. Proc Natl Acad Sci U S A 97: 13637-13642.
116. Wang Z, Shen D, Parsons DW, Bardelli A, Sager J, Szabo S, Ptak J, Silliman N, Peters BA, van der Heijden MS, et al. (2004) Mutational analysis of the tyrosine phosphatome in colorectal cancers. Science 304: 1164-1166.
117. Erdmann KS (2003) The protein tyrosine phosphatase PTP-Basophil/Basophil-like. Interacting proteins and molecular functions. Eur J Biochem 270: 4789-4798.
118. Wansink DG, Peters W, Schaafsma I, Sutmuller RP, Oerlemans F, Adema GJ, Wieringa B, van der Zee CE, Hendriks W (2004) Mild impairment of motor nerve repair in mice lacking PTP-BL tyrosine phosphatase activity. Physiol Genomics 19: 50-60.
119. Lorber B, Hendriks WJ, Van der Zee CE, Berry M, Logan A (2005) Effects of LAR and PTP-BL phosphatase deficiency on adult mouse retinal cells activated by lens injury. Eur J Neurosci 21: 2375-2383.
120. Nakahira M, Tanaka T, Robson BE, Mizgerd JP, Grusby MJ (2007) Regulation of signal transducer and activator of transcription signaling by the tyrosine phosphatase PTP-BL. Immunity 26: 163-176.
121. Park KW, Lee EJ, Lee S, Lee JE, Choi E, Kim BJ, Hwang R, Park KA, Baik J (2000) Molecular cloning and characterization of a protein tyrosine phosphatase enriched in testis, a putative murine homologue of human PTPMEG. Gene 257: 45-55.

122. Pasquali C, Curchod ML, Walchli S, Espanel X, Guerrier M, Arigoni F, Strous G, Van Huijsduijnen RH (2003) Identification of protein tyrosine phosphatases with specificity for the ligand-activated growth hormone receptor. Mol Endocrinol 17: 2228-2239.
123. Pilecka I, Patrignani C, Pescini R, Curchod ML, Perrin D, Xue Y, Yasenchak J, Clark A, Magnone MC, Zaratin P, et al. (2007) Protein-tyrosine phosphatase H1 controls growth hormone receptor signaling and systemic growth. J Biol Chem 282: 35405-35415.
124. Hironaka K, Umemori H, Tezuka T, Mishina M, Yamamoto T (2000) The protein-tyrosine phosphatase PTPMEG interacts with glutamate receptor delta 2 and epsilon subunits. J Biol Chem 275: 16167-16173.
125. Kina S, Tezuka T, Kusakawa S, Kishimoto Y, Kakizawa S, Hashimoto K, Ohsugi M, Kiyama Y, Horai R, Sudo K, et al. (2007) Involvement of protein-tyrosine phosphatase PTPMEG in motor learning and cerebellar long-term depression. Eur J Neurosci 26: 2269-2278.
126. Patrignani C, Magnone MC, Tavano P, Ardizzone M, Muzio V, Greco B, Zaratin PF (2008) Knockout mice reveal a role for protein tyrosine phosphatase H1 in cognition. Behav Brain Funct 4: 36.
127. Whited JL, Robichaux MB, Yang JC, Garrity PA (2007) Ptpmeg is required for the proper establishment and maintenance of axon projections in the central brain of Drosophila. Development 134: 43-53.
128. Jing M, Bohl J, Brimer N, Kinter M, Vande Pol SB (2007) Degradation of tyrosine phosphatase PTPN3 (PTPH1) by association with oncogenic human papillomavirus E6 proteins. J Virol 81: 2231-2239.
129. Spanos WC, Hoover A, Harris GF, Wu S, Strand GL, Anderson ME, Klingelhutz AJ, Hendriks W, Bossler AD, Lee JH (2008) The PDZ binding motif of human papillomavirus type 16 E6 induces PTPN13 loss, which allows anchorage-independent growth and synergizes with ras for invasive growth. J Virol 82: 2493-2500.
130. Topffer S, Muller-Schiffmann A, Matentzoglu K, Scheffner M, Steger G (2007) Protein tyrosine phosphatase H1 is a target of the E6 oncoprotein of high-risk genital human papillomaviruses. J Gen Virol 88: 2956-2965.
131. Tartaglia M, Mehler EL, Goldberg R, Zampino G, Brunner HG, Kremer H, van der Burgt I, Crosby AH, Ion A, Jeffery S, et al. (2001) Mutations in PTPN11, encoding the protein tyrosine phosphatase SHP-2, cause Noonan syndrome. Nat Genet 29: 465-468.
132. Noonan JA (1968) Hypertelorism with Turner phenotype. A new syndrome with associated congenital heart disease. Am J Dis Child 116: 373-380.
133. Keilhack H, David FS, McGregor M, Cantley LC, Neel BG (2005) Diverse biochemical properties of Shp2 mutants. Implications for disease phenotypes. J Biol Chem 280: 30984-30993.
134. Fragale A, Tartaglia M, Wu J, Gelb BD (2004) Noonan syndrome-associated SHP2/PTPN11 mutants cause EGF-dependent prolonged GAB1 binding and sustained ERK2/MAPK1 activation. Hum Mutat 23: 267-277.
135. Gorlin RJ, Anderson RC, Blaw M (1969) Multiple lentigenes syndrome. Am J Dis Child 117: 652-662.

136. Digilio MC, Conti E, Sarkozy A, Mingarelli R, Dottorini T, Marino B, Pizzuti A, Dallapiccola B (2002) Grouping of multiple-lentigines/LEOPARD and Noonan syndromes on the PTPN11 gene. Am J Hum Genet 71: 389-394.
137. Tartaglia M, Martinelli S, Stella L, Bocchinfuso G, Flex E, Cordeddu V, Zampino G, Burgt I, Palleschi A, Petrucci TC, et al. (2006) Diversity and functional consequences of germline and somatic PTPN11 mutations in human disease. Am J Hum Genet 78: 279-290.
138. Hanna N, Montagner A, Lee WH, Miteva M, Vidal M, Vidaud M, Parfait B, Raynal P (2006) Reduced phosphatase activity of SHP-2 in LEOPARD syndrome: consequences for PI3K binding on Gab1. FEBS Lett 580: 2477-2482.
139. Kontaridis MI, Swanson KD, David FS, Barford D, Neel BG (2006) PTPN11 (Shp2) mutations in LEOPARD syndrome have dominant negative, not activating, effects. J Biol Chem 281: 6785-6792.
140. Tartaglia M, Gelb BD (2005) Noonan syndrome and related disorders: genetics and pathogenesis. Annu Rev Genomics Hum Genet 6: 45-68.
141. Edouard T, Montagner A, Dance M, Conte F, Yart A, Parfait B, Tauber M, Salles JP, Raynal P (2007) How do Shp2 mutations that oppositely influence its biochemical activity result in syndromes with overlapping symptoms? Cell Mol Life Sci 64: 1585-1590.
142. Noonan JA (2006) Noonan syndrome and related disorders: alterations in growth and puberty. Rev Endocr Metab Disord 7: 251-255.
143. Neel BG, Gu H, Pao L (2003) The 'Shp'ing news: SH2 domain-containing tyrosine phosphatases in cell signaling. Trends Biochem Sci 28: 284-293.
144. Yusa S, Campbell KS (2003) Src homology region 2-containing protein tyrosine phosphatase-2 (SHP-2) can play a direct role in the inhibitory function of killer cell Ig-like receptors in human NK cells. J Immunol 170: 4539-4547.
145. Yusa S, Catina TL, Campbell KS (2004) KIR2DL5 can inhibit human NK cell activation via recruitment of Src homology region 2-containing protein tyrosine phosphatase-2 (SHP-2). J Immunol 172: 7385-7392.
146. Lee PP, Fitzpatrick DR, Beard C, Jessup HK, Lehar S, Makar KW, Perez-Melgosa M, Sweetser MT, Schlissel MS, Nguyen S, et al. (2001) A critical role for Dnmt1 and DNA methylation in T cell development, function, and survival. Immunity 15: 763-774.
147. Wojchowski DM, Gregory RC, Miller CP, Pandit AK, Pircher TJ (1999) Signal transduction in the erythropoietin receptor system. Exp Cell Res 253: 143-156.
148. De Feo P, Perriello G, Torlone E, Ventura MM, Santeusanio F, Brunetti P, Gerich JE, Bolli GB (1989) Demonstration of a role for growth hormone in glucose counterregulation. Am J Physiol 256: E835-843.
149. Lin AW, Lowe SW (2001) Oncogenic ras activates the ARF-p53 pathway to suppress epithelial cell transformation. Proc Natl Acad Sci U S A 98: 5025-5030.
150. Roper E, Weinberg W, Watt FM, Land H (2001) p19ARF-independent induction of p53 and cell cycle arrest by Raf in murine keratinocytes. EMBO Rep 2: 145-150.
151. Cai T, Nishida K, Hirano T, Khavari PA (2002) Gab1 and SHP-2 promote Ras/MAPK regulation of epidermal growth and differentiation. J Cell Biol 159: 103-112.

152. Feng GS (2007) Shp2-mediated molecular signaling in control of embryonic stem cell self-renewal and differentiation. Cell Res 17: 37-41.
153. Zou GM, Chan RJ, Shelley WC, Yoder MC (2006) Reduction of Shp-2 expression by small interfering RNA reduces murine embryonic stem cell-derived in vitro hematopoietic differentiation. Stem Cells 24: 587-594.
154. Lee CK, Chang BS, Hong YM, Yang SW, Lee CS, Seo JB (2001) Spinal deformities in Noonan syndrome: a clinical review of sixty cases. J Bone Joint Surg Am 83-A: 1495-1502.
155. Sharland M, Burch M, McKenna WM, Paton MA (1992) A clinical study of Noonan syndrome. Arch Dis Child 67: 178-183.
156. Sarkozy A, Digilio MC, Dallapiccola B (2008) Leopard syndrome. Orphanet J Rare Dis 3: 13.
157. Sims NA, Jenkins BJ, Quinn JM, Nakamura A, Glatt M, Gillespie MT, Ernst M, Martin TJ (2004) Glycoprotein 130 regulates bone turnover and bone size by distinct downstream signaling pathways. J Clin Invest 113: 379-389.
158. Lee SE, Chung WJ, Kwak HB, Chung CH, Kwack KB, Lee ZH, Kim HH (2001) Tumor necrosis factor-alpha supports the survival of osteoclasts through the activation of Akt and ERK. J Biol Chem 276: 49343-49349.
159. Lee SE, Woo KM, Kim SY, Kim HM, Kwack K, Lee ZH, Kim HH (2002) The phosphatidylinositol 3-kinase, p38, and extracellular signal-regulated kinase pathways are involved in osteoclast differentiation. Bone 30: 71-77.
160. Wei S, Wang MW, Teitelbaum SL, Ross FP (2002) Interleukin-4 reversibly inhibits osteoclastogenesis via inhibition of NF-kappa B and mitogen-activated protein kinase signaling. J Biol Chem 277: 6622-6630.
161. Miyazaki T, Katagiri H, Kanegae Y, Takayanagi H, Sawada Y, Yamamoto A, Pando MP, Asano T, Verma IM, Oda H, et al. (2000) Reciprocal role of ERK and NF-kappaB pathways in survival and activation of osteoclasts. J Cell Biol 148: 333-342.
162. Wood LD, Parsons DW, Jones S, Lin J, Sjoblom T, Leary RJ, Shen D, Boca SM, Barber T, Ptak J, et al. (2007) The genomic landscapes of human breast and colorectal cancers. Science 318: 1108-1113.
163. Qu CK, Nguyen S, Chen J, Feng GS (2001) Requirement of Shp-2 tyrosine phosphatase in lymphoid and hematopoietic cell development. Blood 97: 911-914.
164. Saxton TM, Ciruna BG, Holmyard D, Kulkarni S, Harpal K, Rossant J, Pawson T (2000) The SH2 tyrosine phosphatase shp2 is required for mammalian limb development. Nat Genet 24: 420-423.
165. Salmond RJ, Huyer G, Kotsoni A, Clements L, Alexander DR (2005) The src homology 2 domain-containing tyrosine phosphatase 2 regulates primary T-dependent immune responses and Th cell differentiation. J Immunol 175: 6498-6508.
166. Yan J, Chen S, Zhang Y, Li X, Li Y, Wu X, Yuan J, Robling AG, Kapur R, Chan RJ, et al. (2008) Rac1 mediates the osteoclast gains-in-function induced by haploinsufficiency of Nf1. Hum Mol Genet 17: 936-948.
167. Yang FC, Chen S, Robling AG, Yu X, Nebesio TD, Yan J, Morgan T, Li X, Yuan J, Hock J, et al. (2006) Hyperactivation of p21ras and PI3K cooperate to alter

murine and human neurofibromatosis type 1-haploinsufficient osteoclast functions. J Clin Invest 116: 2880-2891.
168. Schindeler A, Little DG (2006) Ras-MAPK signaling in osteogenic differentiation: friend or foe? J Bone Miner Res 21: 1331-1338.
169. Illes T, Halmai V, de Jonge T, Dubousset J (2001) Decreased bone mineral density in neurofibromatosis-1 patients with spinal deformities. Osteoporos Int 12: 823-827.
170. Yu X, Chen S, Potter OL, Murthy SM, Li J, Pulcini JM, Ohashi N, Winata T, Everett ET, Ingram D, et al. (2005) Neurofibromin and its inactivation of Ras are prerequisites for osteoblast functioning. Bone 36: 793-802.